ASSESSMENT OF COASTAL VEGETATION DEGRADATION USING REMOTE SENSING IN FALSE BAY, SOUTH AFRICA

by
CIKIZWA MBOLAMBI

Thesis submitted in fulfilment of the requirements for the degree Masters of Science in Geography and Environmental Studies in the faculty of Science at Stellenbosch University

SUPERVISOR: Dr M Lück-Vogel

December 2016

DEPARTMENT OF GEOGRAPHY AND ENVIRONMENTAL STUDIES

DECLARATION

By submitting this thesis electronically, I declare that the entirety of the work contained therein is my own, original work, that I am the owner of the copyright thereof (save to the extent explicitly otherwise stated) that reproduction and publication thereof Stellenbosch University will not infringe any third party rights and that I have not previously in its entirety or in part submitted it for obtaining any qualification.

December 2016

ABSTRACT

The coastal zone, the interface between land and sea, faces much pressure from human activities. These coastal pressures make it difficult for the coastal zones to fulfil their natural functions, so threatening the state of coastal environments and making them vulnerable to coastal disasters and degradation. This study aimed to test whether remote sensing techniques can be implemented to assess the intactness of terrestrial coastal vegetation at the high spatial resolution required for coastal management. The study focused on the northern False Bay coast, Western Cape, South Africa. The research used is a modification of the method developed by Lück-Vogel, O'Farrell & Roberts (2013) which involved image segmentation and a habitat intactness index using image derivatives. The procedure used Worldview-2 (WV-2) images of high spatial, spectral and temporal resolution acquired on 25 February 2014 and 11 October 2014. Both images were pre-processed and segmented into meaningful objects using object-based image analysis (OBIA). Five image derivatives and the eight spectral bands were stacked into a single image to extract field-informed training points. Regression analysis was performed on eight spectral bands and five image derivatives to evaluate the most suitable bands to produce a habitat intactness index in a subsequent decision tree classification. Decision tree classification was generated using two spectral bands, namely the RED and NIR1 bands. These bands were chosen because they gave the best regression results and they are available in most sensors. The bands were also chosen because the study deals with vegetation assessment. The overall accuracy of the results was 80.5% which was a satisfactory result with a kappa value of 0.75 (75%) that indicates a substantial agreement between the remotely sensed result and the reference data. A key finding is the importance of seasonality to delineate natural and alien vegetation which is better achieved in the dry season. Validation of the results was done using the field-validation points of a field visit conducted in June 2016. The output maps generated for habitat intactness consisted of five habitat intactness classes namely highly, moderately and lightly degraded, intact vegetation and alien vegetation. The output maps can be used to inform coastal managers about conservation at a local scale. It is recommended that validation of remote sensing results be done in the same season that satellite images were taken.

KEYWORDS AND PHRASES

Alien vegetation, coastal zone, coastal vegetation, False Bay, habitat intactness, remote sensing, WV-2

OPSOMMING

Die koppelvlak tussen die land en die see, ook bekend as die kussone, verkeer onder druk weens antropologiese invloede. Menslike bedrywighede belemmer die kus se natuurlike funksie en stel die kus en sy nabygeleë omgewing bloot aan kusrampe en degradasie. Hierdie studie probeer bepaal of afstandswaarnemingstegnieke toegepas kan word om habitatsongeskondenheid langs die kus, teen ‘n geskikte resolusie vir kusbestuurdoeleindes, te modelleer. Ons fokus spesifiek op die noordelike deel van Valsbaai in die Wes-Kaap Provinsie van Suid-Afrika. Ons bou voort op metodes wat oorspronklik deur Lück-Vogel, O’Farell & Roberts (2013) gedoen is. Die voorgenoemde studie gebruik beeldsegmentasie en beeldafgeleides ten einde ‘n habitatsongeskondenheidsindeks op te stel. Die metode wat in hierdie studie gebruik word maak gebruik van twee WorldView-2 (WV-2) beelde wat teen ‘n hoë ruimtelike-, spektrale- en tydsresolusie, onderskeidelik, op 25 Februarie en 11 Oktober geneem is. Voorwerpgebasseerde beeldverwerking is toegepas om die voorverwerking en segmentasie op hierdie beelde te doen om sodoende sinvolle beeldvoorwerpe te verkry. Vyf beeldafgeleides en agt spektrale bande is gestapel om ‘n enkele beeld te vorm ten einde die toetspunte te isoleer. Regressie-analise is gedoen om die mees toepaslike bande te bepaal om ‘n habitatsongeskondenheidsindeks daar te stel deur van ‘n klassifikasie-beslissingsboom gebruik te maak. Die RED en NIR1 spektraalbande is gebruik om beslissingsboomklassifikasie te doen. Hierdie bande is gekies omdat hulle die beste regressie resultate gelewer het, beskikbaar is op die meeste sensors en omdat hierdie studie plantegroei-assesering behels. Die algehele akkuraatheid van ons bevindinge is 80.5% en word beskou as ‘n bevredigende resultaat met ‘n kappa waarde van 0.75 (75%) wat aandui dat daar ‘n wesenlike ooreenkoms tussen die afstandswaargenome resultaat en die verwysingsdata is. Een van die sleutelbevindinge is die belangrike rol wat seisonaliteit speel in die beskrywing van inheemse en uitheemse plantegroei. Sulkse beskrywings is meer wesenlik in die droë seisoen. Bevestiging van die resultate is gedoen deur van veld-validasie punte, wat tydens ‘n veldbesoek in 2016 geneem is, gebruik te maak. Die gegenereerde habitatsongeskondenheidskaarte bestaan uit vyf habitatsongeskondenheidsklasse naamlik hoog, matig- en ligtelik gedegradeer, ongeskonde plantegroei en uitheemse plantegroei. Hierdie afvoerkaarte kan gebruik word om kusbestuurders in te lig oor bewaring op 'n lokale skaal. Dit word aanbeveel dat die validasie van die afstandswaarnemingsresultate gedoen word in dieselfde seisoen waarin die satelliet beelde geneem is.

TREFWOORDE EN-FRASES

Uitheemse plantegroei, kussone, kustelike plantegroei, Valsbaai, habitatsongeskondenheid, afstandswaarneming.

ACKNOWLEDGEMENTS

I sincerely thank:

- God almighty for granting me strength, sufficient grace, the ability and wisdom to complete the research.
- My parents for their prayers and constant motivation.
- My supervisor Dr Melanie Lück-Vogel for her constant guidance, support and valuable technical and non-technical advice and input throughout the completion of my thesis.
- My mentor Dr Susan Taljaard for believing in me and supporting me throughout my thesis.
- My Family and friends for their constant motivation and encouragement.
- The Council for Scientific Industrial Research (CSIR) for granting me the studentship and not forgetting the Natural Resources and the Environment (NRE) Coastal Systems and Modelling and Digital Sciences (MDS) group at CSIR for their support.
- Fellow Masters students for their support.
- The City of Cape Town (CoCT) Staff for assisting with data and field visits.

CONTENTS

TABLES

FIGURES

ACRONYMS AND ABBREVIATIONS

AOI	Area of interest
CFDS	Cape Flats Dune Strandveld
CoCT	City of Cape Town
CSIR	Council for Scientific and Industrial Research
DEA	Department of Environmental Affairs
DEAT	Department of Environmental Affairs and Tourism
DN	Digital numbers
DSM	Digital surface model
DTC	Decision Tree Classification
EEA	European Environmental Agency
EEZ	Exclusive Economic Zone
EMS	Electromagnetic spectrum
ESRI	Environmental System Research Institute
FB	False Bay
GIS	Geographic Information Systems
GPS	Global positioning system
HII	Habitat Intactness Index
HWM	High Water Mark
ICMA	Integrated Coastal Management Act
IDP	Integrated Developmental Plan
LiDAR	Light Detection and Ranging
MDS	Modelling and Digital Science
MG	Malmesbury Group
MODIS	Moderate resolution imaging spectrometer
MS	Multispectral Satellite
MSS	Multispectral scanner system
NDVI	Normalized Difference Vegetation Index
NIR	Near-infrared
NLC	National Land Cover
NRE	Natural Resource and the Environment
OBIA	Object-based image analysis
SANSA	South African National Space Agency

SPF	Spatial Planning Framework
SPOT	Systeme Pour Observation de la Terre
TM	Thematic Mapper
TMG	Table Mountain Group
UTM	Universal Transverse Mercator
WV-2	WorldView-2

CHAPTER 1. INTRODUCTION

Chapter one provides a brief background on the study, representing the research problem, research question, aims and objectives as well as research methods and the structure of the thesis.

1.1 BACKGROUND

The coastal zone is the area where the land and sea meet (Nelson 2008; Leewis et al. 2012). The area is characterised by different habitats such as sandy beaches, dunes, cliffs and headlands, mangroves, coral reefs, estuaries, lagoons and salt marshes (Miththapala 2013). These coastal habitats are highly productive areas supporting a variety of biodiversity (Constanza et al. 1997). Moreover, these coastal habitats provide support services for natural ecosystems, for example for shoreline stabilisation, spawning grounds for marine life and buffers against natural hazards; they provide regulation services for climate, nutrient cycles, for detoxification of polluted waters; and coastal provision services like fuelwood, timber, food, coastal protection, natural products, energy resources and recreational activities; and cultural services for religious activities among others (Constanza et al. 1997). These roles highlight the importance of coastal systems and emphasise why they should be studied (EEA 2006; Thompson & Schlacher 2008).

For thousands of years human activities have impacted on coastal environments (Constanza et al. 1997). According to Millennium Ecosystem Assessment (2005), approximately 60% of the world's population is situated within 100 km of the coast. In South Africa, around 40% of the population lives within 100 km of the coast (DEA 2014). Coastal habitats worldwide are encountering rapid environmental change through increasing population and developmental pressures (Nayak & Bahuguna 2001). Global trends show that urbanisation is one of the primary causes of degradation in coastal environments (Nayak et al. 1989). Residential construction in coastal areas exposes them to coastal hazards that impair the functionality of coastal environments. Disturbances of coastal environments caused by anthropogenic factors due to increased population, urban coastal development and urban sprawl cause damage to coastal landscapes through habitat loss, pollution and increased vulnerability to events (Syvitski et al. 2002).

The key pressures affecting terrestrial coastal vegetation include unregulated public access and trampling. Unregulated activities can create pathways on dunes that eventually lead to vegetation destruction that in turn promotes erosion (Moulis & Barbel 1999). Other pressures

arise from sand mining, logging of firewood, motorised vehicles driving through vegetated habitats, urban sprawl, urban development, inappropriate waste deposits and the introduction of invasive species that degrade these habitats (Nayak & Bahuguna 2001). Given all these threats imposed by human activities and the importance of coastal zones, especially regarding the delivery of ecosystem services, there is urgent need to monitor and assess the degradation of terrestrial coastal vegetation to help conserve the natural resources provided by the system for future human generations. Based on the brief background provided in Section 1.1, Section 1.2 states the research problem.

1.2 RESEARCH PROBLEM

Coastal management in South Africa is primarily governed under the National Environmental Management: Integrated Coastal Management Act No. 24 of 2008 (South Africa 2009) as amended in 2014 (DEA 2014; South Africa 2014). Although this Act was the first to mandate the development of coastal management programmes and institutions for cooperative coastal governance, South Africa already had other legislation governing aspects of coastal management (Taljaard 2011; Glavovic & Cullinan 2009; McLean & Glazewski 2009).

Management of the terrestrial coastal zone, delineated as an area above the high water mark (HWM) from the sea inland up to 100 m in urban areas and 1 km in rural areas (South Africa 2009), is largely the responsibility of the respective municipalities (DEA 2014). Under the Municipal Systems Act No. 32 of 2000 (South Africa 2000) municipalities are required to prepare integrated development plans (IDPs) and spatial planning frameworks (SPFs) for the planning and development of their municipalities. A major handicap to municipal managers is the lack of appropriate data and information on the intactness of coastal vegetation at a high spatial resolution suitable for local management. Such high spatial resolution data and information are required to assess existing impacts and to plan conservation in coastal areas (Nayak & Bahuguna 2001). However, assessing the state of degradation of coastal vegetation in the required detail is usually unfeasible given the lack of skilled personnel and limited budgets. Readily available general remote sensing maps usually lack detail on degradation status. Therefore, the problem addressed in this study was the lack of a method to efficiently and cost-effectively measure the intactness of terrestrial coastal vegetation in South Africa at a resolution suitable for local management.

1.3 RESEARCH AIM AND OBJECTIVES

The aim of this research was to test whether remote sensing techniques can be implemented to assess the intactness of terrestrial coastal vegetation at a high spatial resolution required for local management. The study focused on the northern part of the False Bay (FB) coast situated along the south-western coast of the Western Cape Province of South Africa.

The following research question was addressed:

> *Can multispectral Satellite (MS) imagery, such as Worldview-2 (WV-2), be used to assess the intactness of terrestrial coastal vegetation at the northern part of False Bay?*

The research aim and associated research question were pursued through the following objectives:

1. Identify pristine areas and types of degradation in the study area (e.g. pathways, alien vegetation and fire scars) and identify areas with highest and lowest intactness.
2. Derive the spectral, structural and textural information for the intactness gradient of the natural terrestrial coastal vegetation along the northern coast of False Bay from the multi-spectral satellite images.
3. Develop and validate a habitat intactness index (HII) based on the spectral, structural and textural information.
4. Evaluate the remote sensing results.

1.4 RESEARCH METHODS AND RESEARCH DESIGN

1.4.1 Research methods

This study followed a quantitative approach to derive terrestrial coastal vegetation degradation along the northern coast of False Bay. According to Creswell (2003) and Fox (2008), quantitative research methods answer research questions and problems by numerical values to determine, for example, how much a certain area or object has been degraded or to what degree degrading has occurred, that is badly, moderately or slightly degraded using MS imagery. The research was carried out in an untransformed coastal landscape to develop a HII based on the structural, spectral and textural characteristics of environmental features along the northern coast of False Bay. The method implemented in this study was adapted from Lück-Vogel, O'Farrell & Roberts (2013) where it was applied in a study of habitat intactness around Elandsbay in the Sandveld region in the Western Cape Province.

High spatial resolution WorldView-2 (WV-2) imagery with 2x2 m pixel size was acquired from the South African National Space Agency (SANSA). The high resolution of WV-2 imagery was considered suitable for assessing the intactness of terrestrial coastal vegetation by deriving spectral, structural and textural image properties along the northern coast of False Bay. Global position system (GPS) referenced field data were collected for training purposes in the application of the remote sensing processes and for validation of the results. The quantitative method applied in this study used high spatial resolution WV-2 imagery.

1.4.2 Research design

Creswell (2003) describes a research design as a systematic plan or stages of decision used by researchers to answer the research question and to achieve the aim and objectives of the research. The systematic plan employed in this study is shown in Figure 1.1. The research began with a search for and reviews of relevant literature. The second step was the acquisition of high-resolution WV-2 images, as well as field and ancillary data and information from the National Land Cover (NLC) map of 2014 and the geographical information system (GIS) of the City of Cape Town (CoCT) data about habitat condition. Next, the WV-2 imagery was pre-processed to minimise atmospheric and satellite distortions, and subsetted to minimise computation time. A major step was the processing of WV-2 imagery which involved segmenting the imagery as input for developing a HII derived from a decision tree classification. The next step was performing accuracy assessment using field-informed training points and field visit to assess and validate the quality of the remote sensing results.

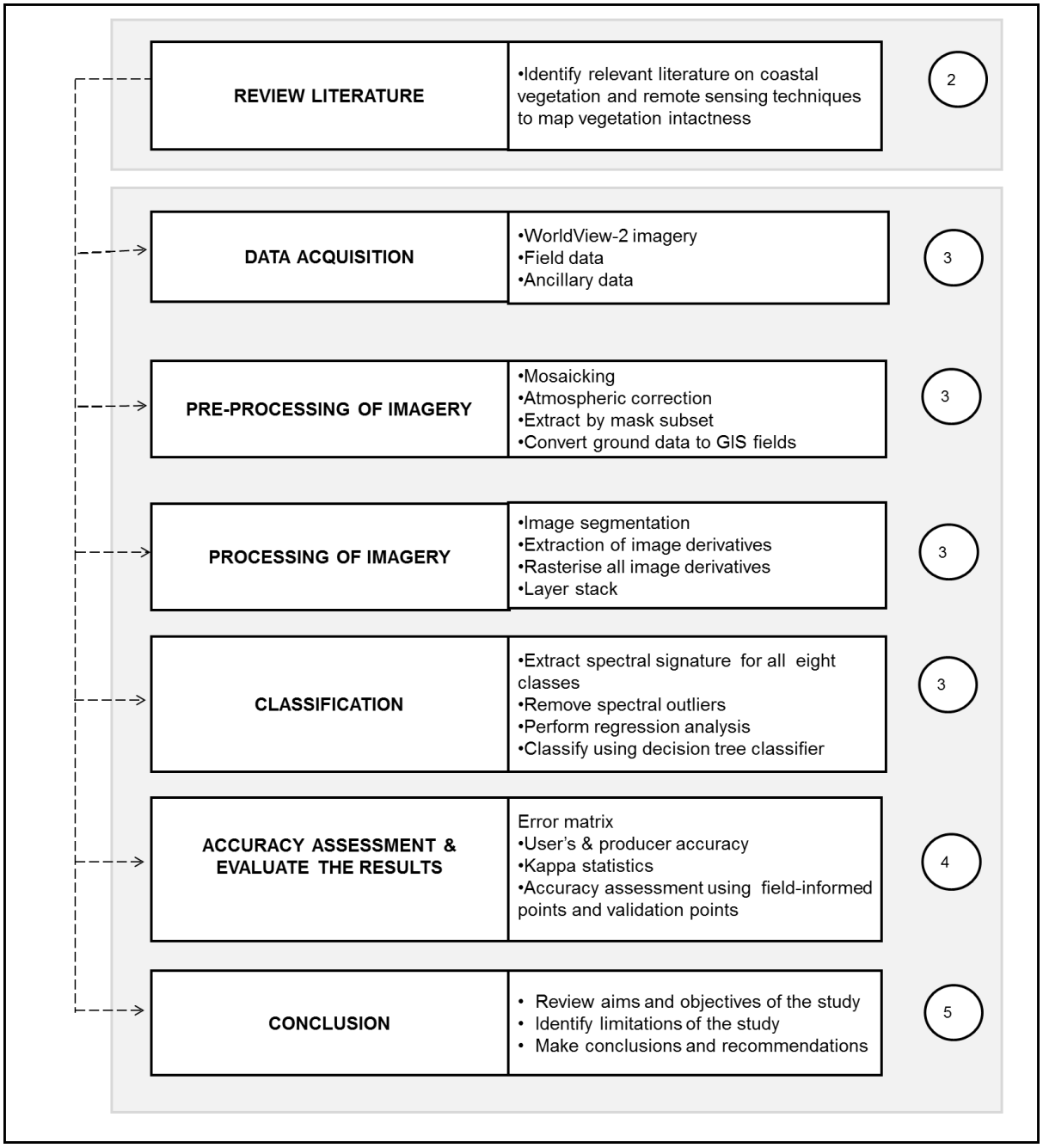

Figure 1.1 The Research design used in this study. Numbers in circles on the right indicate thesis chapters.

1.5 STRUCTURE OF THESIS

This thesis is structured into five chapters. Chapter one introduces the thesis and provides a brief background to the study as well as the research problem, research question, aims and objectives. Chapter two commences with a literature review on coastal terrestrial vegetation and its distribution in South Africa and continues with an overview of the application of remote sensing in mapping in general vegetation and coastal vegetation specifically. Chapter three outlines the study area and methods used in the study to achieve the final results. Chapter four presents and discusses the results of the research. Finally, Chapter five provides the study's conclusions and recommendations.

CHAPTER 2. LITERATURE REVIEW

This chapter is subdivided into two sections. Firstly it provides a review of literature based on coastal environments, its coastal vegetation, the influencing factors and characteristics shaping the coastal environment and vegetation, followed by the description of terrestrial coastal habitats and the key impacts influencing the intactness of these habitats. Secondly the chapter provides the use of remote sensing in coastal environments, based on the selection of different spatial, spectral and temporal resolutions and lastly the classification methods used in vegetation mapping and examples of coastal degradation assessment.

2.1 THE COASTAL ENVIRONMENT

2.1.1 Definition of the coastal zone

The coastal zone is defined internationally as the interface between land and sea (Nelson 2008). Carter (1988) describes the coastal zone as space in which terrestrial environments influence marine environments. The coastal zone has also been characterised as a band of dry land next to ocean space where land use activities directly affect the ocean and vice versa (Ketchum 1972). The National Environmental Management: Integrated Coastal Management Act of South Africa (South Africa 2009), as amended in the National Environmental Management: Integrated Coastal Amendment Management Act (ICMA) (South Africa 2014) defines the coastal zone as a space having the exclusive economic zone (EEZ) (200 nautical miles offshore from the coastline) as the seaward boundary and an area 1 km inland from the HWM in rural areas and 100 m inland from the HWM in urban areas as its landward boundary, as illustrated in Figure 2.1. This definition includes coastal terrestrial habitats, the seashore (area between low- and high-water marks), as well as coastal waters and waterbodies up to the EEZ.

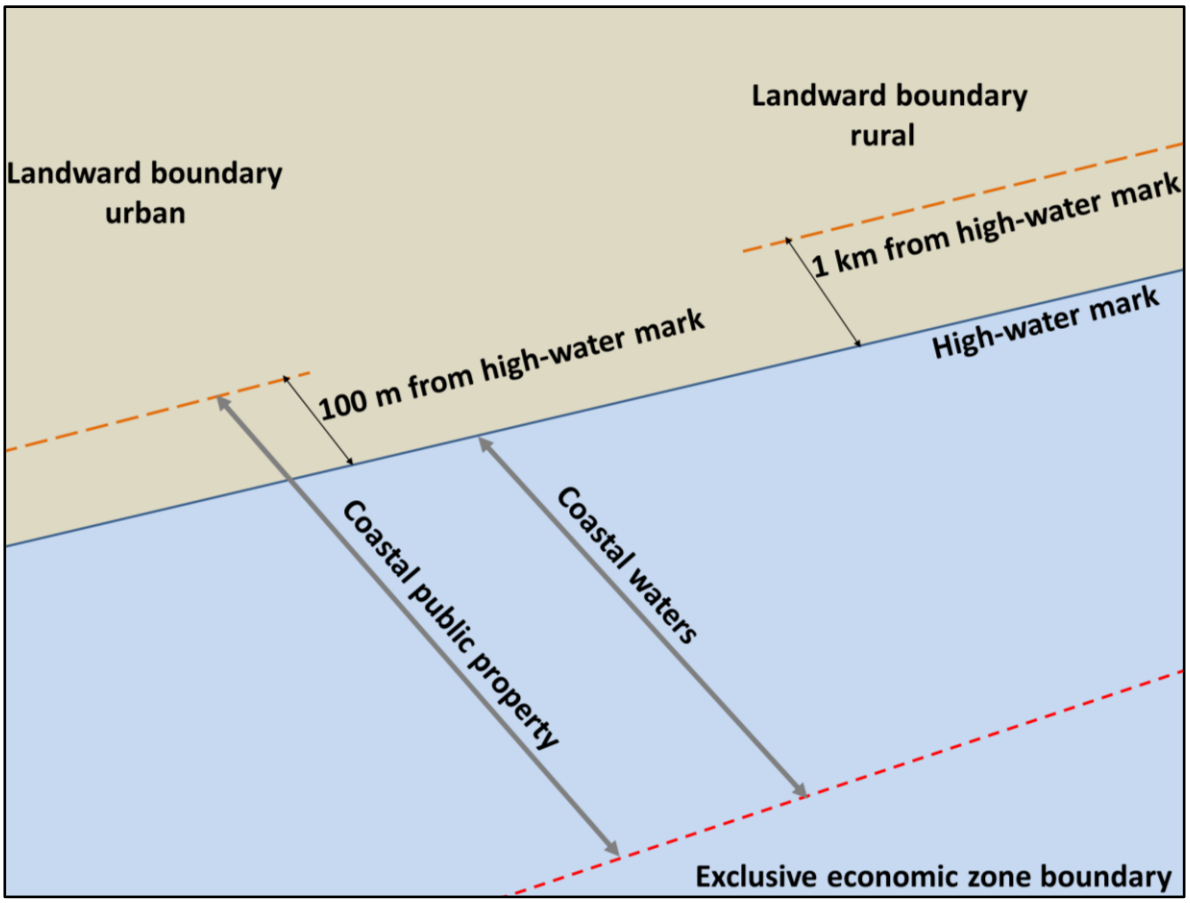

Source: Adapted Celliers et al. (2009)

Figure 2.1 The coastal zone of South Africa according to the Integrated Coastal Management Act in South Africa 2014

This thesis focuses on the coastal zone inland from the high-water mark (highest level reached by the seawater inland) as defined by the ICMA (South Africa 2014), hereafter referred to as the terrestrial coast. It is of importance to understand the key environmental factors shaping the coastal environments and its vegetation, therefore the next Section 2.2 describes the factors.

2.2 KEY ENVIRONMENTAL FACTORS SHAPING THE COASTAL ENVIRONMENT AND VEGETATION

The terrestrial coast is influenced by environmental factors ranging from geology and soil types, climate (e.g. rain, wind and temperature) to oceanographic (e.g. waves, currents and tides) conditions (Nicholls et al. 2007; Zhang 2002; Mucina & Rutherford 2006). Geology and particularly soil type are controlling factors in the distribution of coastal vegetation at local scale (Maun 2004, 2009; Frederiksen et al. 2006; Forey et al. 2008) so that variations in rock and soil types determine the distribution of different vegetation types along the coast. For

example, certain areas along the coast of South Africa are composed of fine-grained sand with limestone and Cape granite that favour the growth of Strandveld vegetation (Jackson 1991).

Variations in rainfall, temperature and wind are the most common climatic factors influencing the distribution of coastal vegetation at regional scale (Cowling et al. 1997; Maun 1998, 2004; Maun & Perumal 1999). Nakamura et al. (2007), Zhao et al. (2007) and Ji et al. (2009) found that rainfall was the most significant environmental factor influencing the distribution of coastal vegetation at regional scale. Wind influences evaporation, transpiration and transport of sand, sandblast and salt spray which occur along the dune profile so influencing the distribution of coastal vegetation (Maun 1998, 2004; Maun & Perumal 1999). Different types of coastal plant communities adapted to strong winds namely southeasters in summer and northwesters in winter also contribute to the distribution of vegetation along the coast (Branch et al. 1994). Section 2.3 outlines the terrestrial coastal habitats, since the study will be focusing in these habitats.

2.3 TERRESTRIAL COASTAL HABITATS

The South African coastline is about 3000 km long (Mucina & Rutherford 2006). The terrestrial coastal habitat is mainly composed of rocky shores consisting of coastal cliffs and headlands, sandy shores and dunes (Mucina & Rutherford 2006). According to Lubke et al. (1997) 70% of South Africa's coastline is sandy shores and 30% rocky shores. Less than 1% of the country's coastline consists of pebbles or shingle beaches (Mucina & Rutherford 2006; Tinley 1985a). Rocky shores include areas between the low-water mark and high-water mark (intertidal) that feature solid rocks (Denny & Gaines 2007). Rocky shores consist of different types of habitats, namely headlands, cliffs and rocky pools (Mucina & Rutherford 2006; Palmer, Van der Elst &Parak 2011). Headlands are coastal structures usually found at the end of bays extending out to the sea. The steep cliffs, also called coastal cliffs, are coastal structures formed along shorelines by erosive wave action. Rocky shore environments are conducive to stress-tolerant plants and animals because of the direct influences of the ocean (such as waves and salt spray) (Mucina & Rutherford 2006). The habitat zones of sandy shores are illustrated in Figure 2.2.

The inshore zone lies below the intertidal zone and is covered by water. The inshore zone is not the focus of this study. Above the inshore zone lies the foreshore zone comprising the intertidal zone (between the low- and high-water marks) that forms the transition zone between the land and the sea (Levinton 1995). The foreshore zone is also not the concern of this study. The

backshore zone extends from the high-water mark inland. The backshore zone of a sandy shore includes sandy beaches and dune habitats (Levinton 1995). The backshore is the focus of this study. It comprises dune habitats that are subdivided into foredunes and backdunes which are the primary and secondary dune habitats respectively. The backshore zone includes five habitat zones, namely plant-free beach zone, strand plant zone, shrub zone, scrub thicket zone and the thicket or forest zone. The five vegetated habitat zones are described in Section 2.3.1.

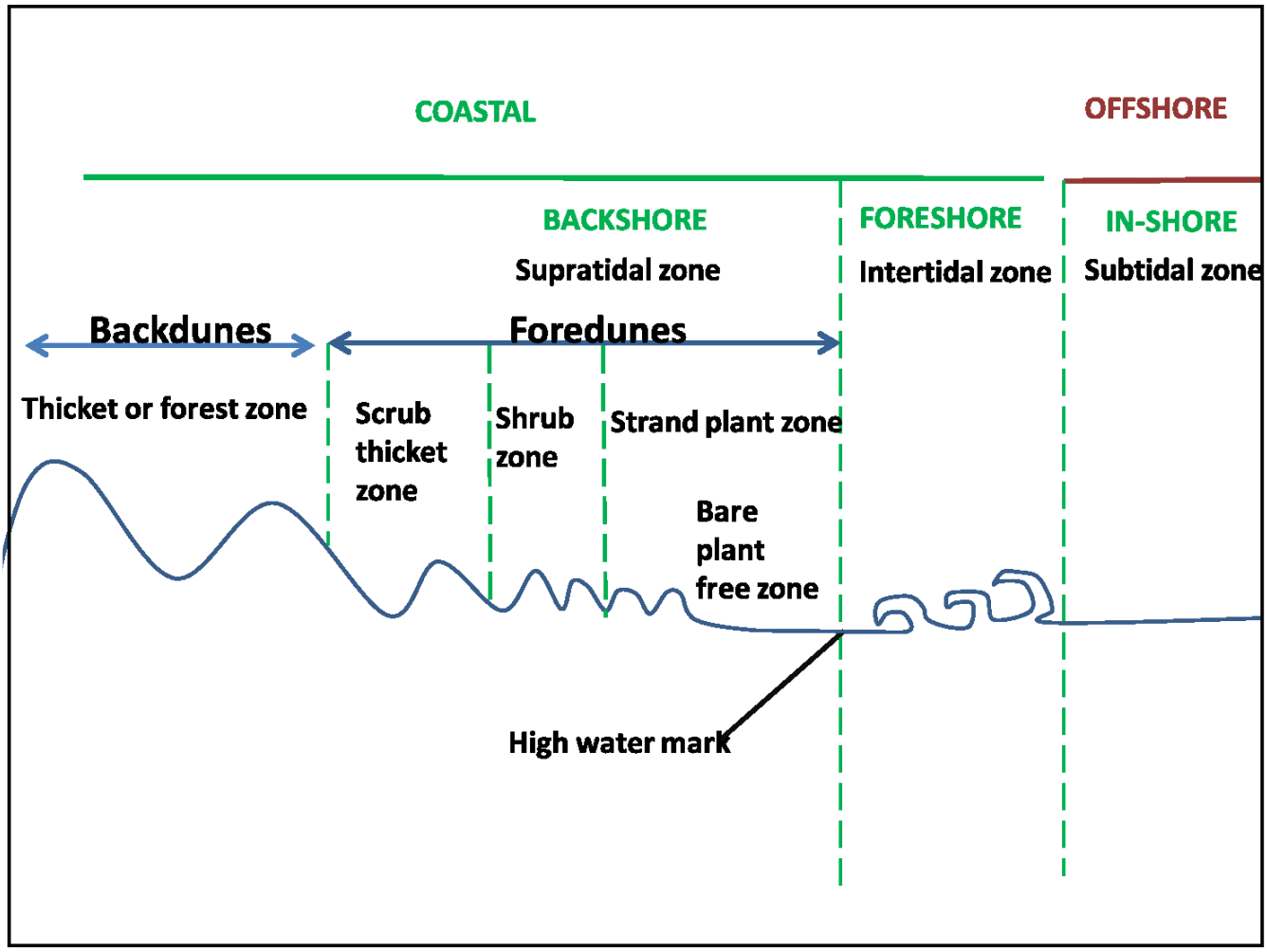

Source: Adapted from Tinley (1985a)

Figure 2.2 Habitat zones in sandy shores

The primary dune habitats consist of bare, plant-free areas and the foredunes that support pioneer plants. The secondary dunes are stabilised backdunes (Levinton 1995). This study focuses on vegetation landward of the high-water mark here referred to as the terrestrial coastal habitat. In terrestrial coastal habitats, it is important to understand the characteristics of vegetation the habitat mainly consists of. Section 2.3.1 briefly provides a description in characterisation of coastal vegetation.

2.3.1 Characterisation of coastal vegetation

The classification of vegetation is done across the dune profile (Tinley 1985b; Mucina & Rutherford 2006). The terrestrial coastal habitat consists of five vegetated zones, namely the strand plant zone, the shrub zone, the scrub thicket zone and the thicket or forest zone and an unvegetated zone (see Figure 2.2).

The *strand plant zone* is the most dynamic zone above the high-water mark in the foredune area. Strand plants are specialised pioneer dune flora that can withstand the extreme conditions of foredune areas (Tinley 1985a). This zone is especially exposed to wave movement and wind. The zone consists of short-lived plant communities (pioneers) that are destroyed at seasonal intervals as a result of storm events while reforming in phases of sand accretion, i.e. in summer (Tinley 1985a). Herbaceous plants and grasses such as sea wheat (*Thinopyrum distichum)* occur in this plant zone. The plants trap windblown sand to form small mounds called hummocks which initiate the development of foredunes (Tinley 1985a). Sea wheat grass is native to South Africa and dominantly found along the south-western coast of South Africa. This grass has been used successfully in dune stabilisation (Cowling et al. 1997; Lubke et al. 1997).

The *shrub zone* is situated on more established foredunes, a bit further inland from the strand plant zone. The plant life forms in this zone include annuals, graminoids, geophytes and succulents (Tinley 1985a; DEA 2014). The *scrub thicket zone* is located in the older and more stabilised dunes behind the shrub zone. This stabilised zone consists of dense dwarf shrubs and shrubs with compact canopies (Tinley 1985a). Examples of plants found in this zone are milkwood (*Sideroxylon inerme)* and sea guarri (*Euclea racemosa)* (Tinley 1985a; DEA 2014).

The *thicket or forest zone* occurs on developed older dunes farther away from the sea (Tinley 1985a; DEA 2014). This zone is only found in areas of higher rainfall and well-developed soils (DEA 2014). The thicket or forest zone comprises a climax plant community representing the final stage of succession (Tinley 1985a). The zone is populated by mature closed coastal dune vegetation composed of between 50% and 60% dense trees (Tinley 1985a).

2.3.2 Biogeographical regions of the South African coast

The South African coast is divided into three biogeographical regions (Figure 2.3), namely the cool temperate west coast, warm temperate south coast and subtropical east coast (Brown & Jarman 1978). In the cool temperate west coast region, the climate is semi-arid with extended periods of low to no rainfall interspersed with short flash-rain events. The south-western part of this region experiences a Mediterranean climate dominated by winter rainfall (Brown & Jarman 1978). In the warm temperate south coast region, rainfall is mainly bimodal with peaks in spring and autumn. The (humid) subtropical region along the east coast is dominated by summer rainfall (Davies & Day 1998).

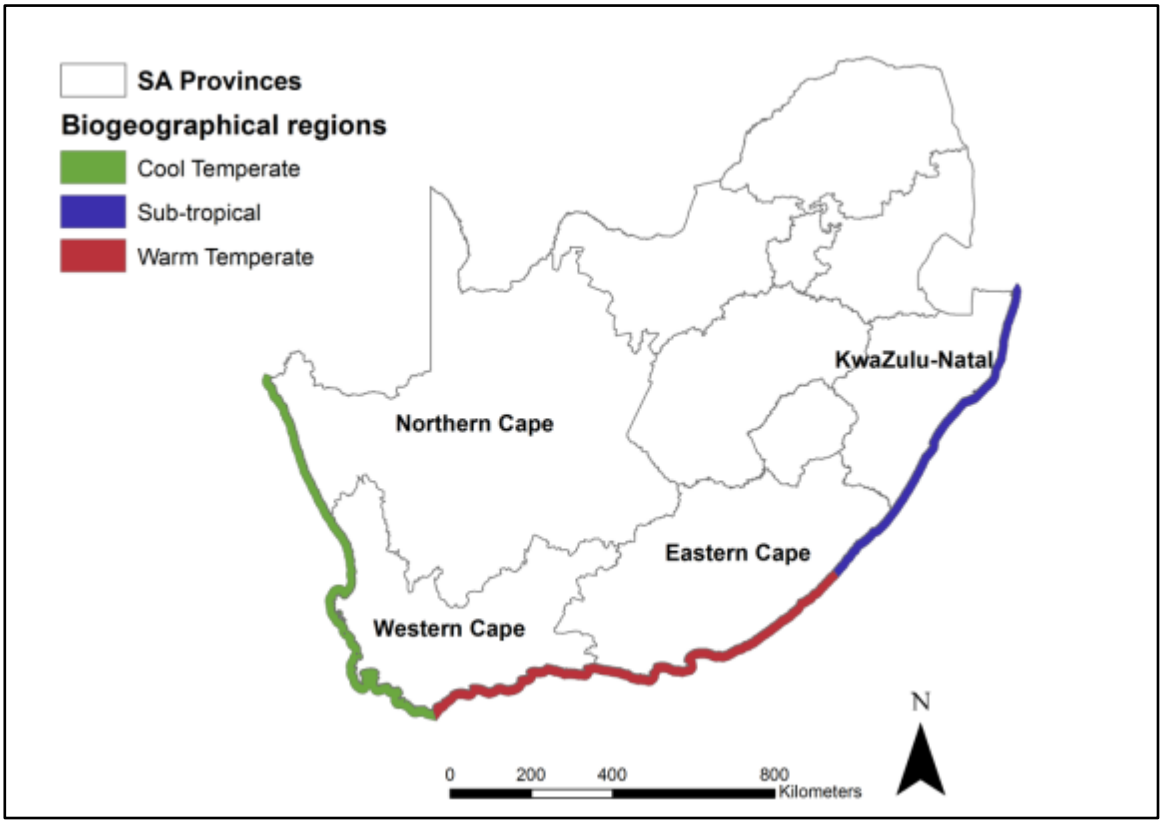

Source: Adapted from DEAT 2008

Figure 2.3 Biogeographical regions of South Africa

Along the coast temperatures are moderated by the influence of the ocean which neither gains nor loses heat as quickly as the land does. As a result temperatures at the shore fluctuate less between high and low as experienced inland (Branch et al. 1994; Zhao et al. 2007). Key oceanographic factors that influence the distribution of terrestrial vegetation are currents, waves and tides (Palmer, Van der Elst &Parak 2011). The oceanographic factors control the presence and adaptability of terrestrial coastal vegetation (Frederisksen et al. 2006). South

Africa's oceanographic patterns are controlled by two major ocean currents, namely the cold Benguela Current which flows northwards along the west coast and the warm south-flowing Agulhas Current along the east and south coasts.

Waves and tides shape the coastline and associated terrestrial coastal vegetation (Palmer, Van der Elst &Parak 2011). The tides control the extent of wave action along the shore (Tinley 1985a) and the state of tides influences the maximum storm level and associated erosion risk at the coast (Barwell 2011). The wave characteristics (e.g. height, length and frequency) determine the presence and type of coastal vegetation along a coastal area (Palmer, Van der Elst &Parak 2011).

2.4 COASTAL VEGETATION TYPES ALONG SOUTH AFRICA'S COASTLINE

The coastal vegetation of South Africa is subdivided into seven regions each comprising characteristic coastal vegetation types (see Figure 2.4) (Lubke et al. 1997). The *West Coast* region extends from Alexander Bay in the north to the Olifants River mouth in the south (see Figure 2.4). The region has low rainfall mainly in winter. Fine grained sandy shores with desert or strandveld vegetation are predominant (Lubke et al. 1997).

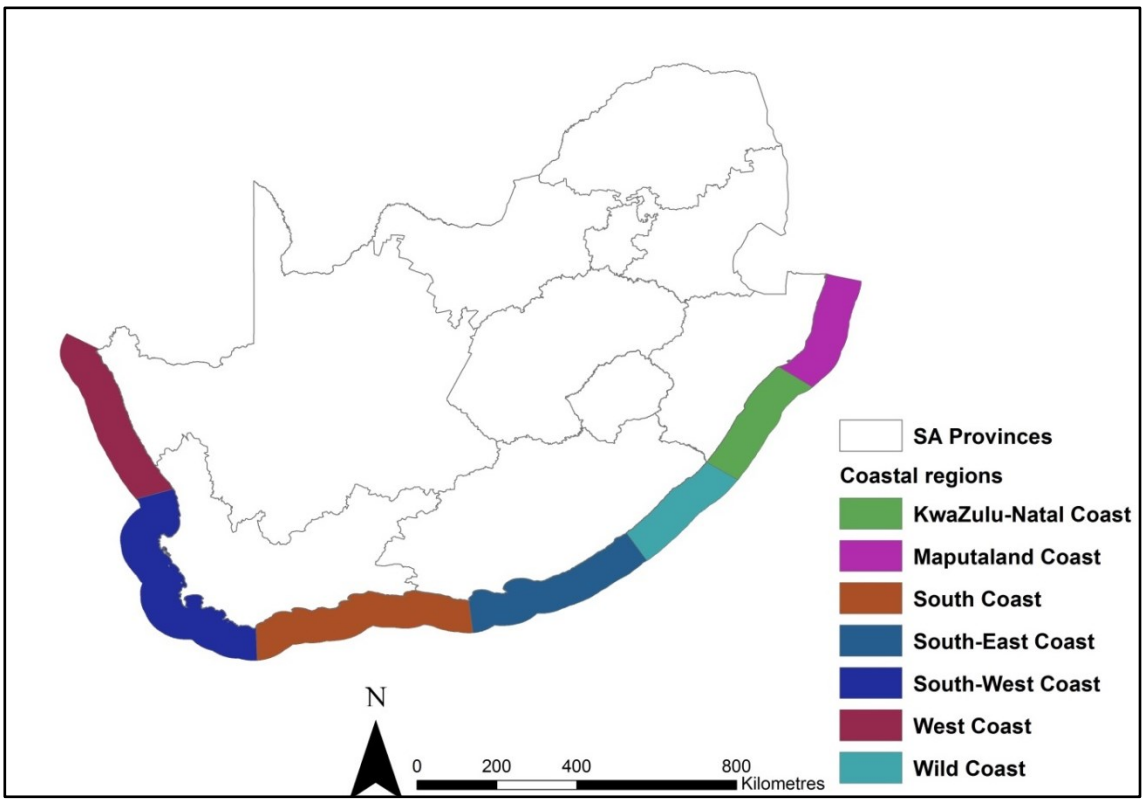

Source: Adapted from Tinley (1985a) and Lubke et al.

Figure 2.4 The coastal vegetation regions of South Africa

The *South West Coast* region extends from the Olifants River Mouth in the north to Cape Agulhas in the south (see Figure 2.4). The region has a cool temperate climate with most of its rainfall in winter (Lubke et al. 1997). This coastal region has fine-grained sandy beaches with exposed rocky shores and it is characterised by fynbos patches, dune thicket vegetation and strandveld (Lubke et al. 1997).

The *South Coast* region extends from Cape Agulhas to Cape St. Francis (see Figure 2.4). The region's warm temperate climate gives rise to all-season rainfall with western parts experiencing mostly winter rainfall (Lubke et al. 1997). This coastal region consists of wave-cut rocky shores and the occasional fine-grained sandy shores (Tinley 1985a). The dune fynbos of the South Coast is characterised by a mosaic of thicket and Afromontane patches (Tinley 1985a).

The *South East Coast* extends from Cape St. Francis to Kei River (see Figure 2.4). The warm temperate climate gives rise to spring, autumn and summer rainfall (Lubke et al. 1997). This region consists of fine-grained sandy shore habitats with dune fynbos vegetation in the western areas and dune thicket with forest vegetation in the eastern parts (Lubke et al. 1997).

The *Wild Coast* region, previously known as the Transkei Coast, extends from Kei River to the Mtamvuna River (see Figure 2.4) (Tinley 1985a; Lubke et al. 1997). The climate in this region is subtropical, characterised by summer rainfall. The Wild Coast has rocky shore habitats and occasional coarse-grained sandy shore habitats. The region's vegetation is characterised by coastal grassland, dune thicket and coastal forests vegetation (Tinley 1985a; Lubke et al. 1997).

The former KwaZulu-Natal coastal region is now subdivided into the KwaZulu-Natal Coast and Maputaland Coast (Lubke et al. 1997). The *KwaZulu-Natal Coast* region stretches from the Mtamvuna River to the Mtunzini River (see Figure 2.4). This coastal region is subtropical, characterised by summer rainfall. It consists of coarse-grained sandy shore habitats and occasionally-exposed headlands. The vegetation is dune thicket and coastal forests such as mangroves (Tinley 1985a; Lubke et al. 1997).

The *Maputaland Coast* extends from the Mtunzini River to Mozambique in the north (see Figure 2.4). Maputaland receives summer rainfall influenced by the subtropical climate. It is characterised by coarse-grained sandy shores and occasionally exposed headlands. The subtropical climate allows lush growth of dune thicket and coastal forest vegetation (Lubke et al. 1997). Tinley (1985b) first described six coastal regions of coastal vegetation, grouping the KwaZulu–Natal and Maputaland regions into one KwaZulu-Natal Coast region which was then

split by Lubke et al. (1997) into two separate regions. The coastal environment is under a lot of pressure mainly caused by humans worldwide. Section 2.5 provides a brief description of the key impacts influencing the intactness of terrestrial coastal vegetation.

2.5 KEY IMPACTS INFLUENCING INTACTNESS OF TERRESTRIAL COASTAL VEGETATION

Coastal environments are among the most productive and valued ecosystems in the world (Constanza et al. 1997). These coastal environments provide services to humans to sustain our well-being. The provision of services involves the benefits people obtain from coastal environments. These benefits include food (fishing), fuelwood, timber, coastal protection (buffer against storms), natural products, energy resources and recreational opportunities (Dayton 2003). Unfortunately, these environments are often heavily degraded by increasing human activity (Millennium Ecosystem Assessment 2005; Dayton 2003). Anthropogenic factors are the main cause of coastal destruction. Loss and degradation of coastal environments occurs through urban development, overgrazing, mining (sand and minerals), pollution (oil spill, dumping, waste disposal), deforestation, informal settlements and introduction of alien invasive species (Constanza et al. 1997).

The consequences of these human activities are erosion and flooding due to the removal of coastal vegetation through inappropriate development along the dune areas and logging of wood (Constanza 1998). The result is that coastal environments can no longer provide their service of coastal protection against storms due to overgrazing and the removal of coastal vegetation that acts as a buffer (Myers 1993; Constanza 1998; Lotze et al. 2006). Mapping and monitoring of coastal environments using field-based assessments is frequently unfeasible, due to the vast extent of the coastline, remoteness or physical inaccessibility. Remote sensing might provide a suitable tool for spatially continuous assessments of the coast.

The loss of vegetation in coastal environments due to human activities has led to an increase in coastal vulnerability. This loss limits the role of coastal vegetation to act as a buffer protecting coastal environments against storms, erosion and wind-blown sand into settlements, habitat loss and fragmentation. Although remote sensing technologies cannot directly reduce the environmental risks, they play an important role in the monitoring and assessment of change and the destruction of coastal environments.

2.6 REMOTE SENSING AND VEGETATION ASSESSMENT

2.6.1 Background

Fischer et al. (1976) describe remote sensing as the acquisition of physical data of an object without direct contact. Lillesand et al. (2008) define remote sensing as "the science of obtaining information on the earth's land and water surfaces, about an object, area, or phenomenon through the analysis of data acquired by a device that is not in contact with object, area, or phenomenon under investigation using electromagnetic radiation."

When electromagnetic radiation hits a surface, some of its energy is absorbed and some is transmitted through the surface and the rest of the energy is reflected back (Ramachandran et al. 1998). Remote sensing is based on the detection of transmitted and reflected electromagnetic radiation by sensors (e.g. cameras and scanners) (Provost et al. 2005). These sensors are attached to platforms (aircrafts and satellites) moving at considerable heights above the earth surface where they record the observations on a suitable medium (Ramachandran et al. 1998). This remotely-sensed data can assist with mapping the present situation, evaluate environmental degradation trends at local and regional scales over time and provide a scientific basis for the management and protection of vegetation (Hantson et al. 2012).

In the past the most commonly used type of remote sensing of the coastal environment had been aerial photographs since the early 1920's (Edwards et al. 2000) as done to map mangroves (Reark & Ross 1975) or changes in the coastline. The major drawback of aerial photography is their limited area of coverage (Friel & Haddad 1992, Mumby et al. 1997). For example, if the area of interest is large the use of aerial photographs is prohibitively expensive (Friel & Haddad 1992, Mumby et al. 1997). Since the launch of Landsat in 1972 remote sensing of coastal areas has proliferated in the 1980s (Edwards et al. 2000) when it was widely used to detect change in coastal environments and for environmental-sensitivity mapping. Other applications are mapping of mangrove areas sensitive to oil spills and the extent of mangrove deforestation, assessment of coastal resources such as salt marshes, coral reefs, mangroves and coastal wetlands, and mapping of boundaries of coastal management zones and aquaculture activities in coastal habitats. The application of coastal remote sensing has been done using different satellites covering areas of interest at regional scale with different spatial, spectral and temporal resolutions such as Landsat Thematic Mapper (TM), Landsat Multispectral Scanner System (MSS) and French Systeme Pour Observation de la Terre (SPOT

XS) (Kenchington & Claasen 1988; Ibrahim & Yosuh 1992; Biňa et al. 1980; Green et al.1997; Loubersac & Populus. 1986).

The application of remote sensing in coastal environments has limitations, the most common being cloud infestation in the images and the turbidity of the coastal waters. In the past the cost of obtaining multiple sets of imagery was high but Landsat imagery is now available at no cost. Most early studies used Landsat images with a medium spatial resolution that gave satisfactory results, but more recently images with high spatial resolution (i.e. WV-2 and IKONOS) for coastal environments are yielding good results in mapping saltmarshes (Wang 2010; McCarthy & Halls 2014). Limitations vary with the use of different sensors where the spatial or spectral resolutions can be too coarse and the temporal resolution too infrequent. Ultimately the suitability depends on the nature of the research problem (Edwards et al. 2000).

2.7 Selection of appropriate sensor resolution

The selection of the appropriate sensor for coastal remote sensing calls for careful consideration of a range of factors relating to spatial, spectral and temporal resolution. These are discussed in the following subsections.

2.7.1.1 Spatial resolution

Spatial resolution is the minimum distance between two objects that a sensor can record (Fischer et al. 1976). Spatial resolution determines the level of detail visible in a satellite image (Gao 1999; Campbell 2006). The higher the spatial resolution of an image, the greater is the visual interpretability (Gao 1999; Nagendra 2001). Therefore, the level of detail required in specific study determines whether fine or coarse spatial resolution imagery is required (Hengl 2006). Cho et al. (2015), for example, used high spatial resolution imagery to identify and map gaps in the tree canopy and pathways in a terrestrial coastal environment.

The first earth-observation satellite launched was Corona in 1960 which used a KH-1 camera with a resolution of 7.5m (Campbell 2011). Subsequently in 1972, Landsat was launched with a medium spatial resolution of 30 m and the imagery has been widely used in mapping and assessing land-cover changes at a regional to global scale. It is currently available at no cost. High-resolution satellite imagery from IKONOS (launched 1999), Quick Bird (launched 2001) and WorldView-2 (launched 2008), is available at 2-m to a 5-m resolution at least and it is used for mapping at regional to local scales (Boyle et al. 2014). Although the high spatial resolution satellite imagery is not free it outperforms medium-resolution (Landsat) imagery by capturing

small habitat patches and its ability to detect forest disturbance and degradation (selective logging) and coastal degradation features (Cho et al. 2015; Mahlalela 2013).

Medium spatial resolutions of satellite imagery such as SPOT 4 with a 20-m pixel size and moderate resolution imaging spectrometer (MODIS) with a pixel size of 250 m to a 1 km have been widely used to map land cover at regional scale (Xie et al. 2008). Studies by Lopez-Portillo & Ezcurra (2008) and Gao (1999) used SPOT data to accurately map mangrove degradation and the impacts of flooding along coastal environments.

2.7.1.2 Spectral resolution

Al-Wassai & Kalyankar (1999), Gao (1999) and Lefsky & Cohen (2001) define spectral resolution as the dimension and number of specific wavelength intervals of a sensor in the electromagnetic spectrum. Spectral resolution denotes the number of spectral bands in which a sensor can collect reflected radiance and the width of the bands in the electromagnetic spectrum. A higher spectral resolution results in a narrower bandwidth. Low spectral resolution ranges from four to eight bands called multispectral imagery and a higher spectral resolution of bands in hundreds is referred to as hyperspectral imagery (Al-Wassai & Kalyankar1999; Campbell 2006). The disadvantage of most high spatial resolution satellite images such as RapidEye, IKONOS and QuickBird is poor spectral resolution, but this does not apply to WV-2 with eight spectral bands. Even though the spatial resolution is high the spectral capabilities of RapidEye and SPOT 5 imagery are limited (Carleer et al. 2004).

2.7.1.3 Temporal resolution

Lefsky & Cohen (2001) see temporal resolution as the time taken by the satellite sensor to complete one orbit cycle and obtain imagery in a certain area. For example, the Landsat satellites view the same area of the world every 16 days. The Landsat sensors are regarded as having low temporal resolution because of the greater number of days they take to revisit an area (Lefsky & Cohen 2001). The French Systeme Pour Observation de la Terre (SPOT 5) sensor is regarded as a high temporal sensor thank to just three days taken to revisit the same area (Al-Wassai & Kalyankar 1999). Oetter et al. (2001) used SPOT 5 satellite images recorded in the same season to detect change in forest structure and biomass. By using multi-date Landsat 7 ETM+ imagery with low temporal resolution, De Colstoun et al. (2003) successfully discriminated natural vegetation in terrestrial coastal habitats.

2.7.2 Examples of mapping of remote sensing coastal degradation

Coastal degradation occurs through human activities such as trampling, pollution, waste disposal, agriculture, mining, deforestation (mangroves) and coastal urban development. The application of remote sensing in this space helps map and monitor the degradation of coastal environments (Nayak 2004).

2.7.2.1 Very high spatial resolution sensors

Very-high resolution sensors such as WV-2, IKONOS and QuickBird can be used to identify and map fine-scale changes in the coastal environment (McCarthy & Halls 2014). All three mentioned sensors were used to map coastal habitat change over a year on Barrier Island in 2014. All the sensors yield good results (McCarthy & Halls 2014). QuickBird was used to map the erosion and disappearing of salt marshes in Jamaica Bay in 2002 (Wang 2010). IKONOS was used to map the deforestation of mangroves in the Caribbean coast of Panama in 2004 (Wang 2010).

2.7.2.2 Medium spatial resolution sensors

Landsat imagery has the longest history of use for monitoring the earth's surface in coastal environments (Nayak 2004). In the 1980s Landsat Thematic Mapper (TM) and SPOT XS were used to distinguish mangroves from adjacent thorn scrub in the Turks and Caicos Island (Ranganath et al. 1989). Biňa et al. 1980 used Landsat Multispectral Scanner System (MSS) in a change-detection study to monitor the clearance of mangroves in the Philippines. Ibrahim & Yosuh (1992) used Landsat to map the impact of deforestation on mangroves in Pulau Redang Marine Park in Malaysia and it was applied to monitor aqua-cultural activities in mangrove forests in the Gulf of Nicoya, Costa Rica (Kapetsky et al. 1990; Loubersac & Populus. 1986).

In the year 2001 Landsat was used to map the destruction of mangroves through deforestation in India (Nayak & Bahuguna 2001). Landsat 7 ETM+ and SPOT 5 were used in combination in South Africa's coastal region to assess the status of the ecosystem (Lück-Vogel, O'Farrell & Roberts 2013). Osei, Merem & Twumasi (2013) used Landsat TM to map the influence of urban development on mangroves in the Nigerian coast. A study in Kenya mapped the impact of coastal development on mangroves using SPOT 5 (Bosire et al. 2014).

2.7.2.3 LiDAR

The light detection and ranging (LiDAR) system is an active sensor that is able to measure surface height and vegetation structure (Campbell 2011). Because it is an active sensor LiDAR does not depend on natural sunlight (Froese & Mei 2008). LiDAR is put to use for various research and commercial purposes. For example, it has been used in coastal environments to map different types of coastal degradation (Wang 2010) and a study of the Norfolk Coast in Great Britain erosion and landslides were monitored (Lee. 2001). Moreover LiDAR was used to assess the impacts of mining on the West Coast of South Africa (Mpe 2015) and to map human-induced changes in coastal wetlands and salt marshes in northern California due to waste disposal (Wang 2010). Further, Lück-Vogel et al. (2016) used LiDAR in combination with high-resolution multispectral satellite imagery to classify coastal and estuarine vegetation in St Lucia.

2.7.3 Classification methods applied in vegetation mapping

Image classification uses the spectral information contained within spectral bands by grouping pixels into different classes (Campbell 2011; Perumal & Bhaskaran 2010). Pixel-based and object-based classification methods apply supervised and unsupervised classification techniques where supervised classifying involves prior knowledge of land cover. The most commonly used supervised classification algorithms are maximum likelihood, parallelepiped and minimum distance classifiers used with multispectral and hyperspectral data sets respectively (Oldeland et al. 2010). Maximum likelihood uses training data to calculate the probability of a given pixel by estimating the mean and variance and then assigning the pixel to the class that it most probably belongs to (Liu & Xia 2010; Lu & Weng 2007; Perumal & Bhaskaran 2010). This algorithm calculates the probability through assuming that the data are normally distributed. Vegetation mapping using remotely sensed images yields better results from supervised classification using samples of known identity such as pixels assigned to informational classes to classify pixels of unknown identity than by unsupervised classification (Zak & Cabido 2002). Supervised classification considers manual identification of a number of areas that are representative for the different classes desired; these are known as training areas (Campbell 2002; Perumal & Bhaskaran 2010). Selection of suitable training areas is essential to instruct the classifier to identify and recognise different classes for classification (Campbell 2002, 2011; Gao et al. 2006; Perumal & Bhaskaran 2010).

Apart from the former stated classifier for land cover identification, there is a method used for classification of remote sensing data called decision tree classification (DTC). DTC originates from machine learning theory. It is regarded an efficient method for solving classification and regression difficulties (De Colstoun et al. 2003; Xu et al. 2005; Zhu et al. 2006). It is based on a hierarchical structure similar to that one of a tree shown in Section 3.4.4. DTC uses continuous data or variables and is regarded as more accurate classification for remote sensing data either using low or high spatial resolution data (Huang et al. 2002). The DTC comprises of nodes and internal nodes that contain the data to derive the classification. The accuracy of the DTC can be assessed using an error matrix (Xu et al. 2005; Campbell 2007).

2.7.3.1 Pixel-based classification

Pixel-based classification is a traditional method based on classifying individual pixels using supervised and unsupervised classification (Liu & Xia 2010; Gao et al. 2006). However, traditional pixel-based classifications based on spectral dissimilarities are not suited to discriminate vegetation species with similar spectral responses. Another problem is that the classification results obtained from pixel-based methods frequently have a salt and pepper effect (Rapinel et al. 2014). The salt-and-pepper effects related to vegetation heterogeneity can be resolved by applying a filtering algorithm on the classification (Rapinel et al. 2014).

2.7.3.2 Object-based classification

Object-based classification is a method that groups pixels into spectrally-homogenous objects through image segmentation and then classifies the individual objects (Gao et al. 2006; Liu & Xia 2010; Campbell 2011). Object-based classification is based on information derived from a set of similar pixels called objects in the image (Syvitski et al. 2002). Image segmentation enables the additional use of various attributes such as shape, colour, size, texture and contextual information to analyse the image objects (Darwish et al. 2003; Syvitski et al. 2002). The performance of object-based classification relies on the quality of the image segments and the accuracy of the segmentation process.

The object-based approach has advantages over the pixel-based approach in two respects. First, the change of classification units from pixels to image objects reduces within-class spectral variation and minimises salt-and-pepper effects that occur in pixel-based classification. Secondly, a large set of features characterising the object's spatial, textural and contextual properties can be derived as complementary information to the direct spectral observations so improving classification accuracy (Gao et al. 2006). Several studies have adopted the object-

based method to monitor vegetation condition and change over time in terrestrial and coastal environments (Blaschke 2004; Gao 2006; 2011; Cho et al. 2015; Lück-Vogel, O'Farrell & Roberts 2013). The study conducted by Lück-Vogel, O'Farrell & Roberts (2013), used an object-based method for assessing the habitat state or the natural vegetation intactness, using segmented multispectral medium spatial resolution satellite imagery. The approach was based on the spectral (brightness), structural (compactness) as well as textural (NIR standard deviation) land cover features. The premises used in Lück-Vogel, O'Farrell & Roberts (2013) are further discussed in Section 3.4.2. The approach yielding sufficient results with an overall accuracy of 76% using Landsat and 70 to 80% for SPOT 5, depending on the habitat type. Lück-Vogel, O'Farrell & Roberts (2013) described the approach as basis for further development to be adopted and modified depending on the respective land cover and land use features.

Whichever method is chosen, there are always limitations. In object-based classification the limitations include errors that occur when performing segmentation either by over-segmentation or under-segmentation (Moller et al. 2007; Kampouraki et al. 2008). The limitations of pixel-based classification are within-class spectral variation, mixed pixels and the salt-and -pepper effect (Liu & Xia 2010). Other methods used for mapping vegetation include a hybrid approach that uses both pixel-based and object-based methods. An example is a study of the French Atlantic coastline using a hybrid method to map the condition of coastal vegetation (Rapinel et al. 2014).

2.7.3.3 Vegetation indices

The ability to measure biomass and vegetative energy by combining two or more spectral bands has been exercised in various ecological studies (Jackson & Huete1991; Jensen 1996; Chaudhury 1990; Campbell 2011). Studies such as that of Pettorelli et al. (2005) have measured the intensity of light reflected off the earth in visible and near-infrared (NIR) wavelengths and quantified the photosynthetic capacity of vegetation in a given pixel of land surface. If the reflected radiation in near-infrared wavelength is much higher than in the visible wavelengths, the vegetation in that pixel is dense and may contain some type of forest vegetation. If there is a little more radiation in the near-infrared than in the red wavelength reflected, the vegetation is probably sparse and may consist of grassland, tundra or desert. Healthy vegetation tends to absorb more visible light due to the chlorophyll in the leaves and reflects greater amounts of NIR energy due to mesophyllic leaf structure and unhealthy

vegetation or sparse vegetation reflecting more visible light and less infrared (Holme et al. 1987). Vegetation indices use a variety of formulas to quantify the density of plant growth and health on earth.

The Normalized Difference Vegetation Index (NDVI) is a frequently applied vegetation index (Jensen 2007; Du Plessis 1999) which uses the red and NIR bands of a sensor. It is employed to assess to which degree the target observed contains live green vegetation (Jackson &Huete 1991). NDVI was first used by Rouse et al. (1973) of the Remote Sensing Centre of Texas University (Jackson & Huete 1991) to study vegetation biomass. NDVI is routinely used as a vegetation index in ecological and conservation studies (Pettorelli et al. 2005). NDVI is a reliable correlative measure for vegetation vigour and functions in a range of diverse ecosystems (Running 1990). NDVI values range from -1.0 to 1.0, where values below zero represent vegetation absence and values above 0.5 represent dense vegetation and much lower values represent inundated areas (Pettorelli et al. 2005; Guerschman et al. 2009). The formula for NDVI is:

$$NDVI = \frac{(NIR - RED)}{(NIR + RED)}$$

NIR is near-infrared and RED is visible red bands (Jackson et al. 1991). NDVI was used by Shalaby & Tateishi (2007) and Nagendra & Rocchini (2008) to assess vegetation health in ecological studies conducted in both terrestrial and coastal habitats. Other studies have shown NDVI to be a good predictor of disturbances to land cover caused by fire drought (Singh, Roy & Kogan 2003) and floods (Wang 2010). Despite the usefulness of NDVI in ecological studies, it has a limitation. NDVI saturates at high biomass, especially in temperate and tropical forests (Huete et al. 2006).

2.8 CONCLUSION

The review has shown that the attributes of different types of image resolutions are key considerations in coastal vegetation mapping (Rapinel et al. 2014). High spatial resolution has been the choice in mapping coastal vegetation in many contexts. However, not all high spatial resolution images have sufficient spectral resolution (Rapinel et al. 2014). Although satellite images such IKONOS at 3 m and QuickBird at 2 m provide high spatial resolutions, they do not possess high spectral resolution. IKONOS images are for example, only provide four spectral bands, namely blue, green, red and near infrared.

Among the very-high spatial resolution sensors, only WV-2 provides both high spatial resolution at 2 m and high spectral resolution with eight spectral bands. WV-2 has been used to map coastal terrestrial vegetation in European studies with good results (Al-Wassai & Kalyankar 1999). Object-based methods are used for classification because of more contextual information on degradation (Marangoz et al. 2009). An efficient and cost-effective method that is object-based has been applied successfully in South Africa to assess habitat intactness (Lück-Vogel, O'Farrell & Roberts 2013). In the light of the successfulness of this method and given the lessons learnt and the insights gained from the literature review, this study investigated the suitability of WV-2 as an efficient tool to assess the intactness of terrestrial coastal vegetation for local management in South Africa. The next chapter provides description of the study and methods used in the study to obtain final results.

CHAPTER 3. RESEARCH METHODS

Chapter 3 provides the outline of methods used in the study as well as the description of the study area with its associated vegetation. A brief description of the input data and its sourcing is included. The data went through pre-processing steps preparing it for further analysis. The analysis of data was followed by an accuracy assessment performed on the derived HII classification.

3.1 STUDY AREA

3.1.1 Selection of the study area

False Bay (FB) was selected as a study area for four reasons. First, FB has a relatively accessible coastal environment for collecting data in the field. Second, given the study's aim of assessing degradation of coastal vegetation, FB is a prime case of coastal environment activities. Third, activities involve some land-use types and alien plants that pose threats to existing areas of pristineness, so providing special interest for investigation. Last, satellite imagery the principal source of data, is available for the study area.

3.1.2 Description of the study area

The area under study is situated in False Bay which is a large, partly protected bay (Figure 3.1-A), situated south of Cape Town in the Western Cape Province of South Africa (Theron & Schoones 2007). The study area extends from Muizenberg to Strand and is surrounded by one of South Africa's fast growing townships called Khayelitsha. The study area extends between 34º04'and 34º23' South and 18º26' and 18º52' East and measures about 35 km by 35 km. False Bay is flanked by two mountain ranges namely the Peninsula mountain chain on the western and the Hottentots Holland Mountains on the eastern side (Spargo 1991).

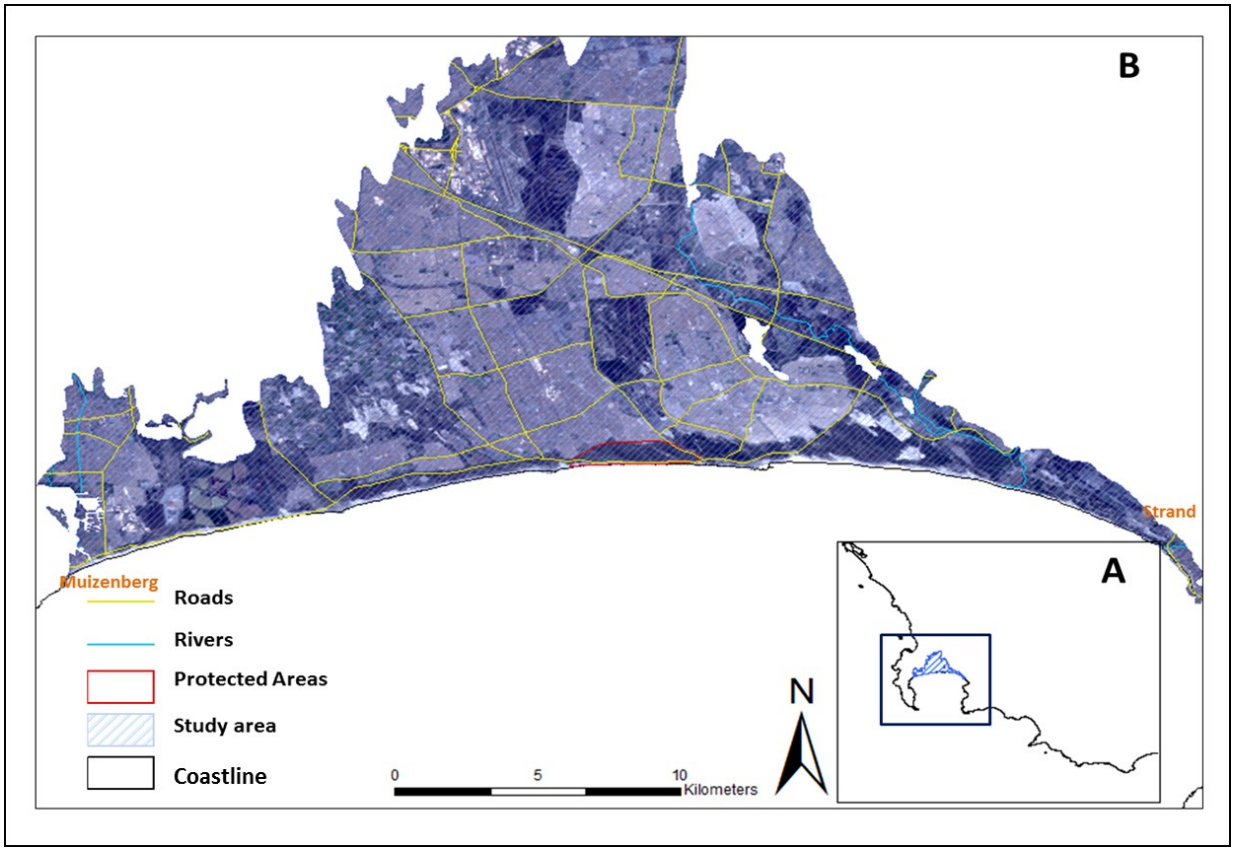

Figure 3.1 Study area: A is the position of the study in the Western Cape; B is the study area on Landsat 8 satellite imagery with band combination R-G-B: bands 5-3-2 (Near Infrared-Green-Blue).

3.1.3 Physical Environment

3.1.3.1 Geology and Soils

The False Bay geology comprises five rock types, namely Greywacke of the Malmesbury Group (MG), Granite of the Cape Granite group, Quartzite of the Table Mountain Group (TMG), Siltstone of the Bokkeveld Group and Limestone of the Cenozoic Cover (Du Plessis & Glass 1991). On western side of False Bay are rocky outcrops of the TMG. The northern part of the Bay is relatively flat with fine sand and the eastern side features rocky outcrops of the MG (Du Plessis & Glass 1991). The study area shown in Figure 3.1 has of two types of soils namely limestone and sandy soil (Du Plessis & Glass 1991).

3.1.3.2 Climate

The southwestern Cape has a different climate from the rest of South Africa. FB has a Mediterranean climate with dry, hot summers from October to March and wet cold winters from April to September (Clark et al. 1996). The minimum and maximum average temperatures in summer are 18ºC and 23ºC respectively. The minimum and maximum average temperature in winter ranges from 11ºC to 15ºC. Figure 3.2 shows a climate diagram of Cape Town with a dry season from October to March.

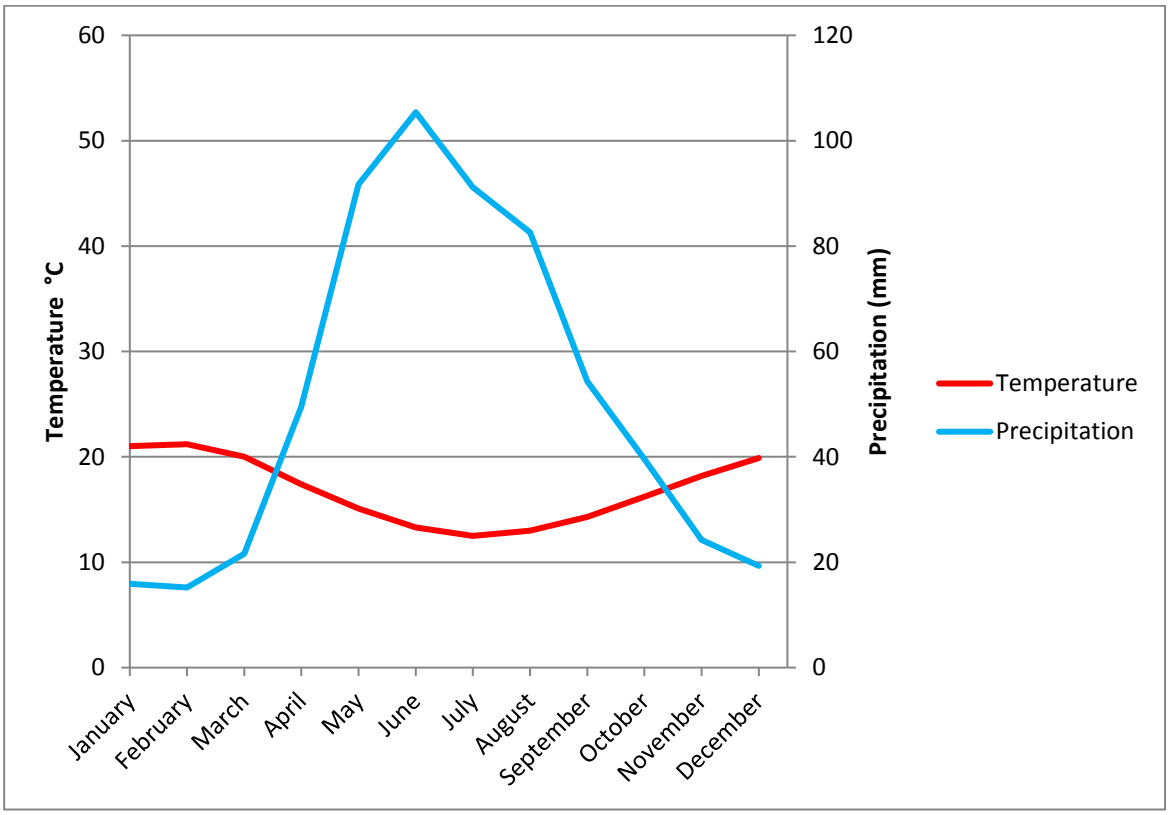

Figure 3.2 Climate diagram of Cape Town with monthly average precipitation and average temperature. Designed by author from data at http://cdnisclimategraphs.blogspot.com.

3.1.4 Coastal vegetation types of northern False Bay

FB has many types of vegetation but this study is focused on the northern part extending from Muizenberg to Strand where the main coastal vegetation is Cape Flats Dune Strandveld (CFDS) shown in Figure 3.3 (Mucina & Rutherford 2006). Further description of the CFDS coastal vegetation is discussed below.

3.1.4.1 Cape Flats Dune Strandveld

Strandveld is an Afrikaans word meaning beach vegetation (Mucina & Rutherford 2006). CFDS vegetation occurs along the Cape West Coast, Cape Flats to the north of False Bay and between Gordon's Bay and Muizenburg including Macassar and Monwabisi (Figure 3.3). At the Cape Flats, CFDS reaches as far inland as north of Bellville, Silverstroomstrand-Table Bay, Atlantis dune plume and small pockets on Cape Peninsula and Robben Island. The study is focused on the CFDS occurring in the Macassar and Monwabisi area. Figure 3.3 shows CFDS in Wolfgat Nature Reserve found in the Monwabisi area.

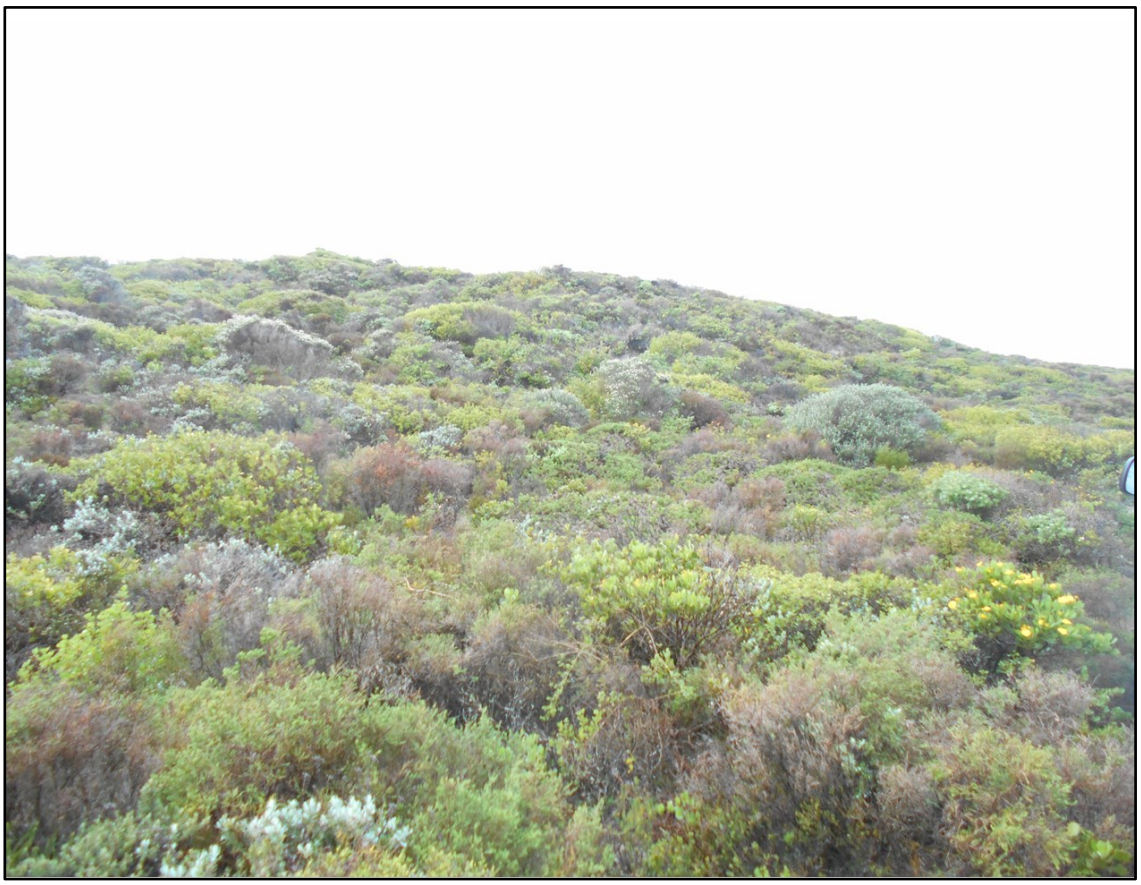

Figure 3.3 Strandveld vegetation in Wolfgat Nature reserve

This type of vegetation grows in deep and well-drained sand along the coast. The sand has a high pH originating from ground seashells which are rich in calcium making the sand alkaline (Mucina & Rutherford 2006; Holmes et al. 2012). Strandveld vegetation grows in habitats under the direct influences of salt spray and other factors associated with seawater, therefore coastal vegetation is azonal (Mucina & Rutherford 2006). Azonal vegetation is vegetation less determined by certain climate conditions, rather by soil types, salt spray and habitats formed in and around stagnant waterbodies exposed to flooding that give rise to the formation of special

soils (Mucina & Rutherford 2006). Strandveld vegetation such as CFDS differs from fynbos and renosterveld in structure, composition and functioning (Holmes et al. 2012; Mucina & Rutherford 2006). Strandveld does not burn easily due to its succulence (high water content). Moreover, Strandveld is not fire dependent for its persistence, as the case of fynbos (Mucina & Rutherford 2006; Holmes et al. 2012).

The Strandveld has tertiary or recent calcareous sands of marine origin mainly blown in as sand dunes. These cover various rock types, but mainly the Tygerberg Formation of the Malmesbury Group. Outcrops of limestone from the Sandveld Group occur at Silwerstroomstrand, on the Cape Peninsula and in the Macassar-Wolfgat area.

The climate of the Strandveld has a winter-rainfall regime, with rainfall peaking from May to August, and varying from an average of 350 mm per annum at Atlantis to 560 mm at Gordon's Bay. The mean daily maximum temperature is 26.7°C in February and the mean daily minimum is 7.5°C in July (Holmes et al. 2012). Strandveld vegetation comprises tall, evergreen, hard-leaved shrubland with abundant grasses and annual herbs growing in a flat to slightly undulating landscape such as dunes (Mucina & Rutherford 2006).

Figure 3.4 is a typical profile of zonation of coastal vegetation in a terrestrial coastal habitat. The vegetation profile starts at the foredunes consisting of pioneer vegetation which acts as a buffer for terrestrial coastal habitats against wind and wave impact. The Strandveld grows from sparse vegetation along the foredunes to dense shrubs and trees at the backdunes which are the old stabilised dunes.

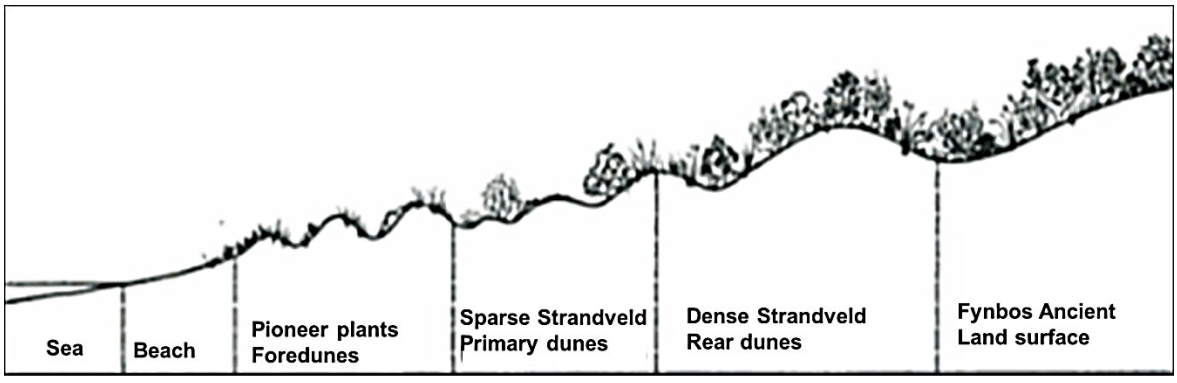

Source: Adapted from Lubke et al. 1997

Figure 3.4 Vegetation zonation in a terrestrial coastal habitat

Typically, Strandveld plants include plants such as Bietou (*Chrysanthemoides monilifera*), Candelabra Lily (*Brunsvigia orientalis*), Sour fig (*Carpobrotus edulis*) and occasional dense

Milkwood (*Sideroxylon inerme*) forest like those that occurred historically in Noordhoek, Olifantsbos and Macassar, and presently found in Nature's Valley Gordon's Bay (

Figure 3.5).

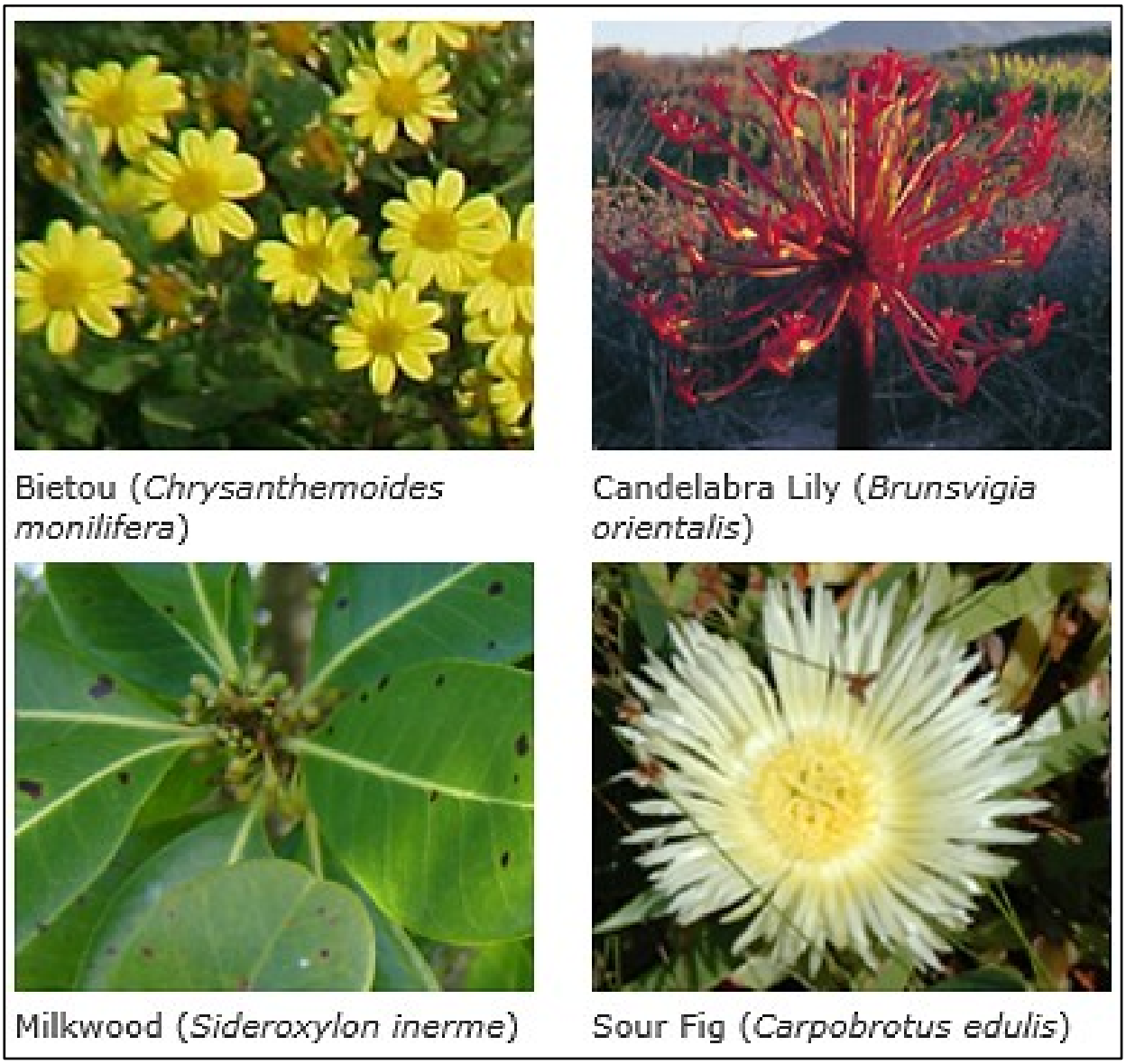

Source: Adapted from Mucina & Rutherford (2006)

Figure 3.5 Strandveld plants

According to Mucina & Rutherford (2006) and Holmes et al. (2012), Strandveld is highly endangered by the invasion of alien plants such as *Acacia cyclops* (Rooikrans) and *Acacia saligna* (Port Jackson wattle), mining, trampling, urban sprawl and coastal development. Yet only 19% of the vegetation is conserved and 51% has already been transformed (Figure 3.6).

The benefit of CFDS is that it provides the communities with ecosystem services such as coastal protection, flood attenuation, recreational space, tourism opportunities, and opportunities for educational programmes, furniture and firewood (Holmes et al. 2012).

3.1.5 Human induced impacts in the study area

The northern FB area (Monwabisi, Wolfgat Nature Reserve and Macassar dune system) is heavily subjected to the influences of human activities that detrimentally affect the surrounding environment. The area comprises dune systems that help to shelter Khayelitsha from flooding and erosion. Khayelitsha's total population in 2011 was greater than 391 700 and continues to grow (Spargo 1991).The detrimental human activities and creations in the area of interest are:

- Informal footpaths
- Illegal woodcutting (selective logging)
- Illegal sand mining
- Informal settlements
- Alien invasive plants
- Overgrazing
- Bush fires
- Illegal waste disposal

The observed human activities in the study area have slow but detrimental effects on coastal intactness. Bush fires are frequent hazards in this coastal environment, especially in areas with a high incidence of *Acacia cyclops* (Rooikrans) invasion. Rooikrans is the dominant alien plant in the study area, although *Acacia saligna* (Port Jackson) invasions are another cause for concern.

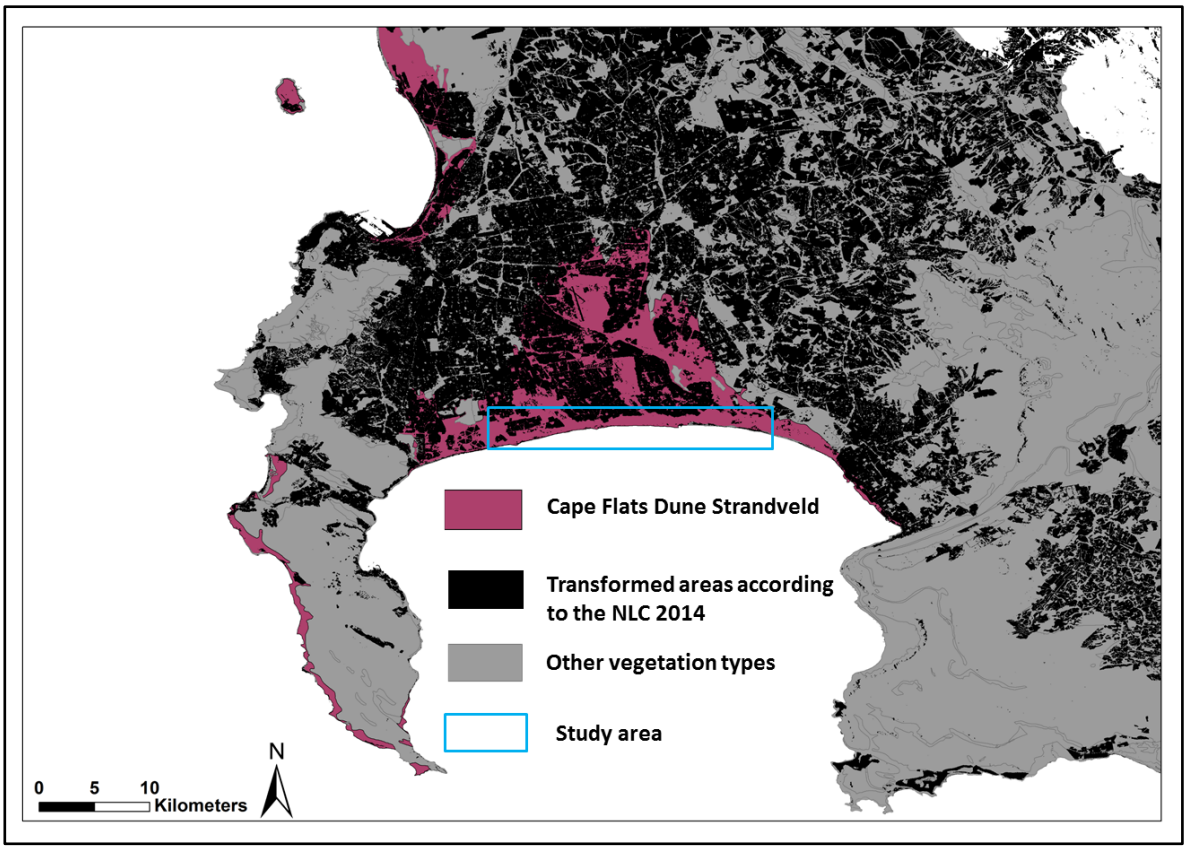

Figure 3.6 Remaining CFDS and transformed areas. (CoCT 2015)

The coastal environment is put under much pressure from human-induced impacts. Figure 3.6 shows the transformed areas and the remaining CFDS vegetation in the study area. This map was derived using the National Land Cover (NLC) of 2014 from the CoCT. The following section describes the input data and methodology used to derived the HII.

3.2 INPUT DATA

3.2.1 Satellite data WorldView-2

The main input data consist of WV-2 satellite images. The WV-2 sensor was launched in October 2009 (see Table 3.1). WV-2 is a Digital Globe owned commercial high-resolution satellite image with eight spectral bands. WV-2 has four standard bands (i.e. blue, green, red, near-infrared1) and four new bands (i.e. coastal, yellow, red edge and near-infrared2). The multispectral bands of the WV-2 image have a 2 m spatial resolution and a temporal resolution (revisit time) of 1 to 2 days. WV-2 has a 16-bit data range which means the image potentially has 65 536 grey values.

WV-2 level 3A data were acquired from the South African National Space Agency (SANSA). Level 3A data means that the images are geometrically corrected and orthorectified. The projection used in orthorectification of the images is Universal Transverse Mercator (UTM) zone 34 south. Radiometric correction was not performed by SANSA.

Table 3.1 Characteristics of the WV-2 sensor

Data	**WorldView-2**		**Spatial resolution**
Band-width interval (micrometres)	**Band**	**µm**	2 m
	1 Coastal	0.4-0.45	
	2 Blue	0.45-0.51	
	3 Green	0.51-0.58	
	4 Yellow	0.58-0.63	
	5 Red	0.63-0.69	
	6 Red Edge	0.70-0.74	
	7 NIR1	0.77-0.89	
	8 NIR2	0.89-1.04	
	Pan	0.45-0.80	0.6 m
Radiometric resolution (bit)	16 bit		
Temporal resolution (days)	1-2 days		
Swath width (km)	16.4 km		

Two WV-2 images from the 25 February 2014 and 11 October 2014 were used in the study for the assessment of terrestrial coastal vegetation degradation. The input images were acquired in a tile format. The February image was provided in five individual tiles, and the October image in six individual tiles. The names of the respective tiles are listed in Table 3.2.

Table 3.2 Image tiles of WV-2 per acquisition date

Acquisition date (WV-2)	Tile name
25 February 2014	14FEB25091310-M2AS_R1C1-054626232010_01_p002.tif 14FEB25091310-M2AS_R1C2-054626232010_01_p002.tif 14FEB25091310-M2AS_R2C1-054626232010_01_p002.tif 14FEB25091310-M2AS_R2C2-054626232010_01_p002.tif 14FEB25091310-M2AS_R2C3-054626232010_01_p002.tif
11 October 2014	14OCT11090443-M2AS_R1_C1-054626232010_01_p001.tif 14OCT11090443-M2AS_R1_C2-054626232010_01_p001.tif 14OCT11090443-M2AS_R1_C3-054626232010_01_p001.tif 14OCT11090443-M2AS_R2_C1-054626232010_01_p001.tif 14OCT11090443-M2AS_R2_C2-054626232010_01_p001.tif 14OCT11090443-M2AS_R2_C3-054626232010_01_p001.tif

Further pre-processing was performed on the image tiles as described in Section 3.3.1.1 below.

3.2.2 Biodiversity network data

The data were also acquired from the CoCT. The data consists of a biodiversity network which provides the subtypes of vegetation in FB such as vegetation growing on limestone and sand. Ancillary data used are habitat condition layer containing different grading. The habitat conditions vary from poor to high. Ancillary data used in the study are in an Environmental Systems Research Institute (ESRI) shapefile format. The data were used for pre-processing the satellite imagery including masking out transformed areas (built-up areas and roads) that are not of immediate interest to the study.

3.2.3 LiDAR data

A LiDAR derived Digital Surface Model (DSM) was acquired from the CoCT that contains the elevation of the area of interest. The DSM acquired from CoCT was pre-processed for the validation of results. Additional data from CoCT, namely biodiversity network and habitat condition were pre-processed to improve the quality of the data.

3.2.4 Field Data

Field reference data were collected in the field to validate the accuracy of remote sensing results in the study. Two field visits were conducted as mentioned in section 3.1 for training and validation as referred to in section 3.4.5.2.

3.2.4.1 Reference data of field-informed random points

A total of 180 field-informed random points were collected in the field. The points were collected based on observations made in the field. The points were collected according to the habitat condition classes observed in the field using WV-2 for visual observation shown in Figure 3.7. Twenty random points were collected per class. The points were later arranged into levels of intactness used for training and validation and as indictors of intactness. A further discussion about the eight field classes is to be found in section 3.4.5.1. The field points in geographical co-ordinates were captured using a GPS and later converted into a shapefile (.shp) to allow for further processing of the data.

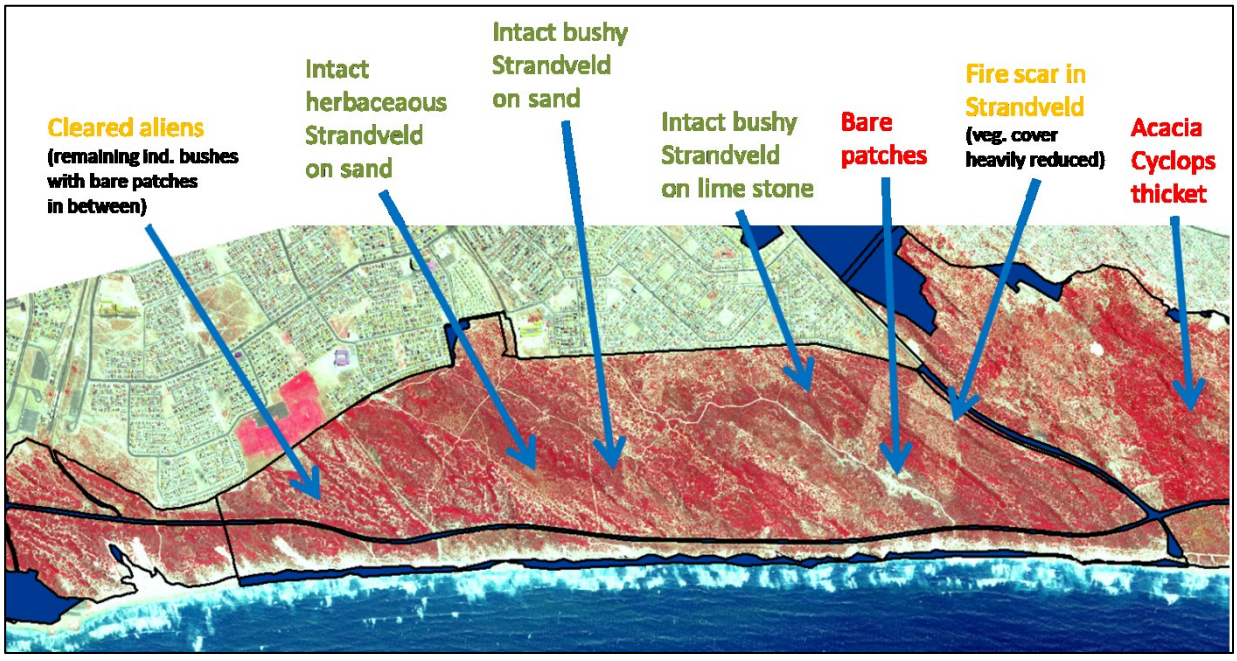

Figure 3.7 Field-informed classes

The points were collected randomly in areas that are accessible. The data was split into training and reference data.

3.3 SATELLITE DATA PRE-PROCESSING

3.3.1 Image pre-processing

Pre-processing of satellite images is an important step prior to image analysis. When satellite images are captured they contain geometric and radiometric distortions. Therefore, it is essential to remove this noise to increase the interpretability of the satellite images. To improve the satellite image quality several pre-processing steps have to be performed before further analysis of the images (Campbell 2011). They are image mosaicking, radiometric correction, subsetting and masking. They are treated in the next section.

3.3.1.1 Mosaicking of satellite imagery

Image mosaicking is the combining of multiple image tiles into one image (Capel 2001). WV-2 images of the two dates (25 February 2014 and 11 October 2014) were used in the study. Both images came in a number of tiles as shown in Table 3.2. The WV-2 image tiles were mosaicked per acquisition date to enhance further processing. Mosaicking on the WV-2 image tiles was performed using ERDAS IMAGINE 2014 (version 14.0) mosaic tool resulting in one image composite per date.

3.3.1.2 Radiometric correction

The mosaicked images were radiometrically corrected. The radiance measured in $W \cdot m^{-2} \cdot sr^{-1}$ by the sensor is stored in the images as digital numbers (DN). The unitless DNs stored by the sensor are not correct representations of ground reflectance. The procedure of radiometric correction involves the conversion of DN values of the image back to spectral radiance. This process requires information of the 'gain and bias' of the sensor in each spectral band (Richter & Schläpfer 2014). The information about the sensor's gain and bias is found in the metadata files. The at sensor radiance L_λ is calculated using the following linear expression (*Richter* & Schläpfer 2014):

$$L_\lambda = gain * DN + bias$$

Radiometric corrections are performed on the WV-2 images to correct for effects caused by the sensor, atmosphere and illumination to convert sensor radiance into desired surface reflectance (%). The software used for atmospheric correction is ATCOR2 for multispectral sensors at flat terrain embedded in ENVI IDL (Richter & Schläpfer 2014).

3.3.1.3 Subsetting and masking

Subsetting is the process of reducing an image to an area of interest (AOI). The input data used for creating a mask were the non-corrected WV-2 images. The Biodiversity network (.shp) from the CoCT consist of vegetation classes 1 and 2. The vegetation class 1 is vegetation growing on sand and vegetation class 2 is vegetation growing on limestone. The Biodiversity network (.shp) was rasterised using the import tool in ERDAS to convert it to an image, to enable subset creation. The projection used for creating a subset was UTM. The subset was created using the spatial modeller (the either-if condition) tool in ERDAS IMAGINE 2014. Buildings, ocean water and other land-use types were masked out using the same dataset since they were not of interest for this study. The subset was created to minimise computation time and to avoid biases in the accuracy of the HII as suggested by Lück-Vogel, O'Farrell & Roberts (2013). The output subset and masked-out images are shown in Figure 3.8. This procedure was conducted on the 25 February 2014 and 11 October 2014 WV-2 images. Analysis of the images is discussed in section 3.4.

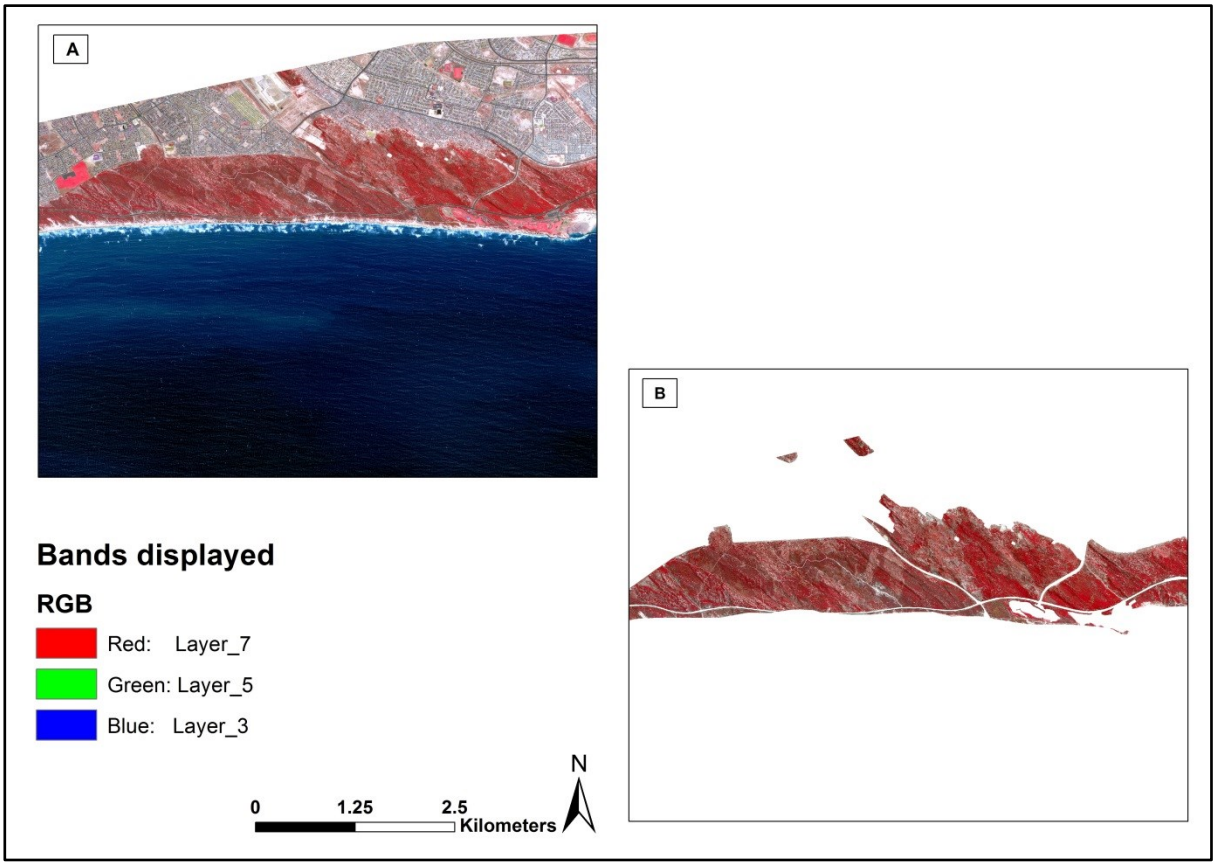

Figure 3.8 Subset and mask output of the WV-2 image. A: Original WV-2 image; B: subsetted WV-2 image

This procedure was conducted on the 25 February 2014 and 11 October 2014 WV-2 images. Analysis of the images is discussed in section 3.4.

3.4 SATELLITE DATA PROCESSING

3.4.1 Image segmentation

Darwish et al. (2003), Wang (2010) and Dragut (2010) define image segmentation simply as dividing the image into spatially and spectrally homogenous regions. Segmentation is the first essential processing step in OBIA through the aggregation of pixels to objects. Segmentation uses image attributes such as shape, colour, size, texture and contextual information to delineate the image objects (Darwish et al. 2003).

Segmentation of image objects was run on the 11 October 2014 and 25 February 2014 WV-2 subsets using eCognition Developer (version 9) software (Definiens 2007). The multiresolution segmentation algorithm was chosen to delineate the image objects of interests. The scale parameter used was 150 as shown in Figure 3.9. The multiresolution segmentation algorithm allows for different individual band weightings. More weight was given to the individual bands important for the extraction of vegetation information, i.e. a weighting of 1 for near-infrared and RED. All other spectral bands were given a weighting of 0.5. The NDVI was calculated in eCognition.

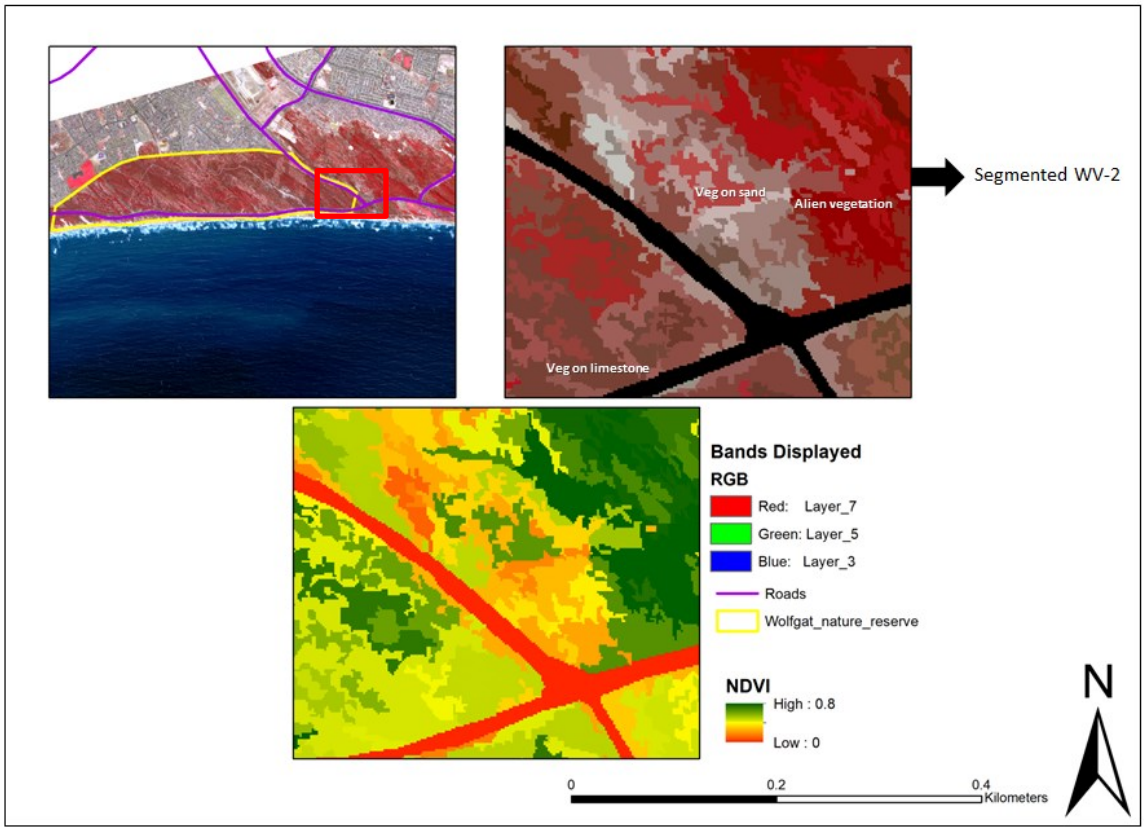

Figure 3.9 WV-2 segmented image and segmented NDVI

Further, the extraction of five image derivatives (Brightness, Compactness, Area, NDVI and NIR standard deviation) was performed to derive additional spectral, structural, textural and contextual properties. This procedure was conducted on both WV-2 images.

3.4.2 Generating image derivatives

The method for deriving the HII using image derivatives was adapted from Lück-Vogel, O'Farrell & Roberts (2013). The modified method aims at assessing how intact or degraded the habitat is using high spatial resolution satellite imagery, whereas Lück-Vogel, O'Farrell & Roberts (2013) used Landsat and SPOT images with medium resolution. This study used high spatial resolution imagery (WV-2) to assess the intactness or degradation of CFDS coastal vegetation. The image derivatives are based on different properties such as spectral, structural, spatial and textural information (Lück-Vogel, O'Farrell & Roberts 2013). An additional derivative was added, namely NDVI and NIR1 standard deviation. The purpose of extracting the image derivatives was to obtain the HII. The procedure of generating image derivatives was performed on both WV-2 images using ERDAS 2014 and eCognition software. The image derivatives and other procedures are set out in the following subsections.

3.4.2.1 Spectral derivative

The spectral derivative is based on the hypothesis that landscapes with less or no vegetation will have higher reflectance in the bands compared to areas with dense vegetation cover. Areas with no vegetation are regarded as degraded but this is no exception for sand dunes (foredunes) which are a natural dune landscape for coastal areas. All transformed areas were masked out as recommended by Lück-Vogel, O'Farrell & Roberts (2013), because they could be confused with degraded areas in terms of brightness. Mean Brightness values were used as proxy for spectral derivative measurement.

3.4.2.2 Structural derivative

In the Sandveld paper Lück-Vogel, O'Farrell & Roberts (2013) hypothesised that the more linear geometry a landscape has, the more degraded it would be due to more anthropogenic factors compared to irregular shapes of natural landscapes. Observations made from satellite images show that man-made features such as buildings and plantations have more square or circular shapes as compared to natural areas which show more irregular shapes. Compactness was used in the Sandveld study by Lück-Vogel, O'Farrell & Roberts (2013) as proxy for vegetation degradation. Compactness is calculated in eCognition (2007) as the ratio of the area of a polygon to the area of a circle with the same perimeter using the formula:

$$\text{Compactness} = \frac{4\pi \times Area}{perimeter^2}$$

Therefore, anthropogenic structures frequently have a high compactness in relation to natural areas that appear less compact (Lück-Vogel, O'Farrell & Roberts 2013). This study tested if this assumption was true in the CFDS as well.

3.4.2.3 Textural derivative

The assumption was made that high spectral heterogeneity is represented by a natural landscape comprising of species that are different in age, height and form of structure per polygons as compared to anthropogenic landscapes that have uniform (homogenous) landscapes (Lück-Vogel, O'Farrell & Roberts 2013). However, anthropogenic landscapes such as agricultural fields were masked out in this study. Standard deviation of NIR range is a proxy for vegetation texture (Lück-Vogel, O'Farrell & Roberts 2013) where an increase in texture is assumed to indicate an increase in ecosystem intactness. This study tested if this assumption was true in the CFDS as well.

3.4.2.4 Area derivative

The area derivative was based on the assumption that natural landscapes have bigger polygons. Degraded areas such as settlements have smaller polygons and were masked out in this study. Area excluding inner polygon in the eCognition software can be used as proxy for the area derivative with the area calculation being:

$$Area = \frac{1}{2}\sum_{i=0}^{x-1} a_i$$

Where:

$$a_i = X_i Y_{i+1} - X_{i+1} Y_i$$

This study tested if this assumption was true in the CFDS as well.

3.4.2.5 Normalized Difference Vegetation Index

NDVI is a vegetation index used to indicate vegetation density and activity. The assumption is that vegetation with low plant activity will have low a NDVI compared to vegetation with high plant activity. NDVI values range from -1.0 to 1.0, where negative NDVI values indicate that water is present (Pettorelli et al. 2005). NDVI values of 0 indicate areas of barren rock and sand, 0.2 to 0.5 indicate sparse vegetation and 0.6 to 0.9 indicate dense vegetation. NDVI is calculated using the following equation:

$$NDVI = \frac{(NIR - red)}{(NIR + red)}$$

NDVI was used as additional spectral derivative.

3.4.2.6 Rasterise image derivatives and WV-2 spectral bands

The segmented eight spectral bands and five image derivatives (Brightness, Compactness, Area, NDVI and NIR1 standard deviation) were exported using eCognition export vector layer function. The spectral bands and image derivatives were exported as smoothed polygons and rasterised in ArcGIS (version 10.1) (ESRI 2010) with a 2 m pixel size using the ‘feature to raster’ function. The output was an ArcGRID format. The “GRID” was then converted into IMG format in ERDAS using the import tool “GRID” read direct. This procedure was performed on both WV-2 images.

3.4.2.7 Layer stack

In the last pre-processing step the eight rasterised spectral bands and the five image derivatives (Brightness, Compactness, Area, NDVI and NIR standard deviation) were stacked (see Table 3.3) to generate a single composite image. The stacked images were used to perform DTC in ERDAS. This procedure was performed on the 25 February 2014 and the 11 October 2014 images.

Table 3.3 Layer stack of all WV-2 spectral bands and image derivatives

Band no	Spectral range	Band no	Image derivatives
1	Coastal	9	Brightness
2	Blue	10	Compactness
3	Green	11	Area
4	Yellow	12	NDVI
5	Red	13	Standard deviation NIR1
6	Red edge		
7	NIR1		
8	NIR2		

3.4.3 Creating training points

As a first attempt, training points were created using the habitat condition (poor, medium and high) obtained from the CoCT biodiversity network data. A total of 160 stratified random points were generated in ERDAS imagine using the accuracy assessment tool based on the CoCT habitat condition (poor, medium and high) data as defined by the CoCT. Layer stack values for each point were extracted using the signature editor tool in ERDAS. The values were exported to Microsoft Excel to determine a relationship between the CoCT habitat condition and 13 layers using linear regression analysis as indicated in Figure 3.10 using the RED band as example.

Figure 3.10 indicates a poor relationship between the habitat condition classes and the red band, with coefficient of determination (R^2) value of 0.14. This attempt failed to produce any significant relationship between the variables and the CoCT habitat condition classes. It failed because the habitat condition data from the CoCT were only presented at a coarse scale. The polygons representing each habitat condition had multiple degradation types per polygon shown in Figure 3.11 i.e. fire scars and pathways. Assumptions made by the CoCT

management regarding each habitat condition were based on course scale and not fine detailed scale. This approach was therefore abandoned.

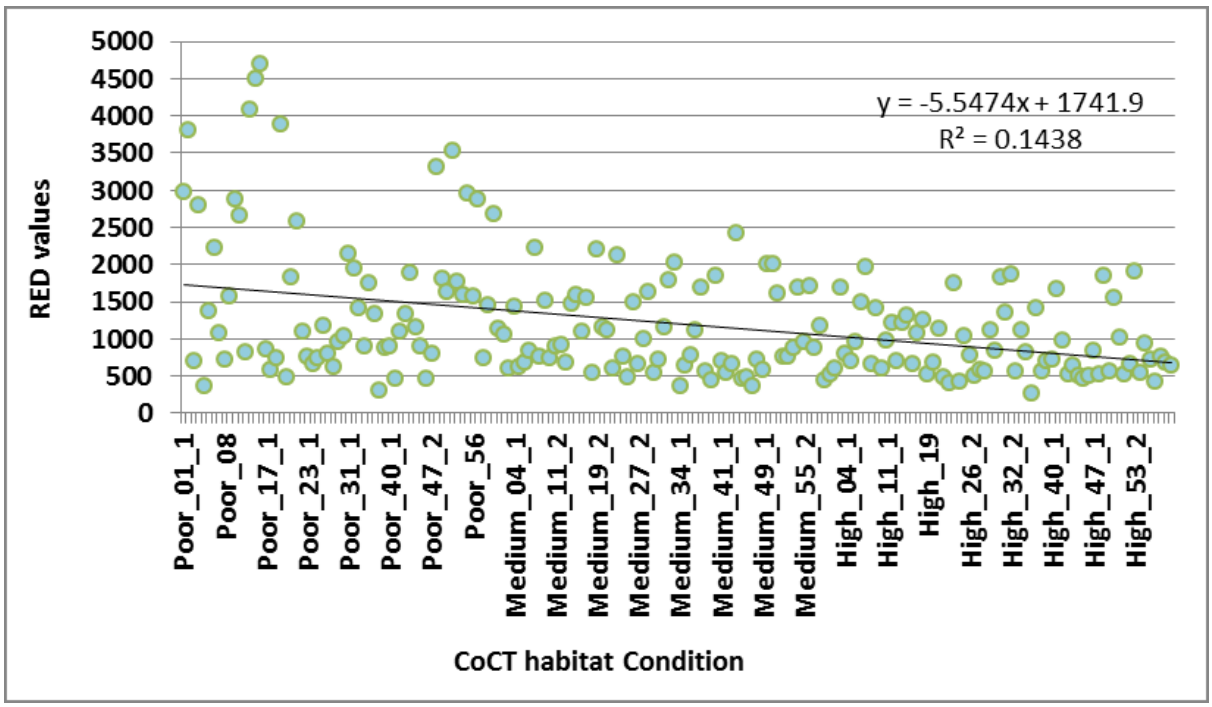

Figure 3.10 Relationship between habitat condition classes and RED spectral values

A second alternative approach was to create random points based on field observations. Points were determined by field-trip observations related to the classes referred to in Table 3.4 according to degree of intactness or degradation. The classes were defined according to the levels of intactness which range from highly degraded (little or no plant cover) to intact (pristine high plant cover) and with the addition of alien vegetation as listed in Table 3.4.

Table 3.4 Identified vegetation classes relating to level of intactness

Number	Description	Levels of intactness
1	Bare Soil	1
2	Cleared vegetation	2
3	Fire scar on limestone	3
4	Fire scar on sand	3
5	Herbaceous vegetation	4
6	Natural vegetation on limestone	4
7	Natural vegetation on sand	4
8	Alien vegetation	5

Alien vegetation is regarded as being not intact vegetation even though it has high plant cover. In this study alien vegetation was placed last on the list.

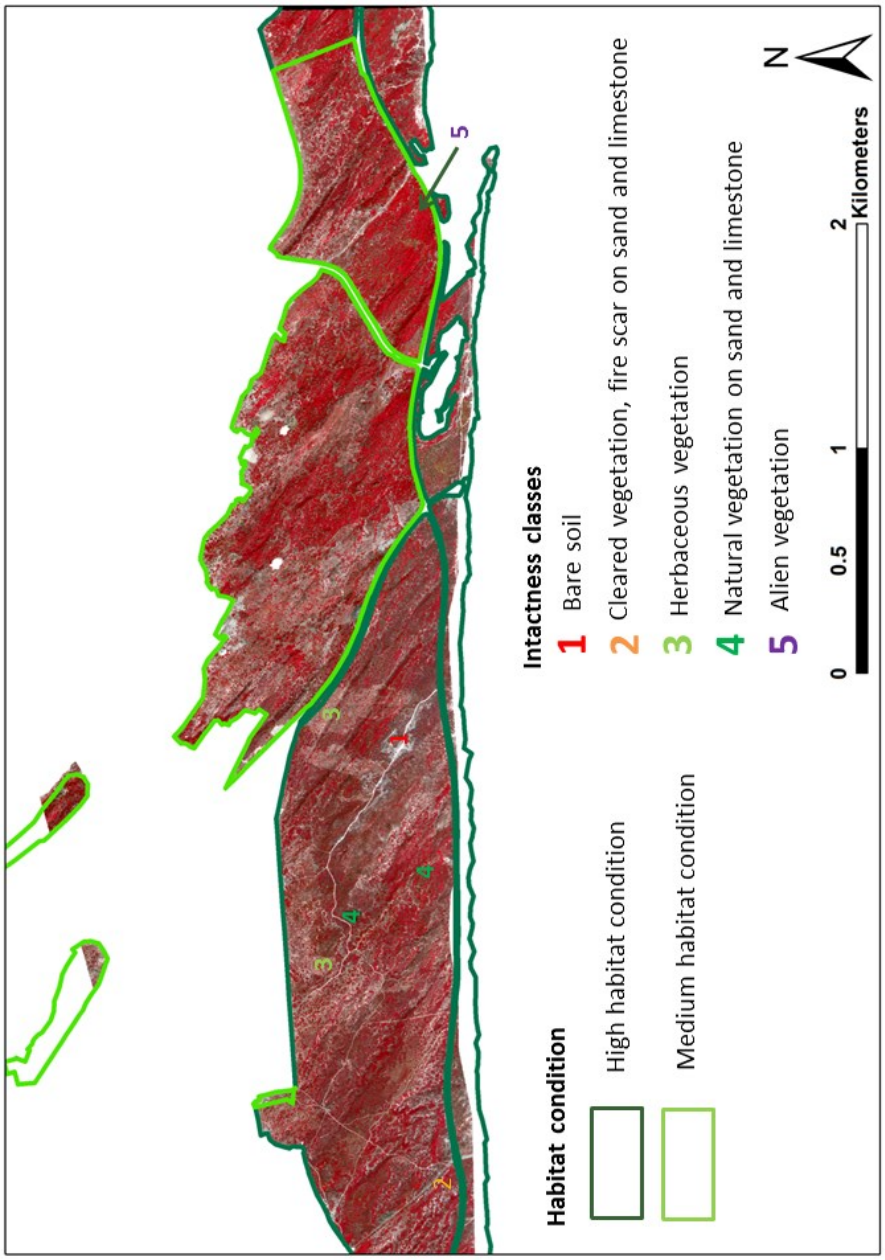

Figure 3.11 CoCT habitat condition polygon outlines versus visible intactness classes on WV-2 image

A total of 160 random points were collected for the eight classes that were visible in the field (Table 3.4). Sample sizes of 20 random points per class were collected. The random points were collected and arranged into levels of intactness as shown in Table 3.4. The collection of random training points was performed using the signature editor tool in ERDAS. The field-informed points were exported to MS Excel for further regression analysis. The results are

dealt with in Section 3.4.4. This procedure was performed on the 25 February 2014 WV-2 image.

The training point values for all eight spectral bands and five image derivatives were exported into MS Excel for further analysis. The correlation between the field-defined classes, spectral bands and image derivatives were assessed using regression analysis (coefficient of determination R^2). The regression analysis values (R^2) range from -1.0 to 1.0. An R^2 value of -1.0 indicates a negative correlation between the variables and a value of 1.0 indicates a positive correlation between the variables. A polynomial regression analysis was used to determine the correlation between the dependent (Y) and independent variables (X). The points were evenly split ("thirds out"), where other points were used as training points for multiple regression analysis and other points used for validation of the DTC.

The resulting spectral signatures from the collected random training points were cleaned to remove spectral outliers that could contribute to bias in the spectral statistics. The spectral mean signatures for the field classes are displayed in Figure 3.12 for the spectral bands.

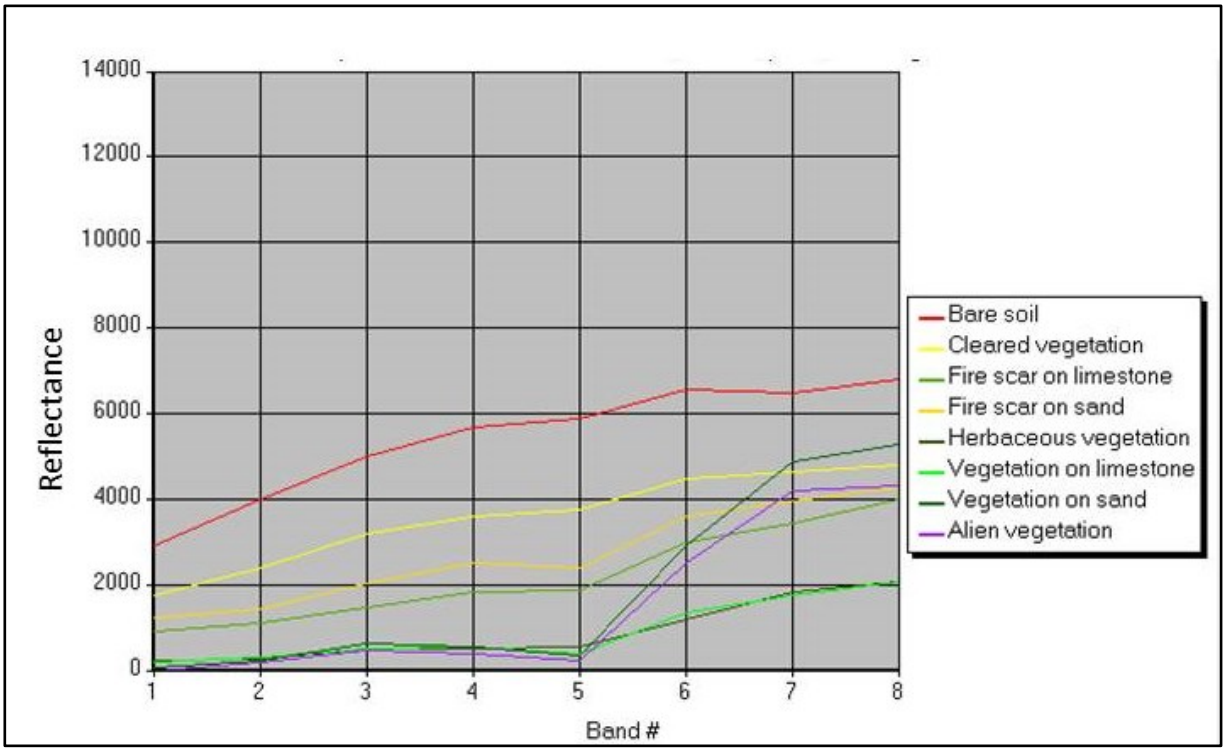

Figure 3.12 Spectral signature of identified classes (mean values)

Figure 3.12 shows typical spectral signatures of the eight observed land cover classes. The bare soil is class assumed the worst state of degradation whereas vegetation growing on sand and

limestone was most pristine, except for alien invasive vegetation. All other classes assumed in-between gradients, with increasing soil signal indicating a decrease in vegetation cover.

3.4.4 Decision tree classification

The regression graphs in Figure 3.14 and Figure 3.15 show the relationship between five intactness classes (X-axis) and mean layer reflectance values for RED and NIR1 respectively (Y-axis). The intactness classes were sorted from highly degraded on the left with an increase in intactness to the right. With exception class 5 (alien vegetation) the relationship between the two variables was determined using polynomial regression analysis. The regression graphs show a smooth curve in the degraded classes with high reflectance values.

The first five spectral bands out of eight spectral bands produced the same regression results just like the one shown in the RED band in Figure 3.14. Therefore, the RED and the NIR1 bands where used to generate the DTC. The choice for using these two bands was based on that most sensors have the RED and NIR band, which are most important for vegetation related studies.

The DTC was generated using the RED and NIR1 multispectral bands. A threshold was created in MS Excel, where the habitat condition classes were split according to degrees of degradation. RED values lower than (<) 757 were regarded as intact vegetation and values greater than (>) 757 but less than 1884 were regarded as lightly degraded. The red band was used since it showed a higher R^2 and smooth, levelled relationship in all habitat condition classes. Figure 3.13 illustrates steps taken to perform a decision tree classification.

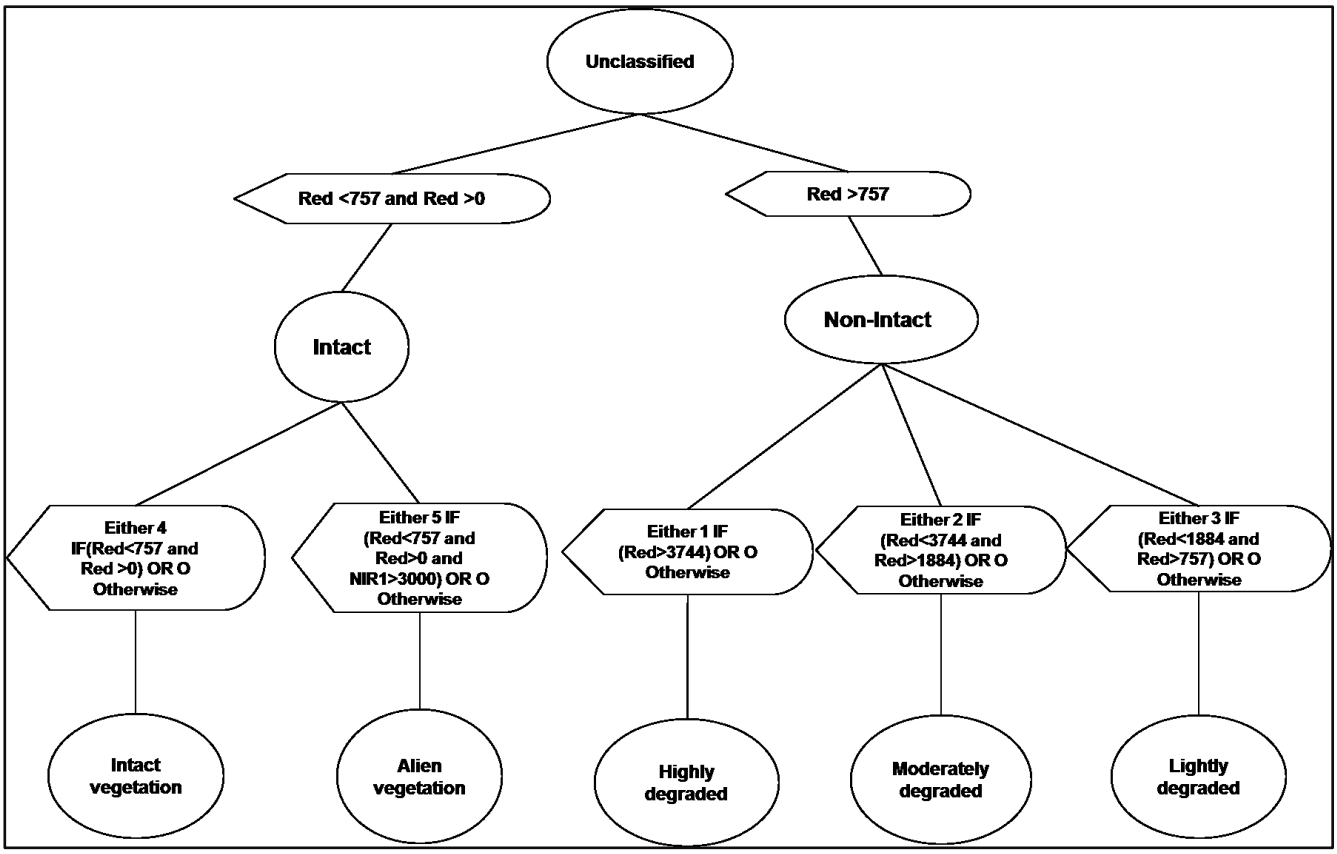

Figure 3.13 Decision tree classification systematic diagram

In order to delineate between intact and alien vegetation habitat condition classes, the NIR band was used. The band was used primary because alien vegetation shows high reflectance in the NIR band while primarily in the RED band looking the same as intact vegetation.

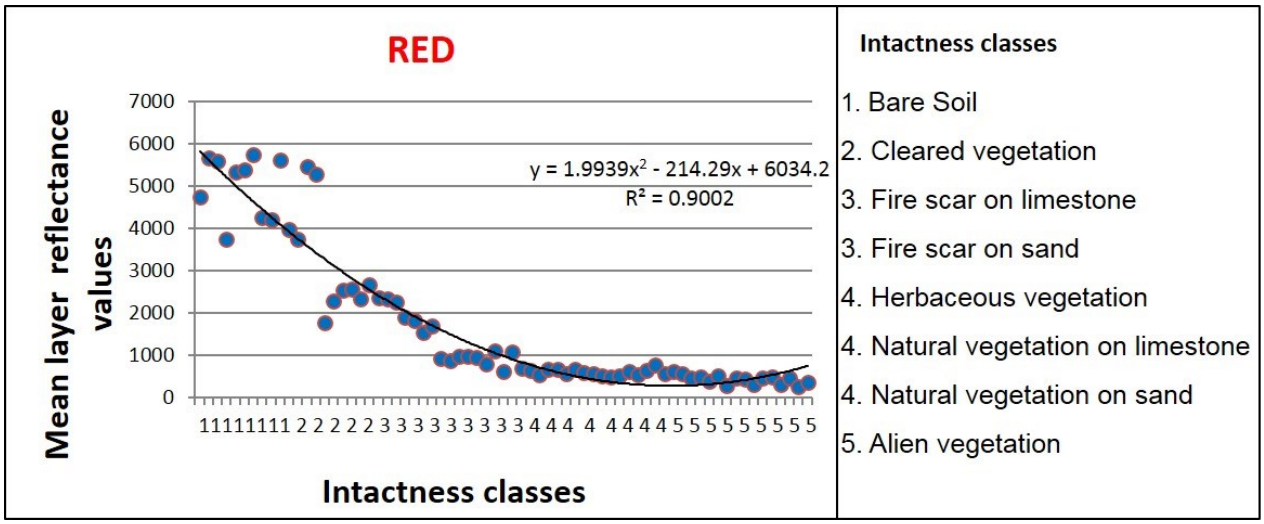

Figure 3.14 Relationship between levels of intactness and each spectral band in the Red band

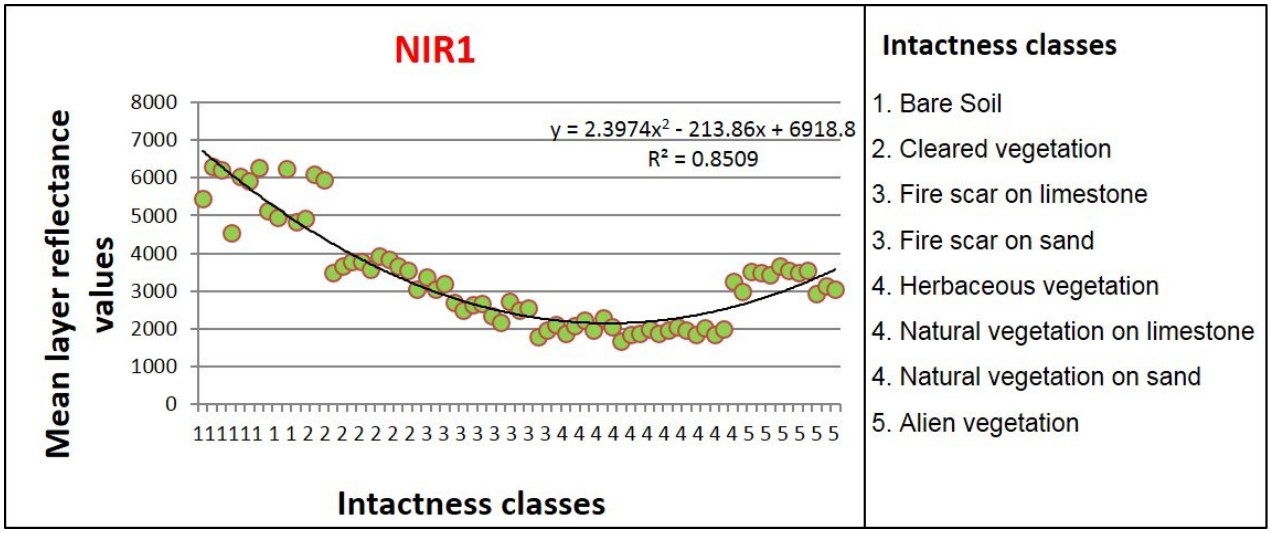

Figure 3.15 Relationship between levels of intactness and each spectral band in the NIR1 band

The five image derivatives were omitted, because they did not produce good regression results to perform the DTC. This procedure was performed separately on the 25 February and 11 October 2014 images.

3.4.5 Validation of results

Two approaches were used to assess the accuracy of the classification results. This included an accuracy assessment using field informed random points and field visit.

3.4.5.1 Accuracy assessment using random points

Accuracy assessment involves evaluating the validity of results derived from remote sensing against ground truth data in order to assess how well the former represent the real world (Congalton & Green 2009). This technique is commonly used to measure the spatial accuracy and help determine the quality of remote sensing outputs. For this study a thematic accuracy assessment was used to measure the accuracy of the outputs of the HII using ground truthing points as reference data.

For the derived DTC an error matrix including kappa statistics, overall, producer's and user's accuracy were calculated analysed using ERDAS's accuracy assessment tool. An error matrix is a comparison between remote sensing results and ground truth data (reference data). It identifies misclassification errors and their quantity. Accuracy of the results is represented not only by overall accuracy but by kappa statics information.

Kappa is a measure of agreement between the remotely sensed classification and the reference data (Congalton & Green 2009). A kappa statistical value greater than 0.80 (80%) indicates a strong agreement between a remotely sensed classification and reference data, while a kappa value between 0.40 (40%) and 0.80 represents a moderate agreement. Kappa value below 0.40 indicates a poor agreement between classification and reference data (Landis & Koch 1977; Congalton & Green 2009).

In order to perform accuracy assessment, a set of validation points derived from field data are needed. Reference data needs to be categorized according to the class values used to create the map (Congalton & Green 2009). The class names are arranged according to levels of intactness, ranging from highly degraded to most intact class. These classes are highly degraded, moderately degraded, lightly degraded, intact vegetation and alien vegetation. A total number of 42 references were used. The accuracy assessment output ASCII tables were exported to MS Excel for further analyses. Results are presented in Section 4.2.

3.4.5.2 Field validation

Further field validation points were collected in the field to assess the validity of the HII results. The printed map results of both February and October 2014 were taken to the field for the selection of points of interest for validation. Investigated points were marked with the GPS. This was done to effectively determine and establish comparable relationship between the HII results and the field validation points. A total number of 31 field validation points were captured and labelled using a GPS. The GPS points were saved and exported to MS Excel and later converted to a shapefile (.shp) for further analysis. Correspondence between appearance in the field and the classification output was analysed. Results are presented and discussed in section 4.1.

CHAPTER 4. RESULTS AND DISCUSSION

The chapter begins with a presentation and discussion of the findings of the DTC of the two WV-2 images. Section 4.2 represents the results of the accuracy assessment that used field-informed random points. The research question whether WV-2 can efficiently assess the intactness of terrestrial coastal vegetation is dealt with. The chapter ends with a detailed exposition and discussion of the results of accuracy assessment based on field validation points.

4.1 THE DERIVED HABITAT INTACTNESS INDEX

Figure 4.1 shows HII derived using DTC of WV-2 image captured on the 25 February 2014 shown in Figure 4.1. The image represents the dry summer season. Five classes were classified, namely highly, moderately and lightly degraded classes, intact vegetation and alien vegetation. The classification identified areas ranging from high degradation to high intactness. Red denotes highly degraded areas which are bare areas of footpaths, pathways (due to vehicles) and open patches without vegetation. Yellow represents moderately degraded areas of cleared alien vegetation that are left bare with in between patches of vegetation. Areas of open low-lying (in vegetation height) herbaceous vegetation in CFDS vegetation are represented by light green. These areas mainly represent regrowth of vegetation recovering from human-caused fires that occur frequently in areas invaded by alien vegetation species such as *Acacia cyclops*. The dark green shading indicates intact indigenous vegetation of the CFDS vegetation growing on limestone and on sand. Purple indicates areas infested with alien invasive *Acacia cyclops* (Rooikrans).

Figure 4.2 demonstrates the HII results derived from the decision tree classification WV-2 image of 11 October 2014. The image represents the wet winter season. The decision tree classification produced five classes that range from highly degraded to highly intact with an exception made for an alien vegetation class. Red shows areas that are highly degraded or bare soil. Close to the coast the areas of open, bare soil are typical natural dune and beach landscape of coastal environments (Lück-Vogel, O'Farrell & Roberts 2013), but farther landward they are due to footpaths and illegal pathways and vehicles tracks. Moderately degraded areas shown in yellow indicate areas with patches of removed vegetation through alien clearing and minimal regrowth of CFDS vegetation. Light green indicates areas of open, low-lying (in vegetation height) herbaceous CFDS vegetation that has not reached its climax stage (full-grown vegetation). Dark green shows areas of high intactness of the CFDS vegetation. Purple again

shows areas infested by *Acacia cyclops* which is the most dominant alien plant species found in Wolfgat Nature Reserve and Macassar dune conservation areas and the entire Monwabisi area.

The red block in Figure 4.1 delineates the area of overlap between the DTC results from 25 February and 11 October 2014. The differentiation of classes in the overlapping areas is shown enlarged in Figure 4.3-A. There is minimal presence of alien vegetation in this area in the February image. The classification shows more alien vegetation in the wet season (October) image compared to the dry season (February) image.

The February classification shows a clear distinction between natural and alien vegetation. This is due to the low plant activity in the natural vegetation in summer as opposed to alien vegetation which is thriving under these environmental conditions. Seasonality is clearly another factor in the classifications of intactness in terrestrial coastal vegetation. The variation caused by seasonality in a period of eight months.

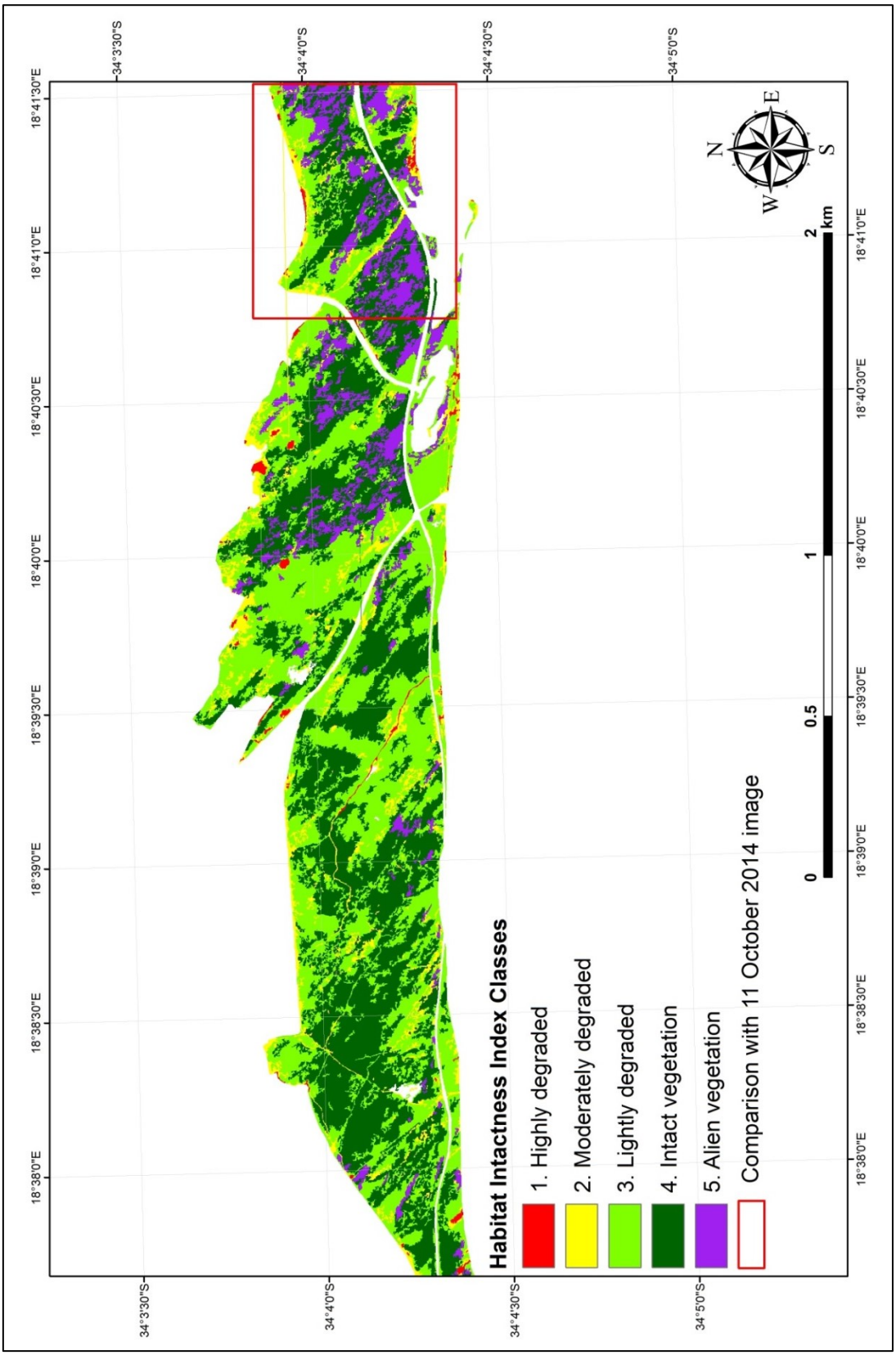

Figure 4.1 HII derived from 25 February 2014 image (dry season).

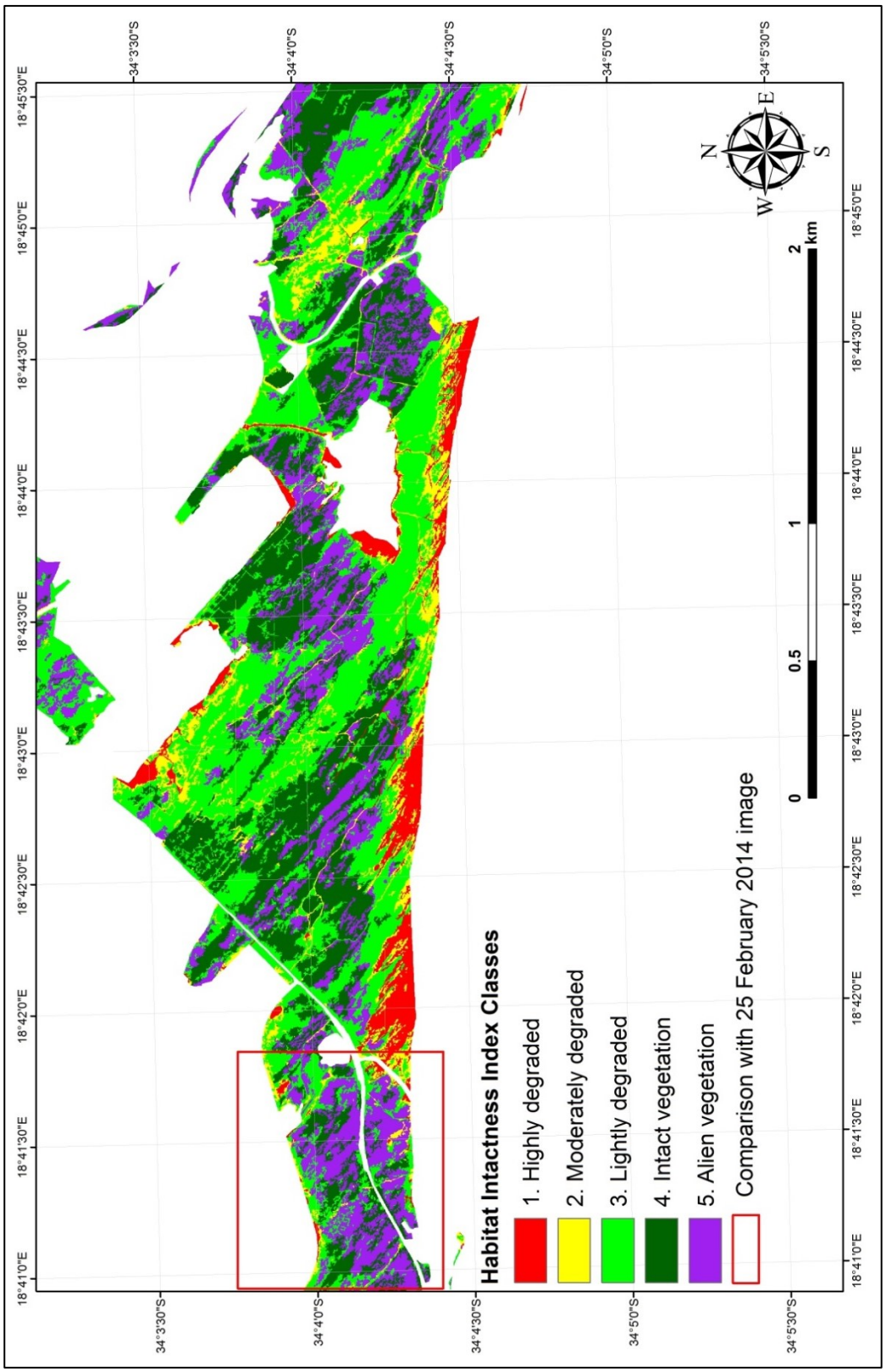

Figure 4.2 HII derived from 11 October 2014 image (wet season).

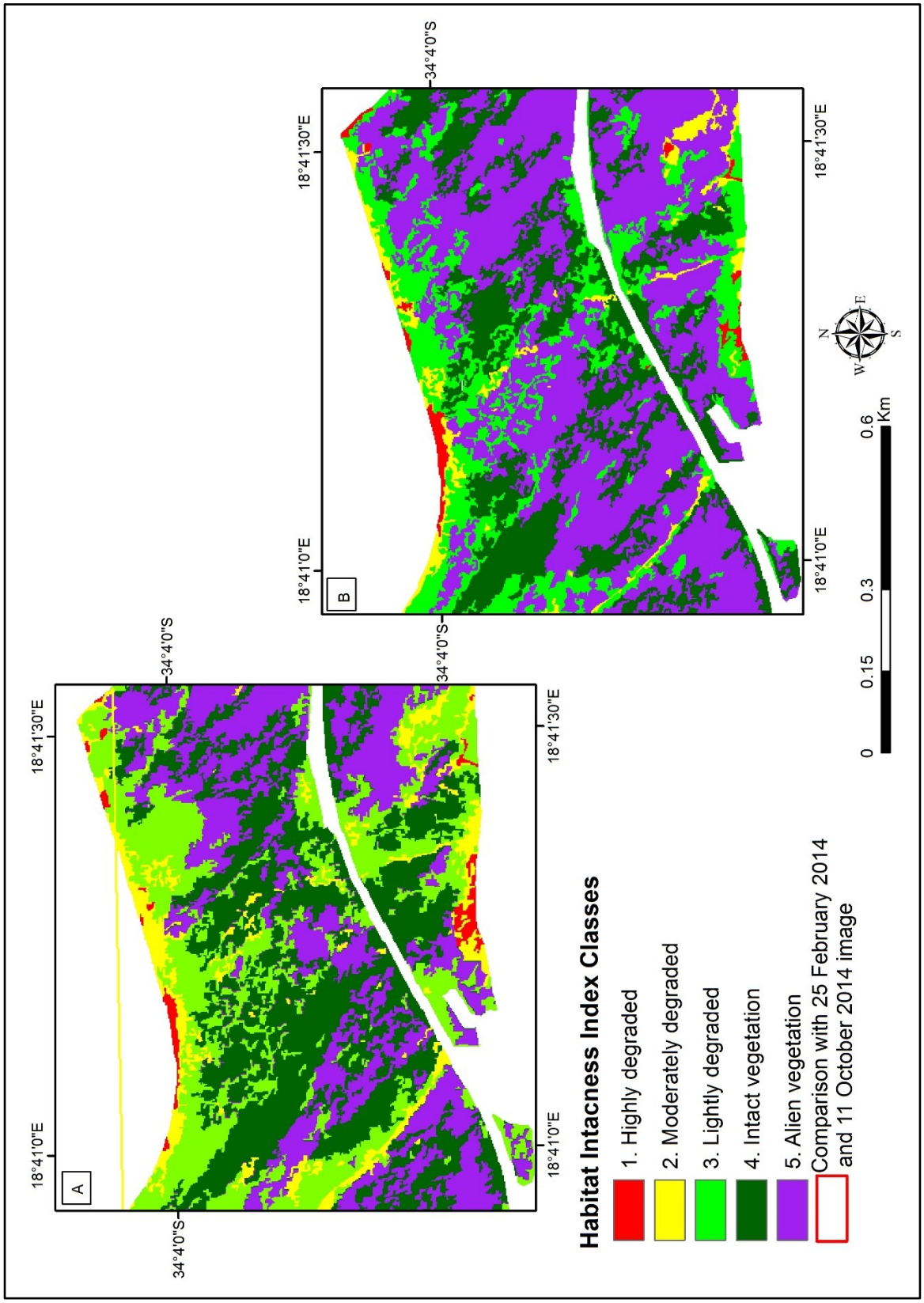

Figure 4.3 A) HII classified areas for the 25 February 2014; B) HII classification of the same area for the 11 October 2014.

The number of pixels per habitat class for each image is given in Table 4.1 which lists the area coverage and area difference between the habitat classes derived for the DTC. Alien vegetation covered a relatively small area of 17.52 ha on the 25 February 2014 image whereas the 11 October 2014 image shows a 1.73 times larger (30.3 ha) total coverage of alien vegetation. These areas are shown in Figure 4.3-A and Figure 4.3-B.

Table 4.1 Area coverage of habitat classes

		February			October				
Colour coding	Class names	Number of pixels	Area (ha)	%	Number of pixels	Area (ha)	%	Feb - Oct Difference (ha)	%
	Highly degraded	1817	0.73	1.19	1722	0.69	1.13	0.04	0.15
	Moderately degraded	12 176	4.87	7.95	5487	2.19	3.60	2.68	10.34
	Lightly degraded	39 962	15.98	26.09	30 450	12.18	19.98	3.80	14.70
	Intact vegetation	55 431	22.17	36.19	38 997	15.60	25.58	6.57	25.39
	Alien vegetation	43 798	17.52	28.59	75 783	30.31	49.71	12.79	49.42

In the case of number of pixel between the February and October image, the highly degraded in February has a greater number of pixels of 1817 compared to 1722 of October. Again the variation in seasonality is the primary reason. The moderately degraded class in October has 5 487 pixels compared to the 12 176 pixel for February. The lightly degraded class for February has 39 962 pixels compared to 30 450 pixels in October. In February the intact vegetation class has 55 431 pixels in comparison to the 38 997 pixels for the October image. The October image has more alien pixels, and fewer pixels for intact vegetation.

The dry-season case shown in Figure 4.3-A exhibits areas with sparse vegetation and more patches without vegetation. The February dry-season image also records less plant activity in natural vegetation. There is also better detection of the alien invasive plant species *Acacia cyclops*. The environmental conditions in February are conducive to the growth of the alien invasive plants. Compared to the October image in Figure 4.3-B, there is less alien invasion shown in purple in the February image Figure 4.3-A of the dry, hot season as. A probable explanation for this difference is that in the dry season there is low plant activity in the natural CFDS vegetation.

The wet-season case depicted in Figure 4.3-B shows fewer areas of sparse vegetation and less patches without vegetation cover. Clearly there is a high degree of plant activity in alien invasive vegetation. Seasonality is the main reason for the greater areal coverage of aliens compared to natural CFDS vegetation after eight months. The high plant (i.e. high biomass) activity of both indigenous and alien invasive vegetation makes it difficult to detect and distinguish between aliens and natural vegetation in this season (wet). This is quite likely due to the spectral confusion between the spectral bands used to produce the DTC. The best season

to better detect alien vegetation from the natural CFDS is the dry season (February) image where there is not much spectral confusion.

Table 4.1 records the greater area coverage of 30 ha (49.71%) alien vegetation in October compared to 17.52 ha (28.59%) in the February image. Table 4.1 shows the areal difference between the February and October images in the area of overlap outlined in Figure 4.3-A and 4.3-B. The difference between the two images is 12.8 compared to the difference of other habitat classes. The accuracy assessment of the classification based on field-informed points and field visit with discussion are dealt with in Sections 4.2 and 4.3.

4.2 ACCURACY ASSESSMENT BASED OF FIELD-INFORMED RANDOM POINTS

The error matrix (Table 4.2) provides evidence of whether classification results reported in Section 4.1 represent actual classes on the ground. The overall accuracy of the classification using field informed random points was high at 80.50 %, yielding a kappa value of 0.75. This kappa value indicates substantial agreement (Congalton & Green 2009; Landis & Koch 1977), that is there is a marked relationship between the classifications results and the reference data. Moreover, the overall accuracy of 80.50 % generated using field-informed random points shows how well the classification worked. The high overall accuracy can be ascribed to the high spatial resolution of 2 metres and the high spectral resolution of the bands of the WV-2 image, as well as the exclusion of transformed areas and non-strandveld vegetation as per recommendation by (Lück-Vogel, O'Farrell & Roberts 2013).

Table 4.2 Error matrix for the classification results of the 25 February 2014 WV-2 image based on random field-informed points.

Classified	Reference					
	Bare soil	Cleared vegetation	Fire scars	Intact vegetation	Alien vegetation	Row total
Bare soil	4	0	0	0	0	4
Cleared vegetation	2	4	0	0	0	6
Fire scars	0	1	6	0	0	7
Intact vegetation	0	0	0	12	0	12
Alien vegetation	0	0	0	5	7	12
Column total	6	5	6	17	7	41
Overall accuracy	80.50%					
Overall kappa statistics	0.75					

Forty-one field-informed random points were used to generate the error matrix. The shaded diagonal cells in Table 4.2 indicate the number of points correctly classified. Four out of six reference points were correctly classified as bare soil; four out of five reference points were correctly classified as cleared vegetation; six out of six reference points were correctly classified as fire scars; twelve out of seventeen reference points were correctly classified as intact vegetation; and seven out of seven reference points were correctly classified as alien vegetation in the WV-2 image for 25 February 2014.

Of the six bare soil reference points two were incorrectly classified as cleared vegetation. A main reason for this error is probably the similarity of the spectral properties of the two classes (Foody 2002). Furthermore, a misclassification of cleared vegetation and fires occurred and there was confusion about intact vegetation and alien vegetation owing to the two classes being spectrally similar. But a clear distinction of alien vegetation on the image was identified as dense homogenous from visual observations.

Table 4.3 summarises the habitat intactness accuracies and kappa values. Forty-one reference points were used to calculate the accuracy of the classification. Thirty-three reference points were correctly classified. The best user's accuracy of the classification was achieved for intact vegetation at 100%, followed by fire scars at 85%. The minimum user's accuracy was achieved for alien vegetation at 58.33% which is considered to be below the desired level for satisfactory accuracy.

Table 4.3 Overall accuracy of the calculated classification results and kappa values

Class names	Reference total	Classified total	Number correct	Producer's accuracy (%)	User's accuracy (%)	Kappa values
Bare soil	6	4	4	66.7	100	1.0
Cleared vegetation	5	6	4	80	66.7	0.6
Fire Scars	6	7	6	100	85.71	0.8
Intact vegetation	17	12	12	70.6	100	1.0
Alien vegetation	7	12	7	100	58.33	0.5
Totals	41	41	33			

The best producer's accuracy was achieved for alien vegetation and fire scars at 100%, with intact vegetation scoring 80%. The least producer's accuracy was registered for bare soil at 66.7%. Kappa values were calculated for each habitat intactness class. Overall the kappa values indicate the level of satisfactory agreement between the reference data and classification results. The best kappa values were achieved for intact vegetation and bare soil at 1.0 and fire scars at 0.8, both values representing marked agreement according to Landis & Koch (1977) and Congalton & Green (2009). Moderate kappa values were achieved for cleared vegetation at 0.6 and alien vegetation at 0.5. The results shown in Table 4.3 confirm the success of the regression analysis for developing a decision tree classification approach for assessing habitat intactness. Although there were some misclassifications, the results allow one to confidently conclude that WV-2 imagery does efficiently assess the intactness of terrestrial coastal vegetation. Section 4.3 represents the validation of the classification results using field visit data.

4.3 ACCURACY ASSESSMENT BASED ON FIELD VALIDATION POINTS

Field validation was conducted for both 25 February 2014 and 11 October 2014 images on June 2016 along areas of interest in the study area. Thirty-one field-validation points were collected and captured using GPS. Figure 4.4 gives an overview of the classification results based on the two images. Figure 4.4 shows the thirty-one captured field-validation called waypoints at points of interest in the study area. The detailed presentation of Figure 4.4 per field-validation waypoint is further discussed from Figure 4.4 to Figure 4.19.

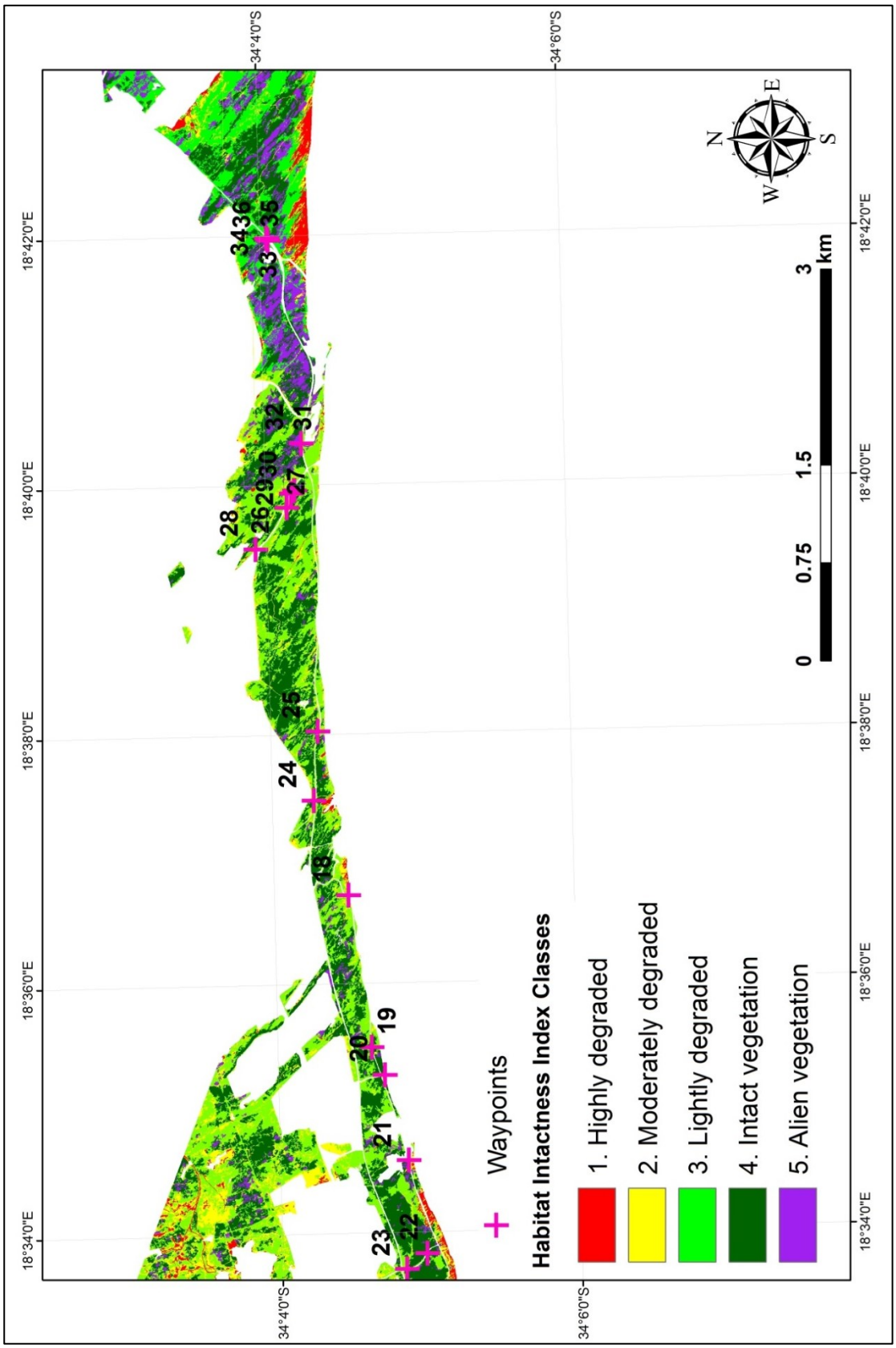

Figure 4.4 Mosaic of the HII classification of WV-2 MS imagery for 25 February 2014 and 11 October 2014.

Figure 4.5-A is a WV-2 satellite image showing the classified validated region for February. The marked waypoint 18 in Figure 4.5-B is a validation point. The validation point represents class 2 of the HII which is a moderately degraded area. Figure 4.5-C is a photograph of waypoint 18 taken during the field-validation visit showing class 2 characterized by dry, cleared alien vegetation stands interspersed with herbaceous vegetation. Apparently, an alien vegetation clearing programme was performed in the area prior to the acquisition of the WV-2 image as confirmed by the CoCT experts. The classification results in Figure 4.5-B are not the same as seen in the field photograph of (Figure 4.5-C) because the alien vegetation that had been cleared had started to recover by the time of the field visit. Therefore, HII classification correctly coincides with the photograph. According to Lück-Vogel et al. (2016), environmental dynamics play a role in validating the classification results. The miss-match between acquisition date of satellite images and field-validation is the main reason for wrongly detected change in the landscapes or environment.

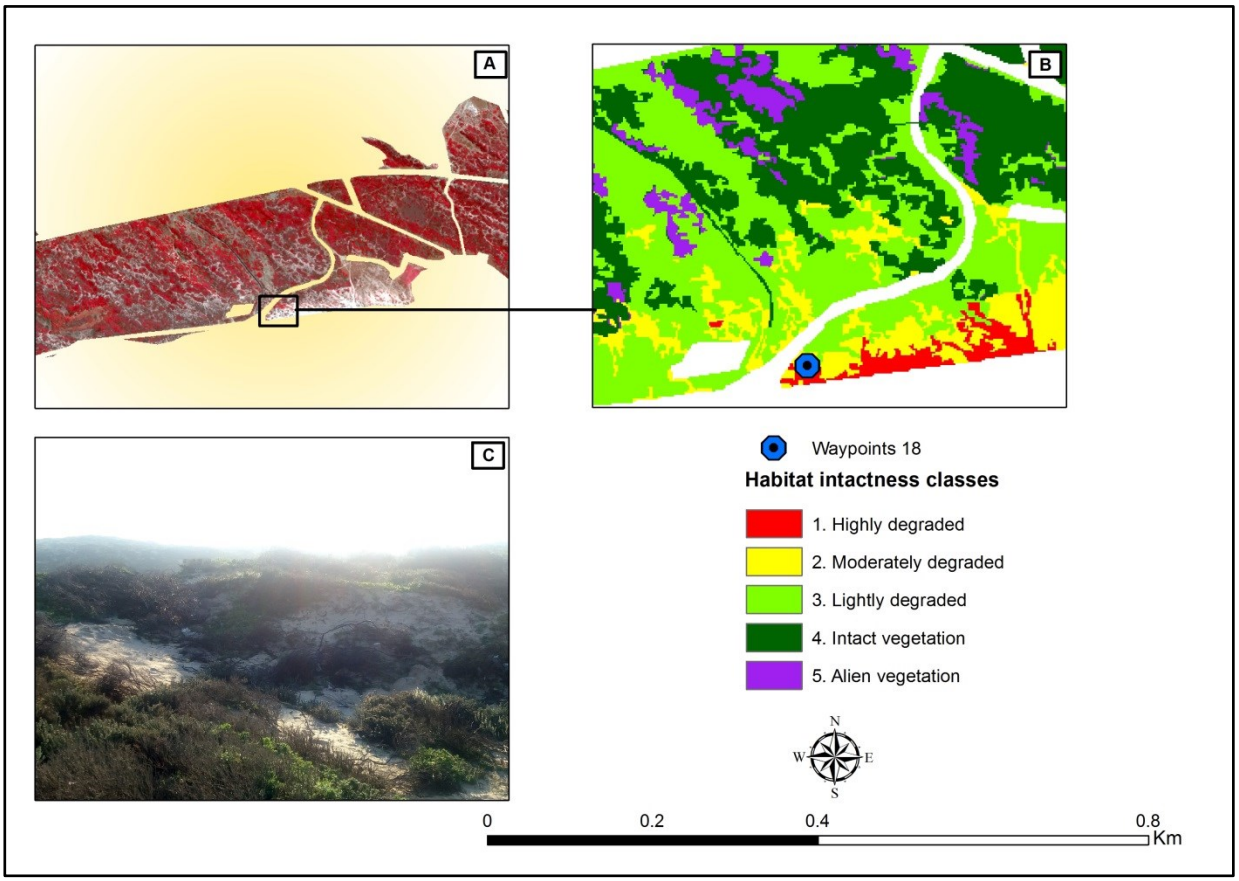

Figure 4.5 (A) is the WV-2 image subset on 25 February 2014 (B) is the classified HII image of the small blocked area in (A); and (C) is a photograph of the star marked validation point in (B).

Figure 4.6-A is a WV-2 satellite image showing a marked region of the validation point in the February image. Figure 4.6-B represents waypoint 19 of class 4 which is intact vegetation and

Figure 4.6-C is a field photograph captured during field visit at waypoint 19 and shows mixture of natural (green) and alien vegetation (brown).

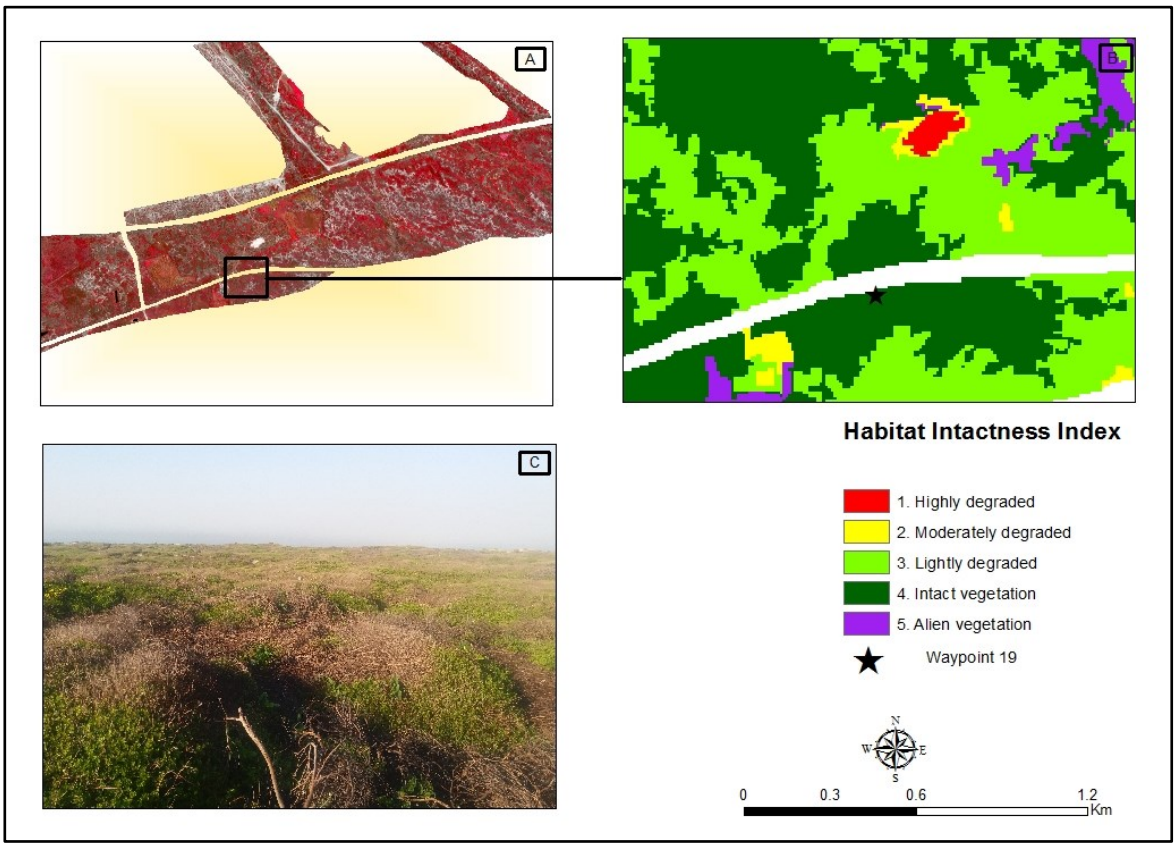

Figure 4.6 (A) is the WV-2 subset image on 25 February 2014; (B) is the classified HII image of the small blocked area in (A) and (C) is a photograph of the star-marked validation point 19 in (B).

The HII classification did not identify alien vegetation at waypoint 19 as shown in Figure 4.6-C. The main reason for this oversight is that waypoint 19 does not show pure alien vegetation class 5 but a mixture of classes 4 and class 5. This is because the NIR1 spectral values used for classification were not high enough to be picked up as pure alien signature.

The WV-2 subset of 25 February 2014 (Figure 4.7-A) shows the area of interest for validation. Figure 4.7-B shows the classified region for waypoint 21 of class 2, the moderately degraded class. Figure 4.7-C is the photograph of the same area taken during the field validation in June 2016 of and shows sparse, grassy vegetation with bare soil bordering the transformed area which is masked out in the satellite image.

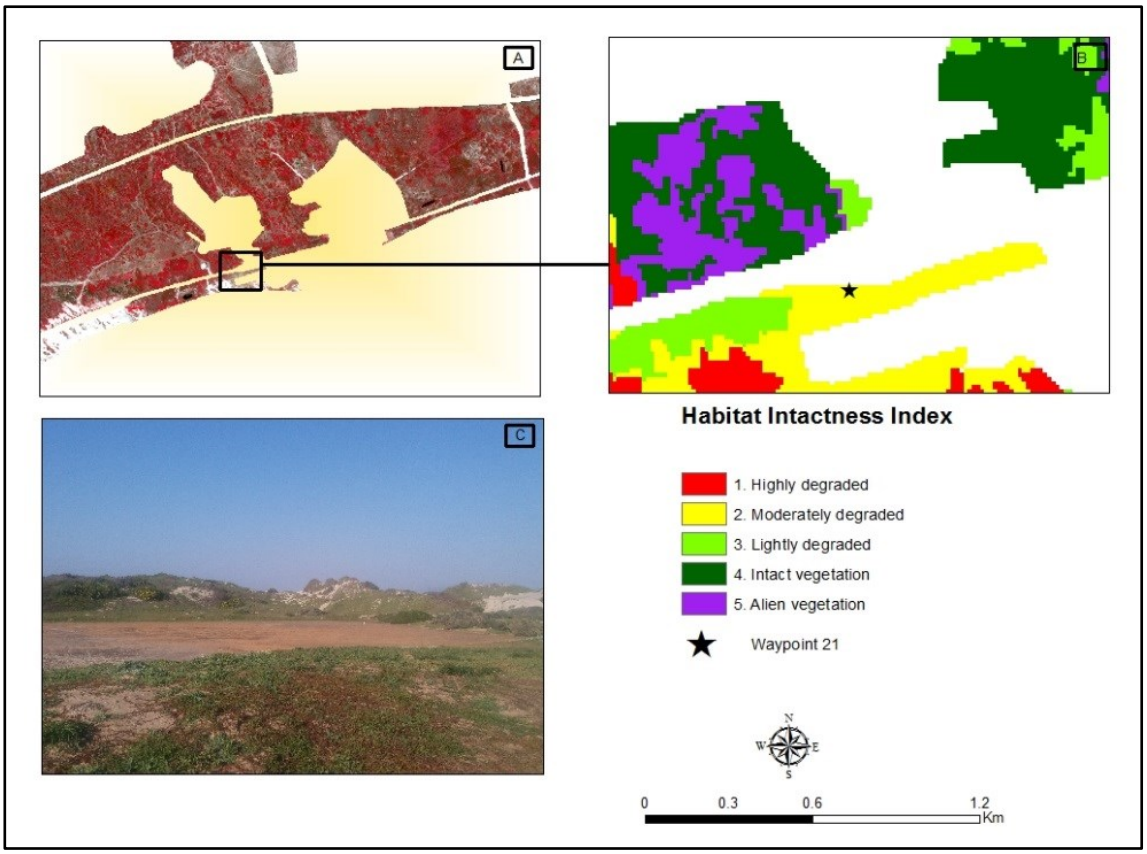

Figure 4.7 (A) is the WV-2 subset image on 25 February 2014; (B) is the showing a classified HII image of the blocked area in (A) and (C) is a photograph validation point 21 in (B)

This confirmed that the HII classification correctly identified class 2 because the spectral values of the NIR band in the segmented polygons in eCognition were able to pick out class 2 clearly.

Figure 4.8-A is the WV-2 subset of 25 February 2014 showing the marked area of interest, Figure 4.8-B shows waypoint 22 classified as intact vegetation (class 4) and Figure 4.8-C is the field photograph of the same area showing dense Rooikrans (*Acacia cyclops)* and Port Jackson *(Acacia saligna)*. The HII classification and the photographed vegetation at waypoint 22 do not agree. The reason is that the NIR1 spectral values for generating the classification were not high enough to identify a pure alien vegetation signature (Foody 2002; Campbell 2002; Xu et al. 2005).

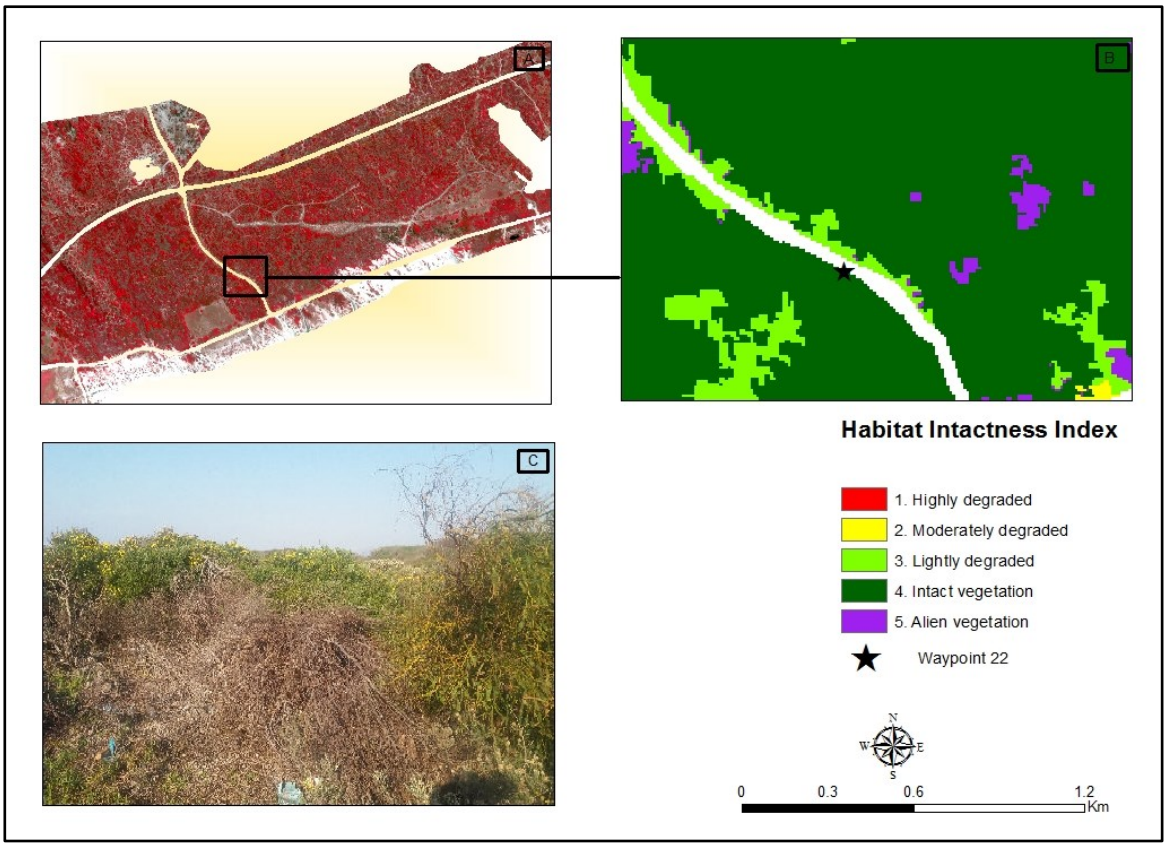

Figure 4.8 A WV-2 subset image of 25 February 2014 presented in (A), with (B) showing a classified image with the marked validation waypoint 22. A photograph of the marked validation point is shown in (C) captured on the 7 June 2016.

Also, the aliens were not very dense, so causing confusion with pristine vegetation. The plant with yellow flowers is alien Rooikrans (*Acacia cyclops*), mostly used for firewood and building material for informal housing.

Figure 4.9-A shows a WV-2 subset of 25 February 2014, Figure 4.9-B is the classified result for the block in Figure 4.9-A. Waypoint 23 is classified as the lightly degraded class 3 and field observations during the accuracy assessment correctly recorded by the photograph in Figure 4.9-C the open grass.

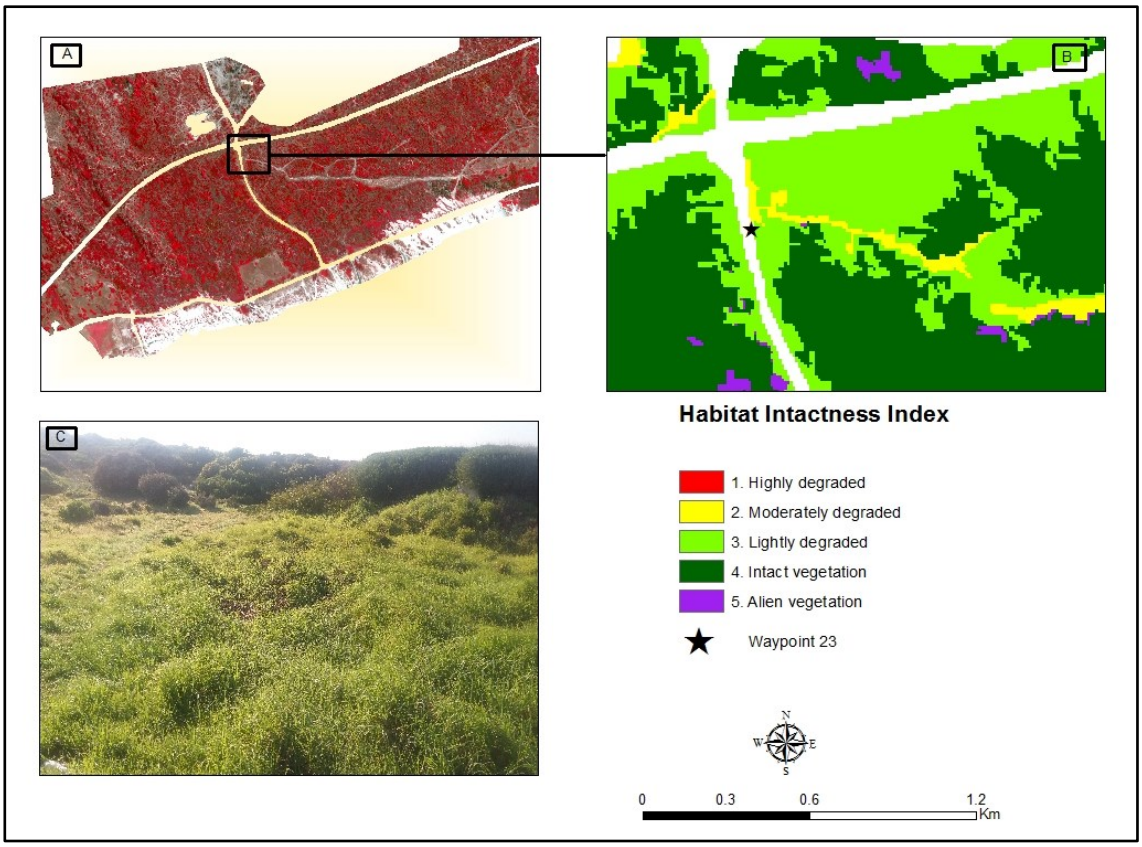

Figure 4.9 (A) is a WV-2 subset image on 25 February 2014 in Monwabisi; (B) is a HII classified image of habitat intactness with a marked validation waypoint 23; and (C) is a photograph (7 June 2016) of open grass representing class 3 at the same area

Figure 4.10-A shows a subsetted WV-2 satellite image of 25 February 2014 and Figure 4.10-B is the HII classification result for the marked block (waypoint 24), namely class 3 (lightly degraded) and characterised by low, shrubby CFDS vegetation. The photograph in Figure 4.10-C indicates low herbaceous vegetation with dwarf, burnt shrubs. The classified result and field observation agree according to CoCT field experts as the dynamics of the CFDS vegetation after a fire event or clearing of alien vegetation is a succession process that takes time for the natural vegetation to reach its climax (fully-grown stage). The class 3 vegetation is too small to be clearly visible in Figure 4.10-C.

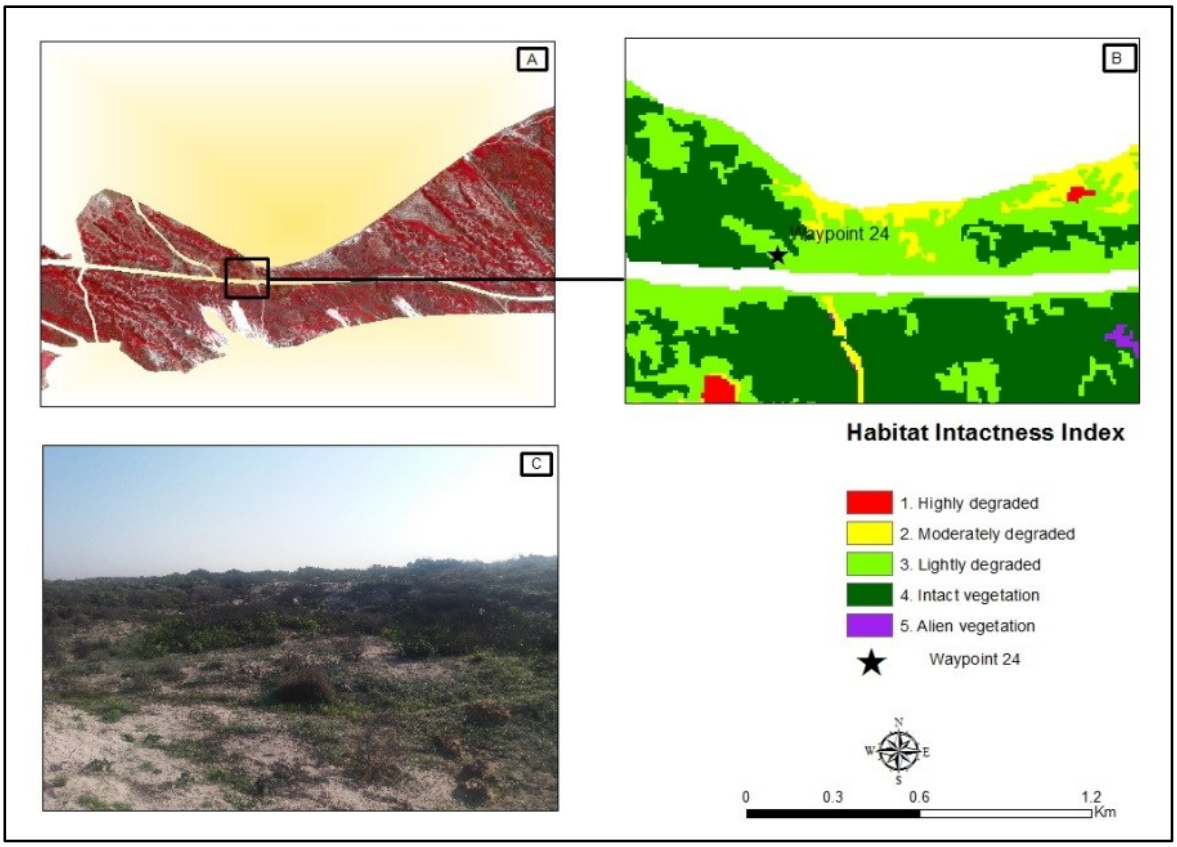

Figure 4.10 (A) is a WV-2 subset image on 25 February 2014 of Wolfgat Nature Reserve (B) is a classified image of the HII with a marked validation waypoint 24, and (C) is photograph (7 June 2016) of open grass representing class 3

Figure 4.11-A is a WV-2 subset of 25 February 2014 and while Figure 4.11-B is the HII classification result for the marked waypoint 25, namely alien vegetation of (class 5). Figure 4.11-D is a photograph of the same area taken during field observation that shows intact vegetation characterised by low, dense shrubby CFDS growing on moist valley-like landscape in a (class 3) lightly degraded condition shown in Figure 4.11-C. The classification is incorrect compared to the evidence from field observation. This area was misclassified as alien vegetation because of the high reflective value in the NIR1 band in the regression analysis before deriving the DTC and the inclusion of valley-like area.

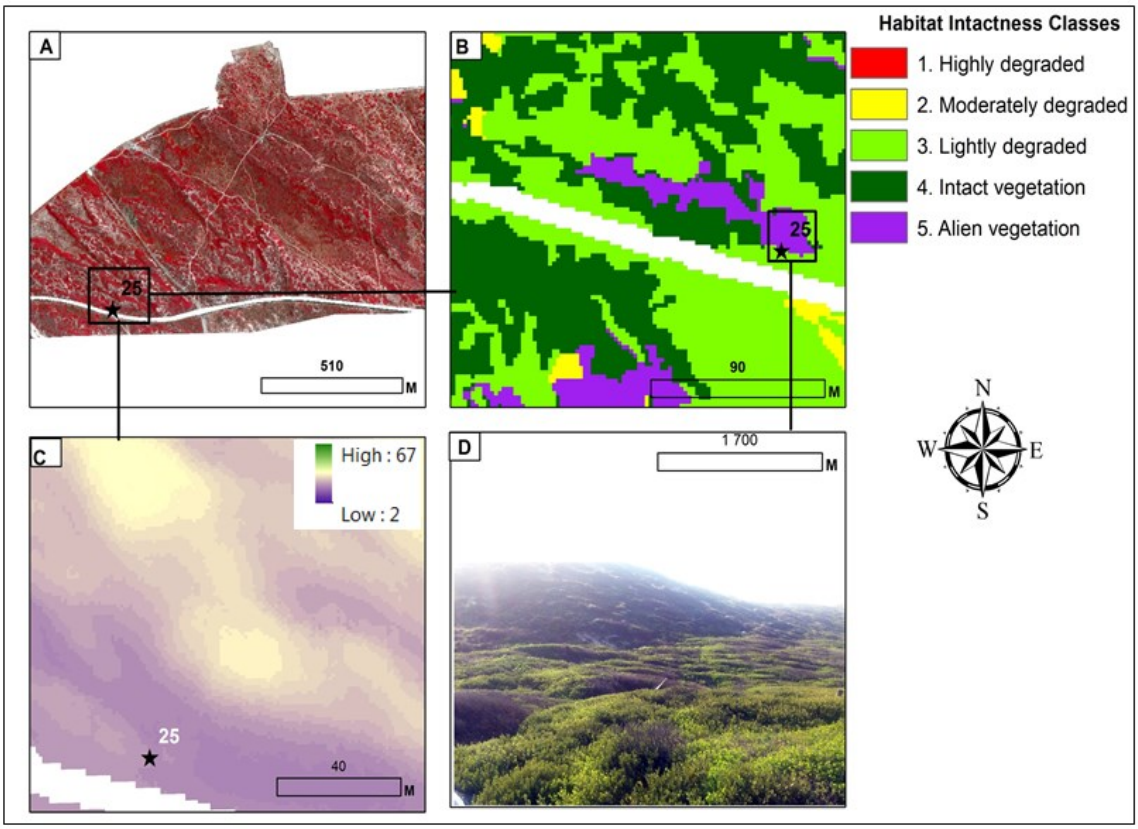

Figure 4.11 (A) is a WV-2 subset image of 25 February 2014 of Wolfgat Nature Reserve; (B) is a classified image of the HII with a marked validation waypoint 25; and (C) is an elevation model for the area in (B) and (D) is a photograph (7 June 2016) of open grass representing class.

Figure 4.12-A is the subsetted WV-2 satellite image from 25 February 2014 and Figure 4.12-B extracted from the marked frame in Figure 4.12-A. It shows the classified result represented by waypoints 26 and 27. Waypoint 26 represents class 2, i.e. moderately degraded. Visual image (WV-2) and field inspections with CoCT vegetation experts showed that north of waypoints 26 is waypoint 27 (marked in a red star) shows a fire scar that occurred in late December 2012. Therefore, the HII classification correctly identified class 3.

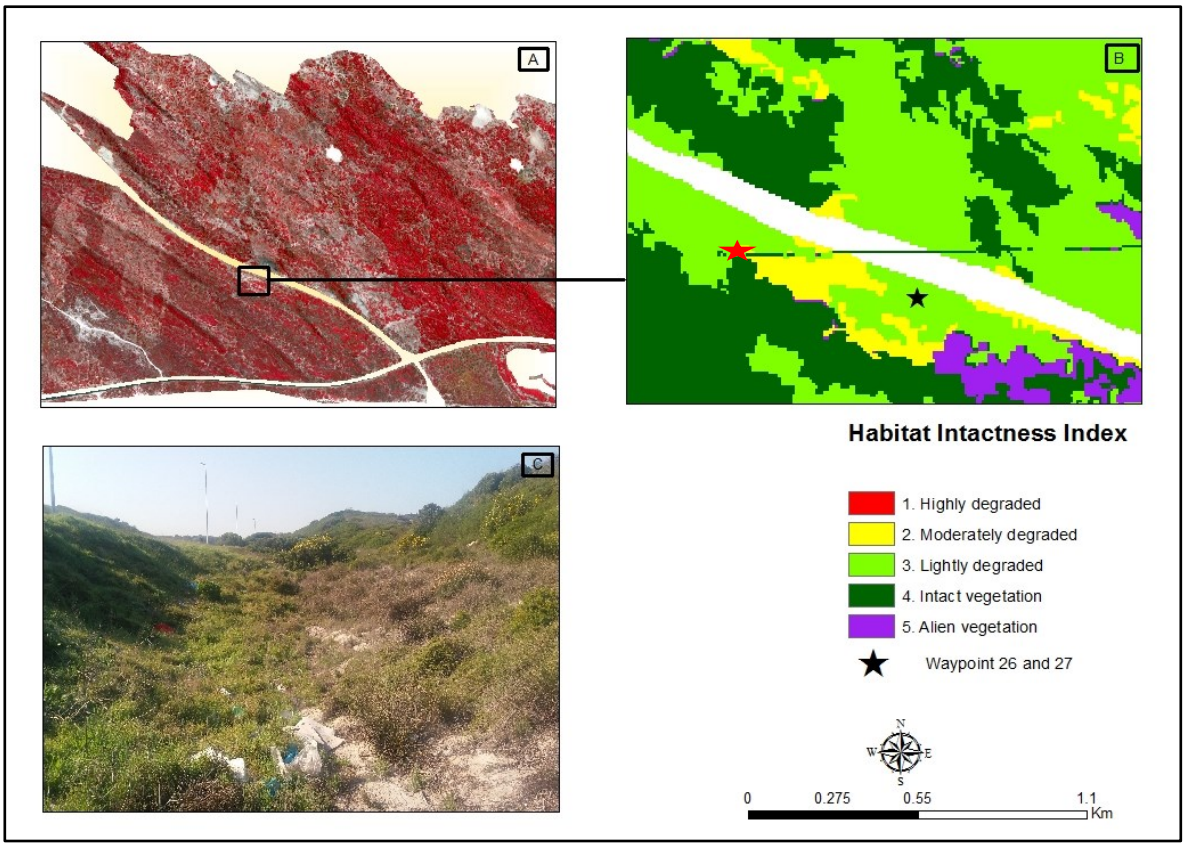

Figure 4.12 (A) is a WV-2 subset image on 25 February 2014 of Wolfgat Nature Reserve; (B) is a classified image of the HII with marked validation waypoints 26 (is a red star marking a previous fire scar) and 27; and (C) is photograph (7 June) of open grass representing class 3.

The marked waypoint 27 in Figure 4.12-B is a validation point for HII classification results of class 3 (lightly degraded). Waypoint 27 is characterised by low CFDS vegetation. The field observation photograph in Figure 4.12-C shows low grassy vegetation with small patches of open sand. The classification and the photographed evidence agree.

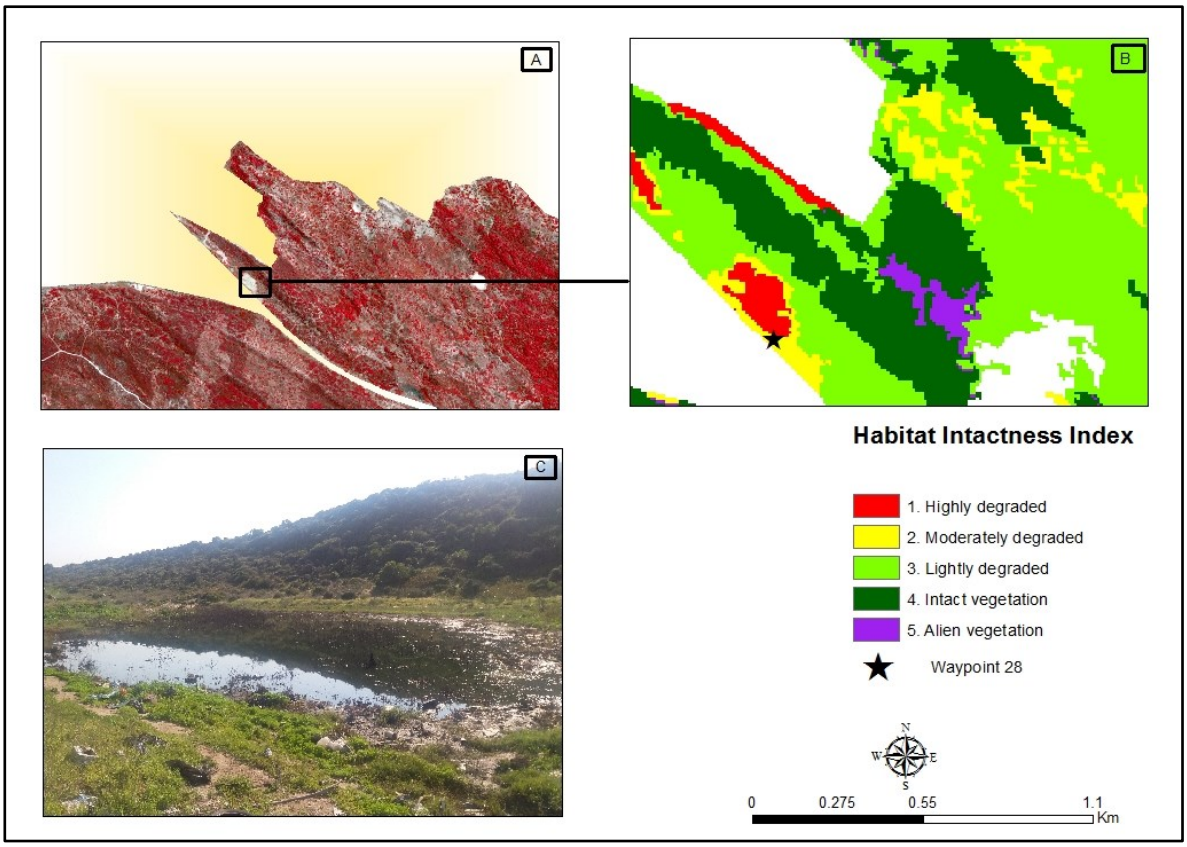

Figure 4.13 (A) is a WV-2 subset image on 25 February 2014 of Wolfgat Nature Reserve; (B) is a classified image of the HII with a marked validation waypoint 28; and (C) is photograph (7 June 2016) of open grass representing classes 1 and 2.

Figure 4.13-A is a WV-2 subsetted image of 25 February 2014 marked with a frame. Figure 4.13-B shows the classified HII results for the frame representing waypoint 28 which indicates a highly degraded class 1. Figure 4.13-C a field-observation photograph of the area recorded during field-visit. The field-validation was conducted during the wet, cold winter when the highly degraded area was filled with water. By comparison the February image taken during the dry, hot summer shows a bare soil, with high spectral reflectance. Figure 4.13-C shows the same area surrounded by open shrubby vegetation. Therefore, the classification is accurate.

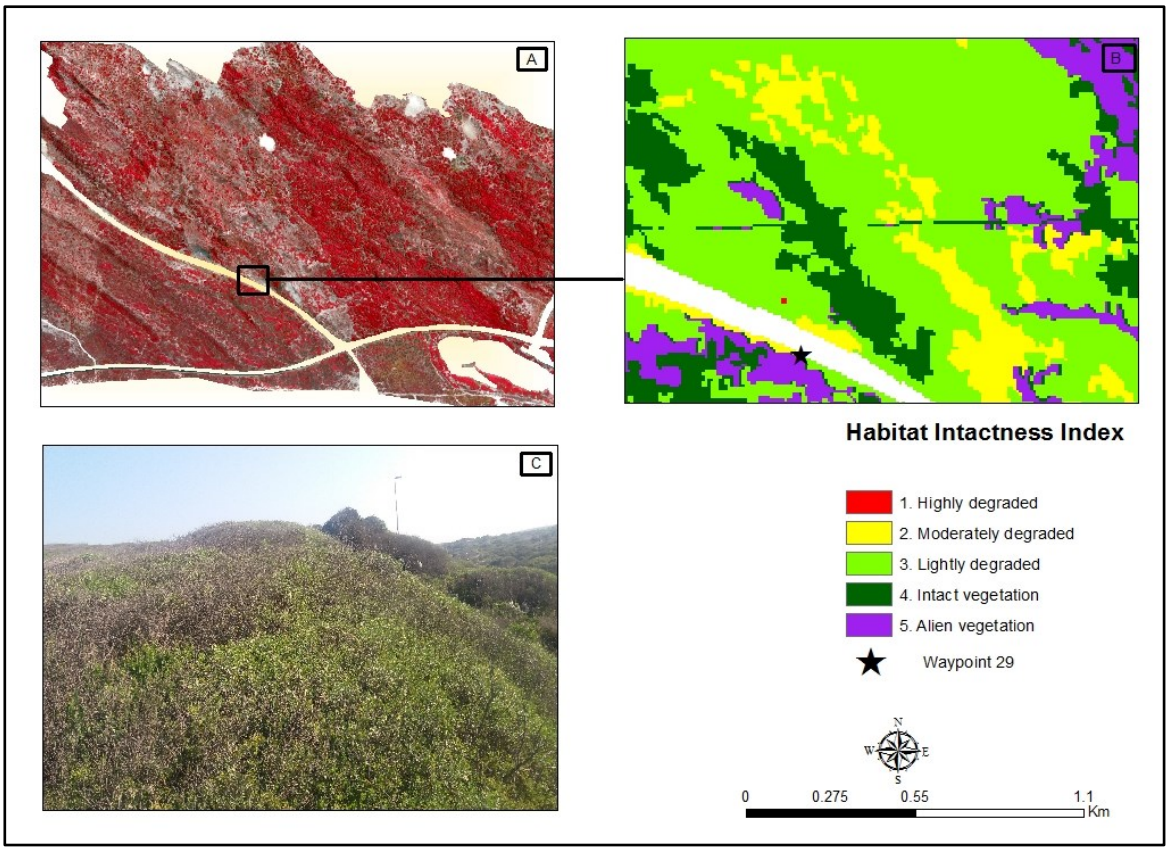

Figure 4.14 (A) is a WV-2 subset image on 25 February 2014 of Wolfgat Nature Reserve;(B) is a classified image of the HII with a marked validation waypoint 29 (B) and (C) is a photograph (7 June 2016) of open grass representing class 5.

Figure 4.14-A is the WV-2 subset image on 25 February 2014 showing the classified result of the HII region marked by the block. Figure 4.14-B is class 5 habitat intactness representing dense alien vegetation. Figure 4.14-C is the field-observation photograph at waypoint 29 which shows dense natural vegetation. The misclassification as alien vegetation arose from the segmentation polygons NIR being spectrally confused as alien vegetation. This error is similar to spectral confusion in Figure 4.5-B.

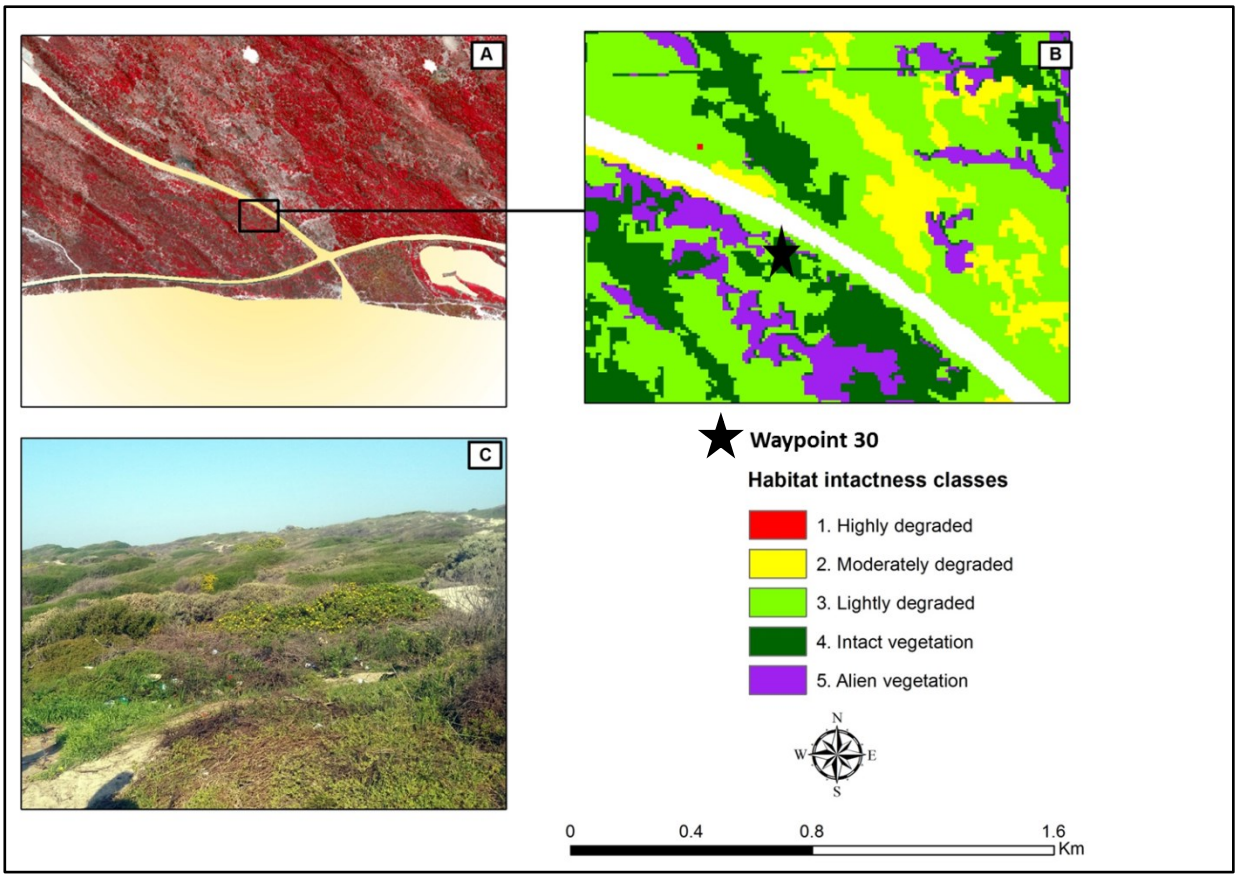

Figure 4.15 (A) is a WV-2 subset image on 25 February 2014 Wolfgat Nature Reserve; (B) is a classified image of the HII with a marked validation waypoint 30; and (C) is photograph (7 June 2016) of open grass representing class 4.

Figure 4.15-A is a subsetted WV-2 image from on 25 February 2014 and Figure 4.15-B shows the classification result of the intact vegetation class 4 (Intact vegetation) in the marked block. Figure 4.15-C, the field-observation photograph, shows dense alien vegetation although the CoCT experts indicated it to be natural CFDS vegetation. The Field visual-observation confirmed that the classification was correct.

Visual observation and the classification results of 11 October 2014 at waypoint 31 indicated the presence of alien vegetation. Due to environmental dynamics and time lag between the dates of the satellite image and field-observations, the field-validation photograph (Figure 4.16-C) recorded during field visit shows herbaceous vegetation regrowth after a fire in November 2015 (CoCT Noxolo Sidzumo and Ludwe Ntantiso field experts).

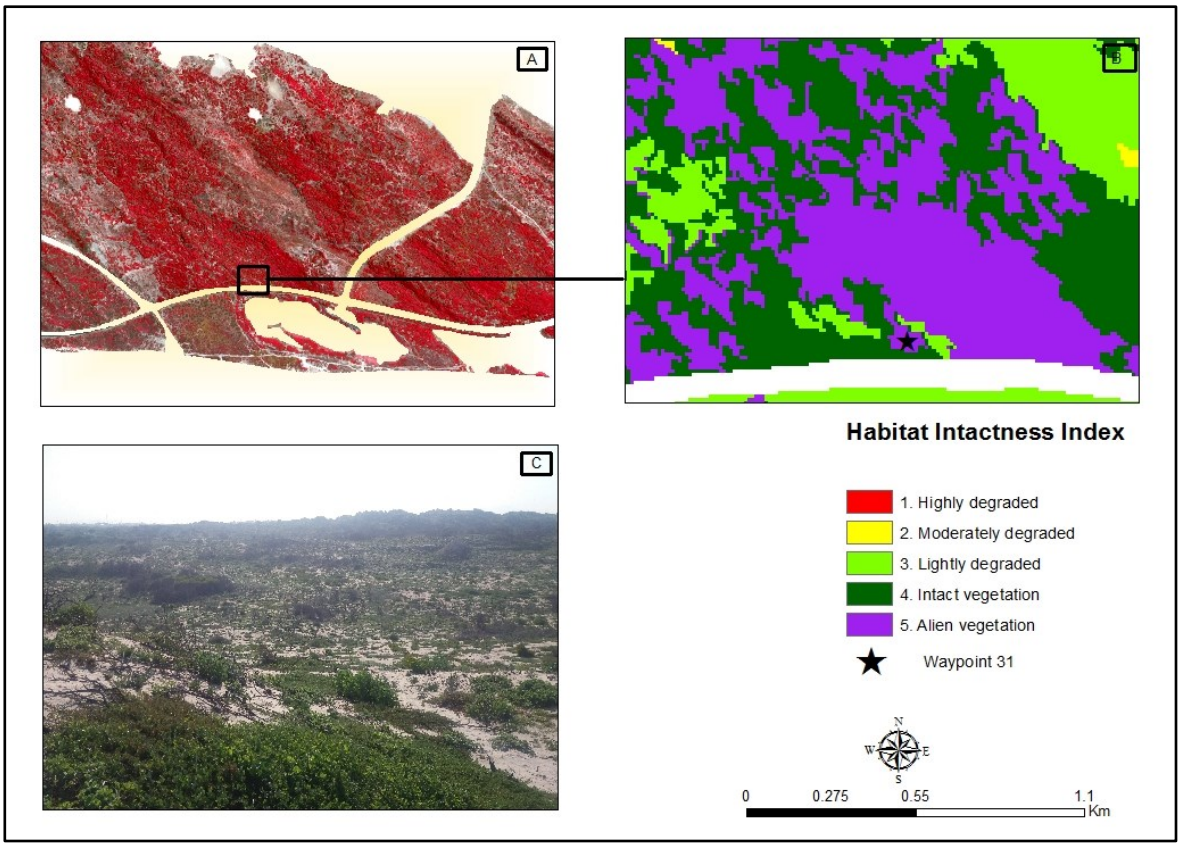

Figure 4.16 (A) is a WV-2 subset image on 11 October 2014 in Monwabisi; (B), is a classified image of HII marked with a field-validation waypoint 31; and (C) is a field validation photograph (7 June 2016) of the marked region

The Rooikrans (*Acacia cyclops*) is the dominant alien plant species occurring in the area. Field validation was not possible because most of the vegetation at waypoint 31 had burnt after image acquisition (alien vegetation is very susceptive to fire). According to Mucina & Rutherford (2006) the regeneration time by Strandveld vegetation to maturity is longer than fynbos vegetation. This explains the dominance of class 3 (lightly degraded) by herbaceous CFDS vegetation and confirms that classification of the satellite image was correct at acquisition time.

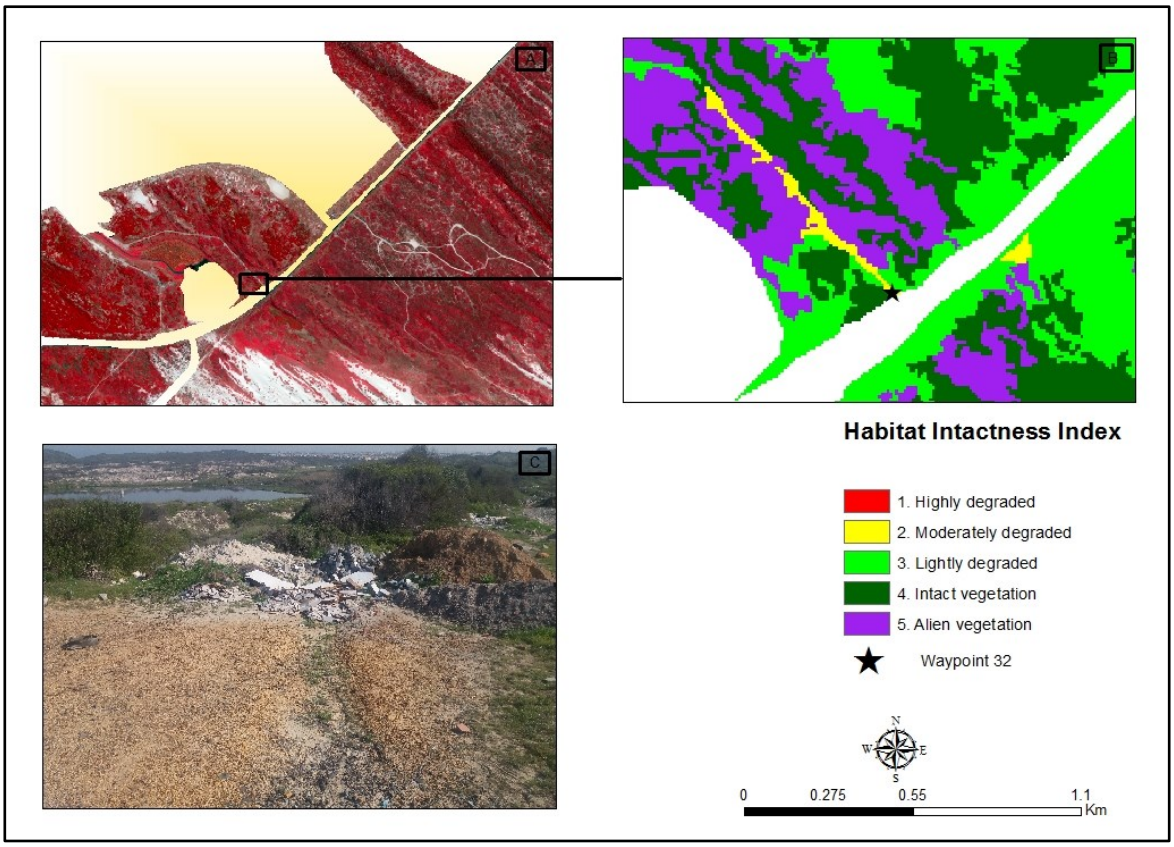

Figure 4.17 (A) is a WV-2 subset image of Macassar dunes on 11 October 2014; (B) is a classified image of HII with a field-validation waypoint 32 and. (C) is a field-validation photograph (7 June 2016) of the marked point

Figure 4.17-A shows the WV-2 subset of 11 October 2014. The HII class of the vegetation at waypoint 32 in Figure 4.17-B is class 2 (moderately degraded). The photograph recorded during field visit shows rubble from building material. The areas next to the field-validation waypoint 32 are the surrounding of shrubby CFDS vegetation. Therefore, the satellite classification was correct as shown by Figure 4.17-C.

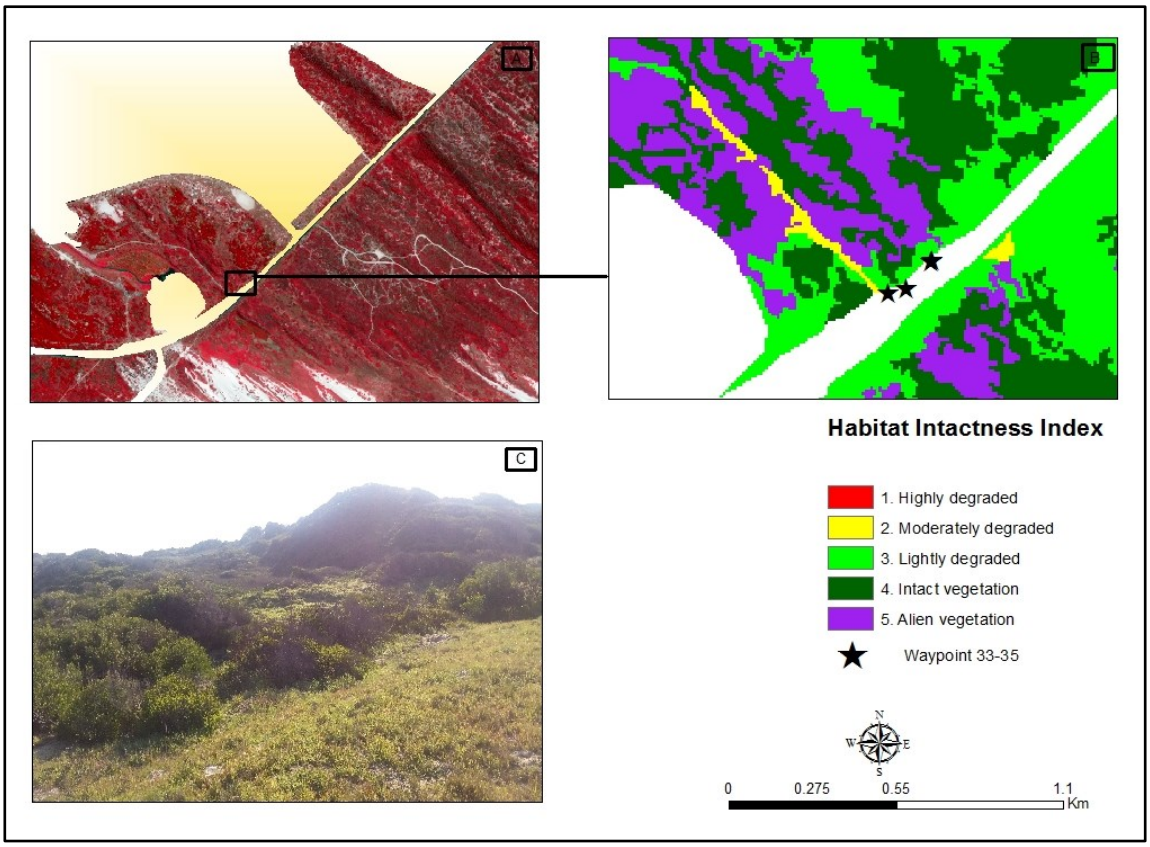

Figure 4.18 (A) is a WV-2 subset image of the Macassar Dunes on 11 October 2014; (B) is a classified image of HII three field-validation waypoints points (33-35) and class 3; (C) is a field-validation photograph (7 June 2016) of the marked areas

Figure 4.18-A indicates a WV-2 subset from the October image. The HII class of the vegetation at field-validation waypoint 33-35 in Figure 4.18-B is class 3 (Lightly degraded). The three waypoints represent the same HII class. The photograph Figure 4.18-C shows open, low-lying CFDS vegetation in the Macassar backdunes. The image was correctly classified with reference to the field photograph.

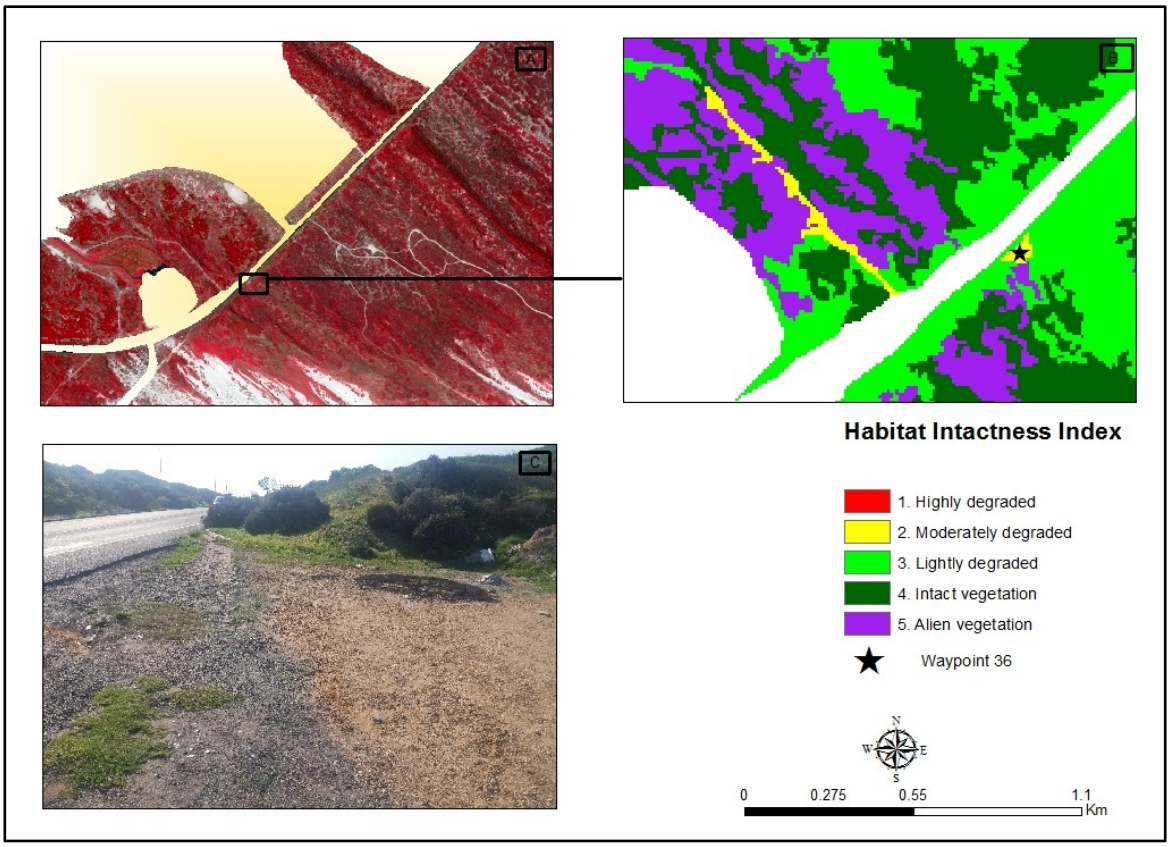

Figure 4.19 (A) is a WV-2 subset image on 11 October 2014 of Wolfgat Nature Reserve; (B) is a classified image of HII with a marked validation waypoint 36 and (C) is a photograph of the same area (7 June 2016) of open grass representing class 2

Figure 4.19-A is the subsetted WV-2 image of 11 October 2014 and Figure 4.19-B portrays the HII for the area marked with the black frame in Figure 4.19-A. The classification at waypoint 36 is class 2 which indicates moderately degraded vegetation. Field observation for accuracy assessment revealed open bare soil and low grassy vegetation Figure 4.19-C. The image classification is correct. Throughout the results, the method adopted from Lück-Vogel, O'Farrell & Roberts (2013) was suitably modified for the study, because all the land-use activities were masked not to decrease the accuracy of the results.

The following chapter 5 briefly gives a summary by revisiting the aims and objectives of the study, setting out limitations of the study and outlining the recommendations and conclusions of the study.

CHAPTER 5. CONCLUSIONS AND RECOMMENDATIONS

This chapter summarises conclusions drawn in this study. The aim and objectives of the study are revisited, the limitations of the study are discussed and recommendations made for future coastal vegetation related studies.

5.1 REVISITING THE OBJECTIVES

The *first objective* was to identify pristine areas and types of degradation. It was achieved by using WV-2 satellite imagery with 2 m spatial resolution and high spectral resolution with eight spectral bands to identify these areas. The remaining total of intact vegetation is 61%. Not only were satellite data used but field visits were carried out to better characterise these areas. Field-informed classes of interest were identified. The field-informed classes were bare soil, cleared vegetation, fire scars on sand and limestone, intact or pristine herbaceous vegetation, pristine woody or shrubby vegetation growing on sand and limestone and alien invasive Rooikrans (*Acacia cyclops)* vegetation. Prior to the field visits WV-2 images for 25 February 2014 and 11 October 2014 were used to visually identify areas of interest for the field visits. The satellite imagery used worked well in identifying different types of degradation.

The *second objective* was to derive spectral, structural and textural properties for the intactness gradient of natural terrestrial coastal vegetation using WV-2 satellite images from 25 February 2014 and 11 October 2014. In order to carry out this objective, the WV-2 satellite images were pre-processed to improve the quality required further analyses. Pre-processing involved mosaicking, atmospheric correction and subsetting of both the 25 February 2014 and 11 October 2014 images. A trial-and-error experiment was done to determine segmentation parameters for both images. Following segmentation five image derivatives namely Brightness (spectral derivative), Compactness (structural derivative), NIR1 standard deviation (textural derivative), Area derivative and NDVI and eight spectral bands were used to develop a HII derived using DTC. The image pre-processing and the segmentation enabled the identification of the respective image objects of interest.

The *third objective* was to develop and validate a HII based on the spectral, structural and textural information. This information together with additional properties (Area and NDVI) was the basis for developing the HII through regression analyses and to perform a DTC. The classification was derived from field-informed classes arranged according to levels of vegetation intactness ranging from highly degraded to most pristine. From the eight WV-2

spectral bands and five image derivatives, only two spectral bands (RED and NIR1) were used to derive the DTC in the end.

The *fourth* and last objective was to evaluate the remote sensing results. An accuracy assessment was performed to assess the quality and accuracy of the results using ground truth data. Prior field data collection, intactness maps were produced and taken with to the field. The results showed that the approach can effectively and efficiently be done on high spatial resolution satellite imagery. The overall accuracy of the results was 80% with kappa statistical value of 0.75 (75%), which represents a strong agreement between remote sensing results and reference data. The objectives were achieved using the transferable modified approach adopted from Lück-Vogel, O'Farrell & Roberts (2013) in producing sufficient results WV-2. The modified method adopted from Lück-Vogel, O'Farrell & Roberts (2013) worked well for the study, since most transformed areas were masked-out in order to increase the accuracy of the results. Two spectral bands namely RED and NIR1 bands were used as ruleset in the DTC to distinguish between intact and alien vegetation.

5.2 LIMITATIONS OF THE STUDY

Difficulties were experienced during field-data collection to identify and establish sufficient and appropriate validation points for assessing the quality of the classification results. Areas of in the field showed variations of intactness in the HII maps due to several environmental dynamics and human-induced factors. Access to validation points in the field was often constrained due to the steep terrain and no road access. Safety during field data collection was also an issue that had to be faced. The major difficulty experienced in the study is the differences between image acquisition dates and field data causing difficulties in proper validation of the results.

5.3 CONCLUSION

On the approach adopted from Lück-Vogel, O'Farrell &Roberts (2013); this study is the first of its kind to be applied in a coastal environment using satellite imagery with high spatial resolution in South Africa. The modification of the methodology in this study has proven that vegetation intactness on CFDS can be assessed with using WV-2. However, during data analysis it was clearly established that seasonality plays an important role for deriving HII since this was a key factor in explaining differences between the classification results based on the two WV-2 images. A major finding regarding the satellite data used in the study revealed that the two-year difference between the images and field observation made ground truthing

confusing due to interim effects of environmental dynamics such as, clearing of alien invasive vegetation and frequent bush fires. The study results revealed that images taken in the dry, summer season better detected invasive alien vegetation. The three image derivatives (brightness, compactness and standard deviation for NIR) adapted from Lück-Vogel, O'Farrell & Roberts (2013) however, did not yield satisfactory regression results for deriving a classification for the coastal environment. This is because of transformed features such as, buildings, play-grounds and agricultural land-uses were masked out in the study. However, the spectral bands important for vegetation assessment, namely the RED, NIR1 and NIR2 worked appropriately and yielded good results in the DTC. The CoCT habitat condition data layer was found to be too coarse for this study thus resulting in low regression results which were not used further for the DTC. This was because to the habitat condition polygons included several types of intactness or degradation.

From this study it can therefore be concluded that the use of high spatial resolution satellite imagery and the masking-out of transformed areas and other vegetation improve the accuracy of the habitat intactness classification results. Areas such as formal urban and informal settlements, roads, camping resorts, playgrounds and other vegetation types were also excluded to improve results accuracy. It was found that the natural dune landscape, which is naturally bare and brightness could be misclassified as habitat degradation.

5.4 RECOMMENDATIONS

The research findings and limitations led to the following recommendations:

- For CFDS vegetation it is better to use WV-2 satellite images of the dry season, not only to better detect alien vegetation but for general classification with the HII.
- HII assessment is best done by using satellite images that match the date of field visit as closely as possible.
- Elevation and relief models should be included in the classification procedures to avoid misclassification between classes occurring in valleys.
- Should the method be applied into a different vegetation type, recalibration of the decision tree threshold for DTC will be required.
- It will be beneficial to test the algorithm or method on a Sentinel-2 satellite image because of cost factor (Sentinel-2 is available for free) and different spatial and spectral resolution.

- Further studies of vegetation assessment are well advised to choose areas that are easily accessible and safe for efficient field data collection.

[24 423 words]

REFERENCES

Al-Wassai & Kalyankar 1999. Major limitations of satellite images. PhD thesis. Bagdad University. Department of Computer Sciences.

Barwell L 2011. Integrity Assessment Procedure for Buffer Dune systems on the Cape South coast, South Africa. MSc Thesis. Stellenbosch: Stellenbosch University.

Biňa RT, Jara RB & Roque CR 1980. Application of multi-level remote sensing survey to mangrove forest resource management in the Philippines. Proceedings of Asian Symposium on Mangrove development, Research and management University of Malaya, Kuala Lumpar, Malaysia.

Blaschke T 2004. Object-based contextual image classification built on image segmentation. Advances in Techniques for Analysis of Remotely Sensed Data, 2003 IEEE. Workshop held 27-28 Oct. 2003 113-119. Salzburg: Austria.

Bosire JO, Kaino JJ, Olagoke AO, Mwihaki LM, Ogendi GM, Kairo JG, Berger U & Macharia 2014. Mangroves in peril: unprecedented degradation rates of peri-urban mangroves in Kenya. *Bio geosciences* 11: 2623-2634.

Boyle SA, Kennedy CM, Torres J, Colman K & Pe´rez-Estigarribia PE (2014). High-Resolution Satellite Imagery is an Important yet Underutilized Resource in Conservation Biology. PLoS ONE 9(1): e86908. doi: 10.1371/journal.pone.0086908.

Branch GM, Griffiths CL, Branch ML & Beckley LE 1994. Two oceans. A guide to the marine life of southern Africa. Cape Town, South Africa: David Philip.

Brown AC & Jarman N. 1978. Coastal marine habitats. in Wiener MJA (ed) Biogeography and ecology of Southern Africa, 1239-1277. The Hague: W. Junk.

Brown AC 2001. Biology of sandy beaches in: Encyclopaedia of Ocean Sciences, Volume 5, ed. J.H. Steele, S. A. Thorpe &K.K. Turekian, pp. 2496-2504. London, UK: Academic Press.

Campbell JB 2002. Introduction to remote sensing. 3rd ed. New York: The Guildford Press.

Campbell JB 2006. Introduction to remote sensing. 4th ed. London: Taylor & Francis.

Campbell JB 2007. Introduction to Remote Sensing. New York: The Guilford Press. London.

Campbell JB 2011. Introduction to Remote Sensing. 5th Ed. New York: The Guilford Press.

Capel DP 2001.Super-resolution and image mosaicking. Doctor of Philosophy. Oxford: University of Oxford, Department of Engineering Science.

Carboni M, Santoro R & Acosta ATR (2010). Are some communities of the coastal dune zonation more susceptible to alien plant invasion? J Plant Ecol-Uk 3: 139-147.

Carleer A, Debeir O & Wolff E 2004. Comparison of very high resolution satellite image segmentation. *Image and Signal processing for remote sensing* 5238: 532-342.

Carter RWG 1988. Coastal Environments: An introduction to physical, ecological and cultural systems of the coastlines. London: Academic Press.

Celliers L, Breetzke T, Moore L & Malan D 2009. A user-friendly guide to South Africa's Integrated Coastal Management Act. Cape Town: Department of Environmental Affairs and SSI Engineers and Environmental Consultants.

Chaudhury MU 1990. Digital analysis of remote sensing data for monitoring the ecological status of the mangroves forests of Sunderbans in Bangladesh. Processing of the 23rd International Symposium of Remote sensing 1: 493-497.

Cho MA, Malahlela O & Ramoelo A 2015. Assessing the utility WorldView-2 imagery for tree species mapping in South African subtropical humid forest and the conservation implications: Dukuduku forest patch as a case study. *International Journal of Applied Earth Observation and Geoformation* 38:349-357.

Clark, BM, Bennet, BA, & Lamberth, SJ, 1996. Factors affecting spatial variability in seine net catches of fish in the surf zone of False Bay, South Africa. *Marine Ecology Progress Series* 131: 14-34.

Congalton R. & Green K 2009. Assessing the Accuracy of Remotely Sensed Data: Principles and Practices. 2nd Ed. Boca Raton: Taylor & Francis.

Constanza R 1998. The Value of ecosystem services. *Ecological Economics* 25, 1:1-2.

Constanza R, D'Arge R, De Groot R, Farberk S, Grasso M, Hannon B, Limburg K, Naem S, O'NeilRV, Paruelo J, Raskin RG, Suttonkk P & Van Den Belt M 1997. The value of the world's ecosystem services and natural capital. Nature 397: 253-260.

Coppin P, Jonckhere I, Nackaerts K, Mays B & Lambin E 2004. Digital change detection methods in ecosystem monitoring: a review. *International Journal of Remote Sensing* 25, 1565-1596.

Cowling RM, Richardson DM & Pierce SM 1997. Vegetation of South Africa. Cambridge: Cambridge University Press.

Creswell JW 2003. Research Design: Qualitative, quantitative and mixed methods approach. New Delhi: Sage.

Darwish A, Leukert K & Reinhardt 2003. Image segmentation for the purpose of object-based classification. Geoscience and Remote Sensing Symposium. IGARSS.'03 Proceedings 2003 IEEE International 3:2039-2041.

Davies B & Day J 1998. Vanishing waters. Cape Town: University of Cape Town Press.

Dayton PK 2003. The importance of the natural sciences to conservation. American Naturalist 162, 1:1-13.

De Colstoun EC, Story MH, Thompson C, Commisso K, Smith TG & Irons JR 2003. National park vegetation mapping using multi-temporal Landsat 7 and decision tree classifier. *Remote Sensing of Environment* 85, 3: 316-327.

DEAT (Department of Environmental Affairs & Tourism) 2008. South Africa's national programme of action for protection of the marine environment from land-based activities. Cape Town: Department of Environmental Affairs.

Definiens 2007. *Definiens Developer 7: User Guide*, document version 7.0.2.936. München, Germany: Definiens AG.

Denny MW, Gaines SD 2007. Encyclopaedia of tidal pools & rocky shores. University of California Press: California.

Department of Environmental Affairs (DEA) 2014. The National Coastal Management Programme of South Africa. Cape Town.

Drăguţ L, Tiede D & Levick SR 2010. ESP: a tool to estimate scale parameter for multi-resolution image segmentation of remotely sensed data. *International Journal of Geographical Information Science* 24, 6:859–871.

Du Plessis A & Glass JG 1991. The geology of False Bay. *Transactions of the Royal Society of South Africa* 47: 495-517.

Du Plessis WP 1999. Linear regression relationships between NDVI, vegetation and rainfall in Etosha National Park, Namibia. *Journal of Arid Environments* 42, 4: 235-260.

Edwards AJ, Green EP, Mumby PJ & Clark CD 2000. Remote Sensing Handbook for Tropical Coastal Management. France: United Nations Educational, Scientific and Cultural Organisation (UNESCO).

EEA (European Environmental Agency). 2006. The changing faces of Europe's coastal areas. EEA Report No 6/2006. EEA - European Environment Agency, Copenhagen.

ESRI 2010. Arc GIS desktop release. Environmental Systems Research Institutes.

Feilhauer H, Thonfeld F, Faude U, He KS, Rocchini D & Schmidtlein S 2013.Assessing floristic composition with multispectral sensors-A comparison based on monotemporal and multiseasonal field spectra. *International Journal Applied Earth Geoformation* 21: 218–229.

Fischer WA, Hemphill WR & Kover A 1976. Progress in remote sensing. *Journal of Photogrammetric* 32, 2: 33-72.

Foody GM & Cutler MEJ 2006. Mapping the species richness and composition of tropical forests from remotely sensed data with neural networks. *Ecological Modelling* 195: 37–42.

Foody GM 2002. Status of land cover classification accuracy assessment. *Remote Sensing of Environment* 80: 185-201.

Forey E, Chapelet B, Vitasse Y, Tilquin M, Touzard B & Michalet R 2008.The relative importance of disturbance and environmental stress at local and regional scales in French coastal sand dunes. *Journal of Vegetation Science* 19: 493-502.

Fox NJ 2008. Post-positivism. In: Given L (ed) Encyclopedia of Qualitative Research Methods. London: Sage.

Frederiksen L, Kollmann J, Vestergaard P & Bruun HH 2006. A multivariate approach to plant community distribution in the coastal dune zonation of NW Denmark. *Phytocoenologia* 36:321-342.

Friel C & Haddad K 1992. GIS manages marine resources. *GIS World* 5: 33-36.

Froese C & Mei S 2008. Mapping and monitoring coal mine subsidence using LiDAR and SAR. Canada. GeoEdmonton.

Gao J 1999. A comparative study on spatial and spectral resolution of satellite data in mapping mangrove forests. *International Journal of Remote Sensing* 20: 2823-2833.

Gao Y, Mas JF, Maathuis BHP, Xiangmins Z & Van Dijk PM 2006. Comparison of pixel-based and object-oriented image classification approaches: a case study in a coal fire area, Wuda, Inner Mongolia, China. *International journal of Remote Sensing* 27, 18: 4039-4055.

Glavovic BC & Cullinan C 2009. The coast in Strydom HA & King ND (eds) Environmental Management in South Africa (2nd ed), 868-920. Cape Town, South Africa: Juta Law.

Green EP, Mumby PJ, Edwards AJ & Clark CD 1997. Estimating leaf area index of mangroves from satellite data. *Aquatic Botany* 58:11-19.

Guerschman JP, Hill MJ, Renzullo LJ, Barrett DJ, Marks AS & Botha EJ 2009. Estimating fractional cover of photosynthetic vegetation, non-photosynthetic vegetation and bare soil in the Australian tropical savannah region up scaling the EO-1 Hyperion and MODIS sensors. *Remote Sensing of Environment* 113: 928–945.

Hantson W & Kooistra L & Slim PA 2012. Mapping invasive woody species in coastal dunes in the Netherlands: a remote sensing approach using LIDAR and high-resolution aerial photographs. *Applied Vegetation Science* 12: 35-41.

Hengl T 2006. Finding the right pixel size. *Computers and Sciences* 32:1283-1298.

Holme A, Burnside DG & Mitchell AA 1987. The development of a system for monitoring trend in range condition in the arid shrub lands of Western Australia. *Australian Rangeland Journal* 9:14-20.

Holmes PM, Dorse C, Stipinovich A, Purves A, Wood J, Gibbs D & Ernst Zen R 2012. Conservation implementation plan for strandveld in the metro south-east environmental Resource Management Department (ERMD), City of Cape Town.

Huang C, Davis LS, & Townshend JRG 2002. An assessment of support vector machines for land cover classification. *International Journal of Remote Sensing* 23, 4: 725-749.

Huete AR, Didan K, Shimabukuro YE, Ratana P, Saleska SR, Hutyra LR, Yang W, Nemani RR & Myneni R 2006. Amazon rainforests green-up with sunlight in dry season. *Geophysical Research Letters* 33: 1-4.

Huete AR, Liu H, Batchily K, & van Leeuwen W 1991. A Comparison of vegetation Indices over a global set of TM Images for EOS-MODIS. Remote Sensing of Environment 59, 3: 440-451.

Ibrahim M & Yosuh M 1992. Monitoring the development impacts on coastal resources of Pulau Redang Marine Park by remote sensing in: Third ASIAN Science and Technology week conference 407-413.

Jackson RD & Huete AR 1991. Interpreting vegetation indices. *Preventive Veterinary Medicine* 11:185-200.

Jackson WPU 1991. False Bay an environmental assessment: Transitions of the Royal Society of South Africa: Cape Town.

Jacobs K & Jangle R 2008. Coastal Ecosystem Management Plan: Western Cape. Unpublished, the Nature Conservation Corporation, Cape Town.

Jensen JR 1996. Introductory digital image processing: a remote sensing perspective. Upper Saddle River, N.J. Prentice Hall.

Jensen JR 2007. Introductory to Digital Image Processing: A Remote Sensing Perspective. Prentice Hall Series in Geographic Information Science.

Ji Y, Zhou G & New T 2009. Abiotic Factors Influencing the Distribution of Vegetation in Coastal Estuary of the Liaohe Delta, Northeast China. *Estuaries Coasts* 32: 937-942.

Kampouraki M, Wood GA & Brewer 2008. Opportunities and limitations of object-based image analysis for detecting urban impervious and vegetated surfaces using tur-colour aerial photography. *Geoformation and Cartography* 555-569.

Kapetsky JM, Hill JM, Worthy LD &Evans DL 1990. Assessing Potential for Aquaculture Development with Geographic Information System. *Journal of the World Aquaculture Society* 21, 4: 241-249.

Kenchington RA, Claasen DR 1988. Australia's Great Barrier reef management technology. Proceedings of Symposium on remote sensing of the coastal zone, Gold Coast, Queensland (Brisbane: Department of Geographical Information Systems) 2, 2: 2-13.

Ketchum BH 1972. The water's edge: Critical problems of the coastal zone. London.

Klemas V 2007. Remote sensing of coastal wetlands and estuaries. Proceedings of Coastal Zone 07. Charleston, South Carolina: NOAA Coastal Services Centre.

Landis JR & Koch GG 1977. The measurement of observer agreement for categorical data. *Biometrics* 33: 159-174.

Lee M, 2001. Coastal defence and the habitats directive: predictions of habitat change in England and Wales. *Geographical Journal* 167:57-71.

Leewis L, van Bodegom PM, Rozema J & Janssen GM 2012. Does beach nourishment have long-term effects on intertidal macroinvertebrate species abundance? *Estuarine. Coastal Shelf* 113:172-181.

Lefsky MA & Cohen WB 2001. Selection of remote sensing data. PhD thesis. Oregon University. Department of Forest Science.

Levinton JS 1995. Marine biology: function, biodiversity, ecology. Oxford University Press. 420.

Lillesand TM, Kiefer RW and Chipman JW 2008. Remote sensing and image interpretation. 6th ed. Hoboken (NJ): Wiley.

Liu D & Xia F 2010. Assessing object-based classification: advantages and limitations. *Remote Sensing Letters* 1, 4:187-194.

Lopez-Portillo J & Ezcurra E 2008. Zonation in mangrove and salt marsh vegetation at Laguna de Mexico. *Tropical Biology and Conservation* 21, 2: 107-114.

Lotze HK, Lenihan HS, Bourque BJ, Bradury HR, Cooke RG, Kay MC, Kidwell SM, Kirby MX, Peterson CH, Jackson JBC 2006. Depletion, degradation and recovery potential of estuaries and coastal seas. *Science* 312: 1806-1809.

Loubersac L & Populus J 1986. The application of high resolution satellite for coastal management and planning in a pacific coral island. *Geocarto International* 2:17-31.

Lu D & Weng Q 2007. A survey of image classification methods and techniques for improving classification performance. *International Journal of Remote Sensing* 28, 5: 823-870.

Lubke RA, Avis AM, Steinke TD & Boucher C 1997. Coastal Vegetation. Cambridge: University Press pp300-321.

Lück-Vogel M, Mbolambi C, Rautenbach K, Adams J, Van Niekerk L 2016. Vegetation mapping in the St Lucia estuary using very high resolution multispectral imagery and LiDAR. *South African Journal of Botany*, for Special Issue on Estuaries, available online at http://dx.doi.org/10.1016/j.sajb.2016.04.010.

Lück-Vogel M, O'Farrell P & Roberts W 2013. Remote sensing based ecosystem state assessment in the Sandveld Region, South Africa. *Ecological Indicators* 33: 60-70.

Malahlela O 2013. Integrating environmental variables with WorldView-2 data to model probability of occurrence of invasive Chromolaena adorata in forest canopy gaps: Dukuduku forest in KwaZulu Natal, South Africa. Master's thesis. University of KwaZulu Natal, department of Earth and environmental Sciences.

Marangoz AM, Oruc M, Karakis S & Sahin H 2009. Comparison of pixel based and object oriented classification using IKONOS imagery for automatic building extraction. International Journal of Remote Sensing 114: 220-225.

Maun MA & Perumal J 1999 Zonation of vegetation on lacustrine coastal dunes: effects of burial by sand. *Ecological Letters* 2:14-18.

Maun MA 1998. Adaptations of plants to burial in coastal sand dunes. Canadian *Journal of Botany* 76:713-738.

Maun MA 2004. Burial of plants as a selective force in sand dunes. Martínez ML, Psuty NP (eds) Coastal dunes. *Ecology and Conservation Journal* 119-135.

Maun MA 2009. The biology of coastal sand dunes. Oxford University Press: Oxford.

McCarthy MJ, Halls JN 2014. Habitat mapping and change assessment of coastal environments: an examination of WorldView-2, QuickBird and IKONOS satellite imagery and airborne island habitats. *International Journal of Geo-Informatics* 3:297-325.

McLean B & Glazewski JI 2009. Marine systems. Environmental management: An introduction. In: Strydom HA & King ND (eds) Environmental management in South Africa (2nd ed), 455-512. Cape Town, South Africa: Juta Law.

Millenium Ecosystem Assessment 2005. Ecosystems and Human Well-being. Millennium ecosystem assessment: Synthesis Report. World Resources Institute. Washington, DC: Island press.

Miththapala S 2013. Lagoons and Estuaries. Coastal Ecosystems Series (Vol 4). vi 73. IUCN Sri Lanka Country Office, Colombo.

Moller M, Lymburner & Volk M 2007. The comparison index: A tool for assessing the accuracy of image segmentation. *International Journal of Applied Earth Observation and Geoinformation*

Moulis D, Barbel P & 1999. Restauration des dunes. Réhabilitation et gestion des dunes littorals Méditerranéennes Françaises. Collection: *Manuels et Méthodes. BRGM Ed* 75-91.

Mpe HT 2015. Assessment of mining impacts on the west coast of Western Cape using LiDAR data. Honours research report. Stellenbosch: Stellenbosch University, Department of Geography and Environmental Studies.

Mucina L & Rutherford MC 2006. The vegetation of South Africa, Lesotho and Swaziland. Pretoria: South African National Biodiversity Institute.

Mumby PJ, Green EP, Edwards AJ & Clark CD 1997. Measurement of seagrass standing crop using satellite and digital airborne remote sensing. *Marine Ecology Progress Series* 159:57-60.

Myers R 1993. Slope Stabilization and Erosion Control Using Vegetation. Department of Ecology, State of Washington 131: 17-34.

Nagendra H & Rocchini D 2008. High resolution satellite imagery for tropical biodiversity studies: The devil is in the detail. *Biodiversity and Conservation* 17: 3431–3442.

Nagendra H 2001. Using remote sensing to assess biodiversity. *International Journal of Remote Sensing* 22, 12: 2377-2400.

Nakamura Y, Krestov PV, & Omelko AM 2007. Bioclimate and zonal vegetation in Northeast Asia: First approximation to an integrated study. *Phytocoenologia* 37:443-470.

Nayak S & Bahuguna A 2001. Application of remote sensing data to monitor mangroves and other coastal vegetation in India. *Indian Journal of Marine Science* 30, 4: 195-213.

Nayak S 2004. Application of remote sensing for implementation of coastal zone regulation: A case study of India. Global Spatial Data Infrastructure 7th conference.

Nayak S Pandeya A, Gupta MC, Trivede CR, Prassad KN & Kadri SA 1989. Application of satellite data monitoring degradation of tidal wetlands in the Gulf of Kachchh, West India. *Acta Astronautical* 20: 171-178.

Nelson SA 2008. Coastal zones. Retrieved 101, from Tulane University: httpWwww.tulane.edu/sanelson/geo/204/coastalzones.htm.

Nicholls RJ, Wong PP, Burkett VR, Codignotto JO, Hay JE, McLean RF, Ragoonaden S & Woodroffe CD 2007. The Coastal systems and low-lying areas. Climate Change 2007: Impacts, Adaptation and Vulnerability. Contribution of Working Group II to the Fourth Assessment Report of the Intergovernmental Panel on Climate Change. Cambridge, UK, 315-356: Cambridge University Press.

Nobre AM & JG Ferreira 2009. Integration of ecosystem-based tools to support coastal zone management. *Journal of Coastal Res*. SI 56:1676-1680.

Oetter DR, Cohen WB, Berterretche M, Maiersperger TK & Kennedy RE 2001. Land cover mapping in an agricultural setting using multiseasonal thematic mapper data. *Remote Sensing of Environment* 76:139-155.

Oldeland J, Dorigo W, Lieckfeld L, Lucieer A & Jurgens N 2010. Combining vegetation indices, constrained ordination and fuzzy classification for mapping semi-natural vegetation units from hyperspectral imagery. *Remote sensing of Environment* 114, 6: 115-120.

Osei A, Merem EC & Twumasi 2013. The use of remote sensing data to detect environmental degradation in coastal region of south Nigeria.

Palmer B, van der Elst R & Parak O 2011. Understanding our Coast: A synopsis of KZN's coastal zone. KwaZulu-Natal Department of Agriculture, Environmental Affairs and Rural Development, Cedara, Pietermaritzburg. 32 pp.

Perumal K & Bhaskaran 2010. Supervised classification performance of multispectral images. *Journal of computing* 2, 2:11.

Pettorelli N, Vik JO, Mysterud A, Gaillard J, Tucker CJ & Stenseth NC 2005. Using the satellite-derived NDVI to assess ecological responses to environmental change. *Trends in Ecology and Evolution* 20, 9: 503-510.

Provost S, Van Til M, Deronde B & Knotters A 2005. Remote sensing of coastal vegetation in the Netherlands and Belgium. International Conference on Nature Restoration.

Ramachandran S, Sundramoorthy S, Krishnamoorthy R, Devasenapathy J, & Thanikachalam M 1998. Application of Remote Sensing and GIS to Coastal Wetland Ecology of Tamilnadu and Andaman and Nicobar group of Islands with special reference to Mangroves. *Current Science* 75(3):101-109.

Ranganath BK, Dutt CBS & Manikan B 1989. Digital mapping of mangroves in middle Andamans of India. *Proceedings of the 6th Symposium on coastal and ocean management* 1:741-750.

Rapinel S, Clement B, Magnanon S, Sellin V & Hubert-Moy L 2014. Identification and mapping of natural vegetation on a coastal site using a Worldview-2 satellite image. *Journal of Environmental Management* 144:236-246.

Reark P & Ross PS 1975. Mangrove vegetation stratification using Salyut 7 photographs and satellite images. *Geocarto International* 3: 31-47.

Richter R & Schläpfer D 2014. ATCOR-2/3 user guide [online]. Wil: ReSe Applications. Available from http://www.rese.ch/pdf/atcor3_manual.pdf [Accessed 22 February 2015].

Rouse JWRH, Haas JA, Schell & Deering DW 1973. Monitoring vegetation systems in the Great Plains with ERTS. Third ERTS Symposium. NASA SP-351 I 309- 317.

Running SW 1990. Estimating primary productivity by combining remote sensing with ecosystem simulation. *Remote Sensing of Biosphere Functioning* 79: 65-86.

Schlacher TA, Schoeman DS, Dugan J, Lastra M, Jones A, Scapini F& McLachlan A. 2008. Sandy beach ecosystems: key features, sampling issues, management challenges and climate change impacts. *Marine Ecology*. 29:70-90.

Shalaby A & Tateishi 2007. Remote sensing and GIS for mapping and monitoring land cover and land-use changes in the North-western coastal zone of Egypt. *Applied Geography* 27: 28-41.

Short AD & Hesp PA 1982. Wave, beach and dune interactions in South Eastern Australia. *Marine Geology* 48: 259-284.

Singh RP, Roy S & Kogan F 2003. Vegetation and temperature condition indices from NOAA AVHRR data for drought monitoring over India. *International Journal of Remote Sensing* 24, 22-30

South Africa 2000b. Local Government: Municipal Systems Act, Act 32 of 2000. Government Gazette of the Republic of South Africa 425: 21776, 20.11.2000:1.

South Africa 2009. National Environmental Management: Integrated Coastal Management Act, Act 24 of 2008. Government Gazette of the Republic of South Africa 524: 31884, 11.02. 2009:1.

South Africa 2014. National Environmental Management: Integrated Coastal Management Amendment Act, Act 36 of 2014. Government Gazette of the Republic of South Africa 592: 38171, 31.10.2014:2.

Spargo PE 1991. False Bay, South Africa: An historic and scientific overview. *Transactions of the Royal Society of South Africa* 47: 363-375.

Strahler AH, Woodcock CE & Smith JA 1986. The nature of models in remote sensing. *Remote Sensing of Environment* 20: 121-139.

Syvitski JPM, Harvey N, Walanski E, Burnett WC, Perillo GME & Gornitz V 2002. Dynamics of coastal zone.

Taljaard S 2011. An implementation model for integrated coastal management in South Africa-from legislation to practice. PhD thesis. Stellenbosch: Stellenbosch University, Department of Geography and Environmental Studies.

Thackway R & Lesslie R 2005. Vegetation Assets, States, and Transitions: accounting for vegetation condition in the Australian landscape. Technical Report, Bureau of Rural Sciences, Australian Government Department of Agriculture, Fisheries and Forestry. Canberra, A.C.T.

Thackway R & Lesslie R 2006. Reporting vegetation condition using the Vegetation Assets, States and Transitions (VAST) framework. *Ecological Management and Restoration* 7,1: S53-S62.

The Nature Conservancy and Environmental Systems Research Institute (TNC and ESRI). 1994a. NBS/NPS Vegetation Mapping Program: Final Draft, Standardized National Vegetation Classification System. Prepared for USDI – National Biological Survey and National Park Service. Arlington, Virginia. Wiley-Blackwell ltd. 1-367.

Theron AK & Schoones 2007. Sand transport at and shoreline response to a breakwater attached to a large tidal pool at Monwabisi, Cape Town. *Journal of the South African Institution of Civil Engineering* 49, 2: 2-9.

Thompson LMC & Schlacher TA 2008. Physical damage to coastal dunes and ecological impacts caused by vehicle tracks associated with beach camping on sandy shores: a case study from Fraser Island Australia. *Journal Coastal Conservation* 12:67-82.

Tinley KL 1985a. Coastal dunes of South Africa. South African National Science Programme report 109. Pretoria: Council for Scientific and Industrial Research FRD-CSIR.

Tinley KL 1985b. Framework of Gorongose ecosystem, Mozambique. DSC thesis. Pretoria: University of Pretoria.

Townsend DW 2006. Oceanography and Marine Biology: An introduction to Marine Science. University of Maine.

Tzatzanis M, Wrbka T & Sauberer N 2003. Landscape and vegetation responses to human impact in sandy coasts of Western Crete, Greece. *Journal for Nature Conservation* 11, 187-195.

Wang Y 2010. Remote Sensing of Coastal environments. United States: Taylor and Francis.

Welby CW 1978. Application of Landsat imagery to shoreline erosion. *Photogrammetric Engineering and Remote Sensing* 44: 1173-1177.

Xiao XM, Zhang Q & Braswell B 2004. Modelling gross primary production of temperate deciduous broadleaf forest using satellite images and climate data. *Remote Sensing of Environment* 91:256-70.

Xie Y, Sha Z & Yu M 2008. Remote sensing imagery in vegetation mapping; review. *Journal of Plant Ecology* 1, 1: 9-23.

Xu M, Watanachaturaporn P, Varshney PK & Arora MJ 2005. Decision tree regression for soft classification of remote sensing data. *Remote Sensing of Environment* 97: 332-336.

Zak M & Cabido M 2002. Spatial patterns of the Chaco vegetation of central Argentina: integration of remote sensing and phytosociology. *Applied Vegetation Science* 5: 213-226.

Zhang JT 2002. A study on relations of vegetation, climate and soils in Shanxi province, China. *Plant Ecology* 162: 23-31.

Zhao B, Guo H, Yan Y, Wang Q, Li B 2007. A simple waterline approach for tidelands using multi-temporal satellite images: A case study in Yangtze Delta. *Estuarine, Coastal and Shelf Science* 77:134-142.

Zhu GB, Liu XL & Jia Z 2006. A multi-resolution hierarchy classification study compared with conservative methods. Workshop on Multiple representation and interoperability of spatial data, Hannover, Germany.